Supplementary Information

Supporting Information

Mild Catalytic Deoxygenation of Amides Promoted by Thorium Metallocene

Sayantani Saha and Moris S. Eisen*

Schulich Faculty of Chemistry, Technion − Israel Institute of Technology,
Haifa City, 320008, Israel
Fax: + 972-4-8295703; Tel: + 972-4-8292680
E-mail: chmoris@tx.technion.ac.il
* To whom correspondence should be addressed.

Contents

1. Experimental Section

1.1. General considerations. All manipulations of air sensitive materials were performed with the rigorous exclusion of oxygen and moisture in flamed Schlenk-type glassware or J-Young NMR tubes on a dual manifold Schlenk line interfaced to a high vacuum (10−5 Torr) line, or in a nitrogen-filled 'Innovative Technologies' glovebox with a medium capacity recirculator (1−2 ppm of O_2). Argon and nitrogen were purified by passage through a MnO oxygen-removal column and a Davison 4 Å molecular sieve column. Hydrocarbon solvents benzene−d_6 (Cambridge Isotopes), toluene (Bio-Lab), and diethyl ether (Bio-Lab) were distilled under vacuum from Na/K alloy. A few amides were bought from Sigma-Aldrich and others were synthesised using literature procedure.[1] All the solid substrates used in catalysis reaction were dried under vacuum (10−6) for 12 h on a high vacuum line. All the liquid substrates used in catalysis reaction were distilled and stored over activated 4 Å molecular sieves. Cp*$_2$ThMe$_2$ [**Th1**],[2] thorium metallacycle [**Th2**],[3] Th-complex [**Th3**][4] and deuterated pinacolborane (DBpin)[5] were prepared according to published procedures. All the afore mentioned reagents were stored in an inert atmosphere glovebox prior to use. Thorium complexes are radioactive (caution)!

NMR spectra were recorded on Bruker Advance 300, Bruker Advance III 400 spectrometers. Chemical shifts for ^{1}H and ^{13}C NMR are referenced to internal protio solvent and reported relative to tetramethylsilane. J-values are reported for ^{1}H NMR coupling constants in the unit of hertz (Hz).

2. Kinetic studies

2.1. Hydroboration of tertiary amide: In a J. Young NMR tube, typical amount of precatalyst **Th1** (1.88 ~ 18.78 μmol), *N*,*N*–diethyl–2,2,2–trifluoroacetamide (0.08 ~ 0.50 mmol), HBpin (0.08 ~ 1.0 mmol), and total volume was made up to 0.6 mL with C_6D_6 in the glove box and then the tube was sealed. The NMR tube was taken out of the glove box and freeze it in an ice bath until the ^1H NMR experiment began at 70° C. All the experiments were done by changing either one substrate or the catalyst while keeping the other reagents constant, and the data was collected up to 10–15% conversion. The product concentrations were measured by the area ratio of starting material and product from the in situ formed reaction mixture. Reaction rates were determined by least–square fit of the initial product concentration versus time, and the plots were shown in Figures S1–S10. Activation parameters including enthalpy ($\Delta H^{\neq}$), entropy ($\Delta S^{\neq}$) and activation energy (E_a) were calculated from kinetic data using Eyring and Arrhenius plots. In a typical sample, the J. Young tube was loaded with desired amount of catalyst **Th1** (0.564 μmol), *N*,*N*-diethyl-2,2,2-trifluoroacetamide (0.1879 mmol), HBpin (0.376 mmol) and sealed. Then the sample was inserted into Bruker Advance 300 spectrometer which had been previously set to the desired temperature (50 ºC, 60 ºC, 70 ºC, 80 ºC, 90 ºC). The data was collected up tro 10–15% conversion. Reaction rates were determined by the least square fit of initial product concentration versus time, and Eyring and Arrhenius plots were shown in Figures S11–S13. Enthalpy ($\Delta H^{\neq}$), entropy ($\Delta S^{\neq}$) and activation energy (E_a) were calculated from the slope and intercept of the least–square fit.

N,*N*–diethyl–2,2,2–trifluoroacetamide (0.1879 mmol) HBpin (0.3758 mmol)			
Rate (mmol/sec) × 10^{-5}	**Th1** (mmol)	ln(Rate)	ln(**Th1**)
2.32	0.00188	-10.67	-6.28
5.32	0.0047	-9.84	-5.36
11.96	0.009393	-9.03	-4.67
21.2	0.0141	-8.46	-4.26
28.12	0.0188	-8.18	-3.97
		Slope	1.09

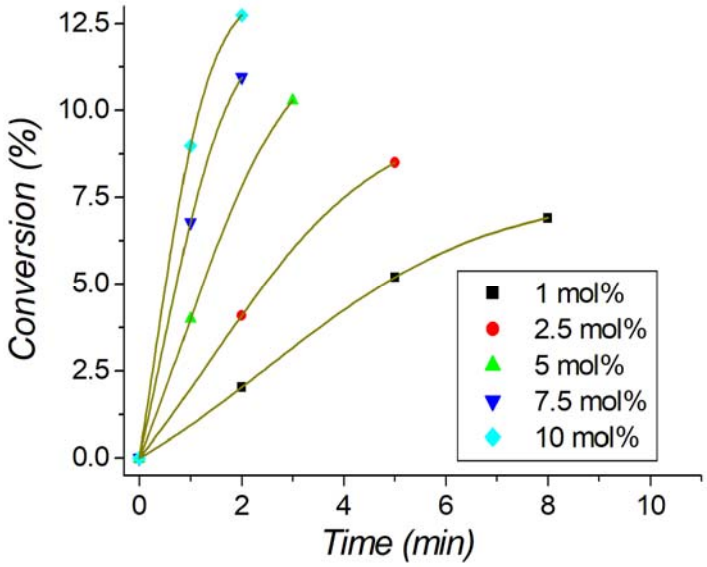

Figure S1. Plot of conversion (%) vs time (min) at different **Th1** concentrations in the reaction of *N*,*N*-diethyl-2,2,2-trifluoroacetamide and HBpin catalyzed by complex **Th1** at 70 ºC.

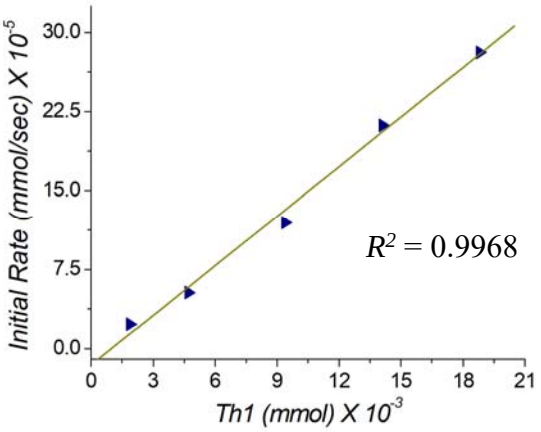

Figure S2. Plot of Initial rate *vs.* [**Th1**] in the reaction of *N*,*N*-diethyl-2,2,2-trifluoroacetamide and HBpin catalyzed by complex **Th1** at 70 ºC.

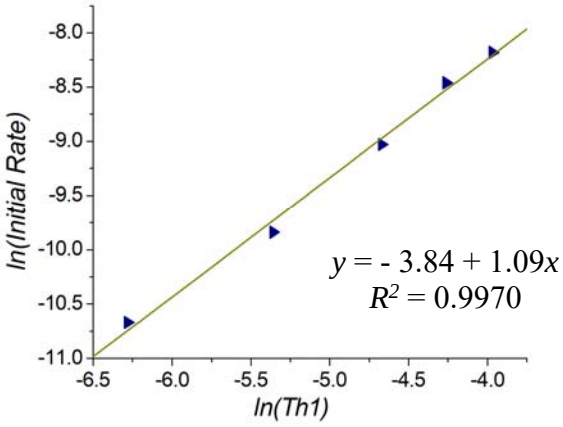

Figure S3. Plot of ln[Initial Rate] *vs.* ln[**Th1**].

N,*N*–diethyl–2,2,2–trifluoroacetamide (0.4 mmol) **Th1** (0.0093 mmol)			
Rate (mmol/sec) × 10^{-6}	HBpin (mmol)	ln(Rate)	ln(HBpin)
3.1	0.08	− 12.68	− 2.53
4.5	0.12	− 12.31	− 2.12
7.2	0.16	− 11.84	− 1.83
9.3	0.25	− 11.58	− 1.38
13.7	0.35	− 11.19	− 1.05
		Slope	0.99

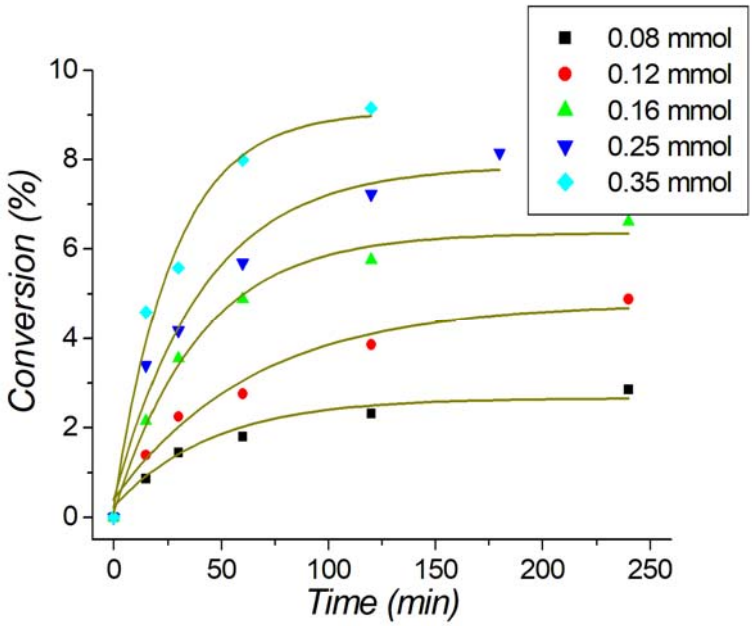

Figure S4. Plot of conversion (%) vs time (min) at different HBpin concentrations in the reaction of *N*,*N*-diethyl-2,2,2-trifluoroacetamide and HBpin catalyzed by complex **Th1** at 70 °C.

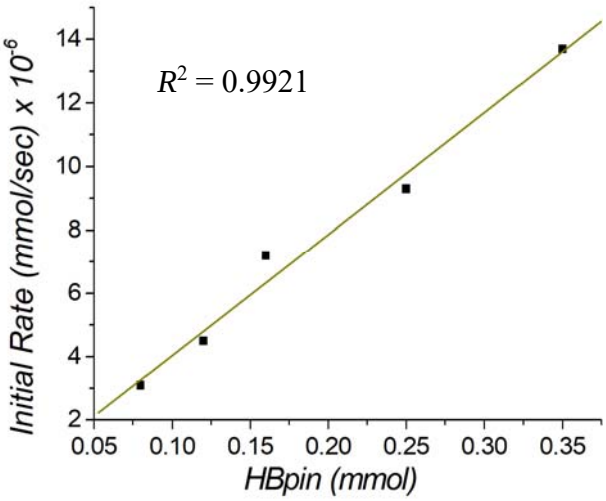

Figure S5. Plot of Initial rate *vs*. [HBpin] in the reaction of *N*,*N*-diethyl-2,2,2-trifluoroacetamide and HBpin catalyzed by complex **Th1** at 70 °C.

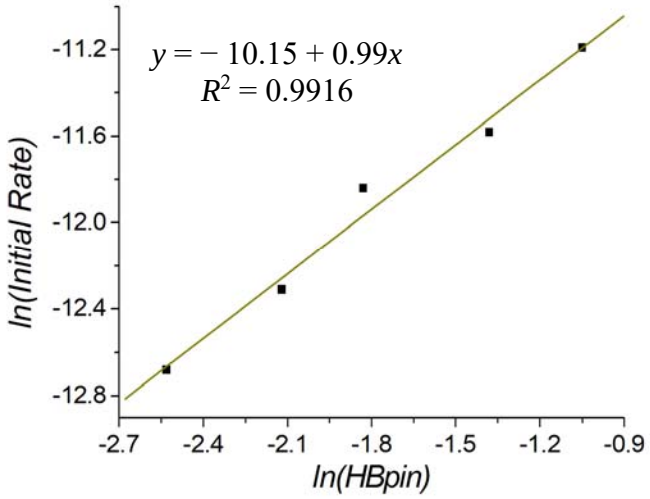

Figure S6. Plot of ln[Initial rate] *vs*. [HBpin].

Th1 (0.0062 mmol) HBpin (0.8 mmol)	
Rate (mmol/sec) × 10^{-5}	Amide (mmol)
4.44	0.08
5.92	0.16
6.1	0.25
3.96	0.40
5.6	0.50

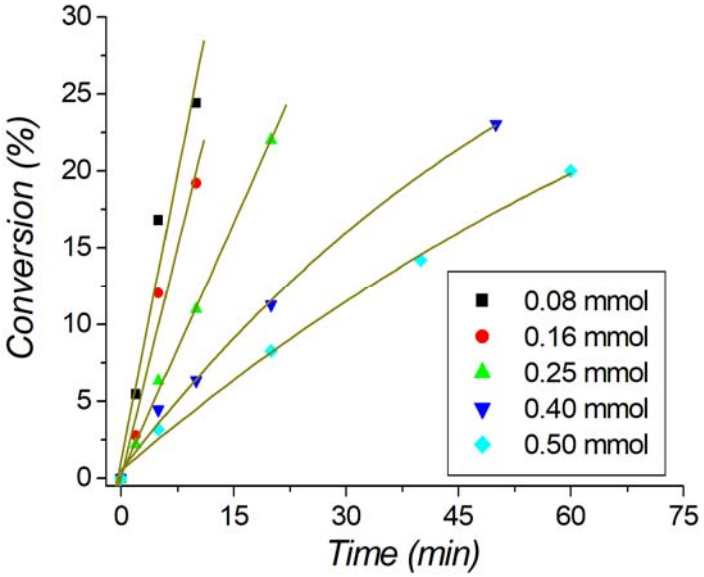

Figure S7. Plot of conversion (%) vs time (min) at different amide concentrations in the reaction of *N*,*N*-diethyl-2,2,2-trifluoroacetamide and HBpin catalyzed by complex **Th1** at 70 °C.

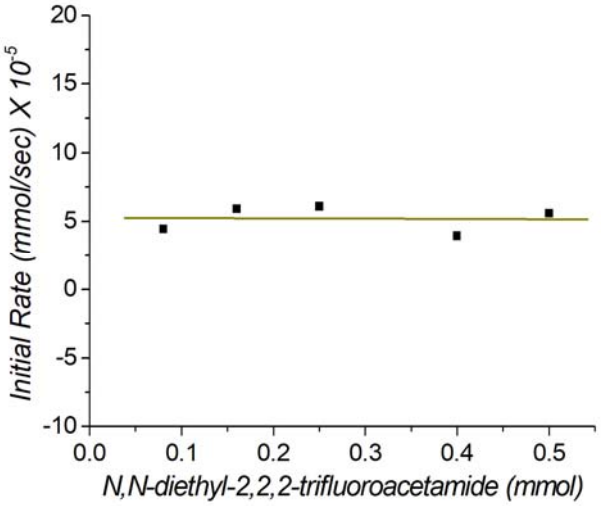

Figure S8. Plot of Initial rate *vs*. [Amide] in the reaction of *N*,*N*-diethyl-2,2,2-trifluoroacetamide and HBpin catalyzed by complex **Th1** at 70 ºC.

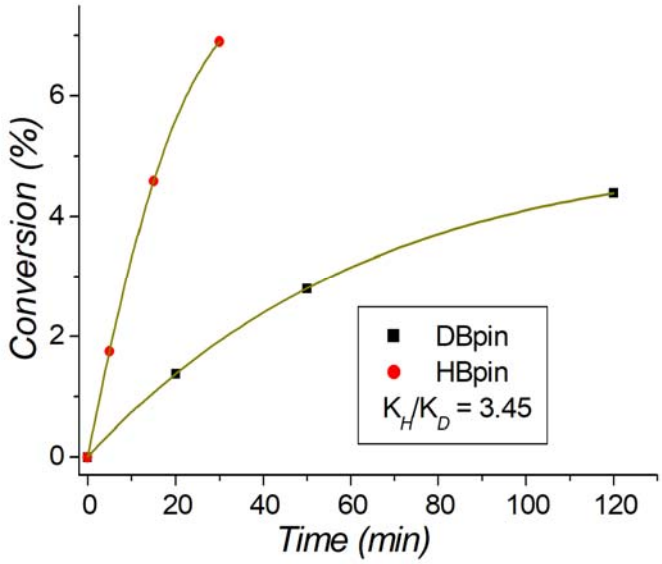

Figure S9. Plot of conversion (%) *vs*. time (min) in the reaction of *a*) *N*,*N*–diethyl–2,2,2–trifluoroacetamide and HBpin (2.0 equiv.) and *b*) *N*,*N*–diethyl–2,2,2–trifluoroacetamide and DBpin (2.0 equiv.) catalyzed by 3 mol% of complex **Th1** at 70 ºC.

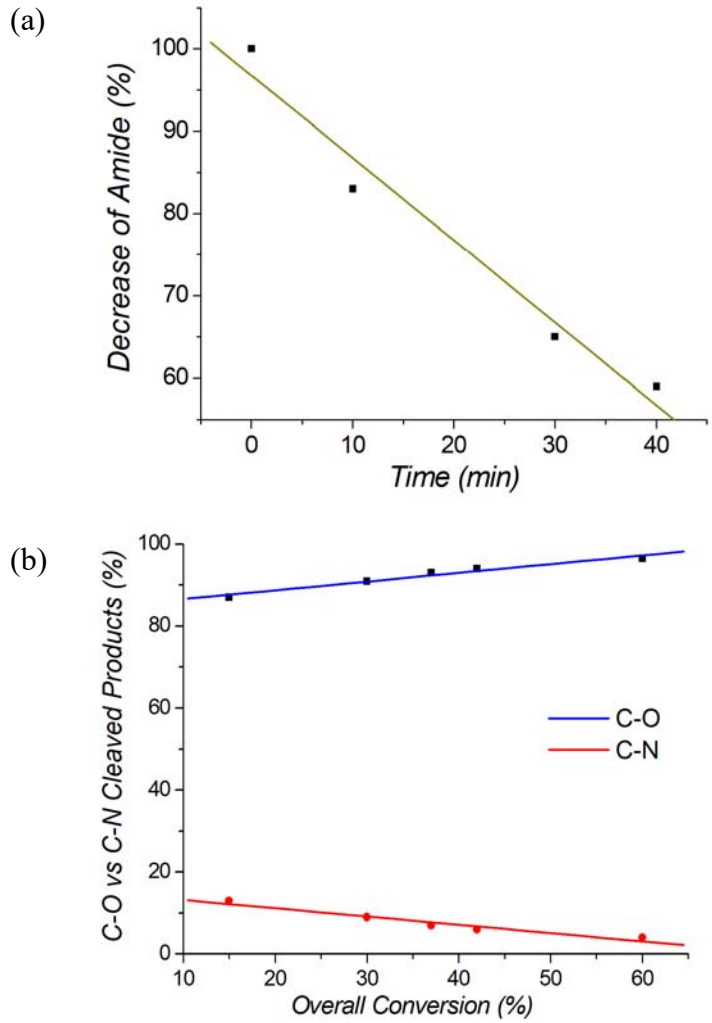

Figure S10. a) Plot of decrease (%) of *N*,*N*-dimethylbenzamide vs time, and b) Plot of C-O/C-N cleaved products (%) *vs.* overall conversion (%) in the reaction of *N*,*N*-dimethylbenzamide + HBpin (2 equiv.) in presence of **Th1** (3 mol%) 70 °C.

N,*N*–diethyl–2,2,2–trifluoroacetamide (0.1879 mmol) HBpin (0.3758 mmol) **Th1** (0.0093 mmol)				
k	ln(k/T)	ln(k)	T (K)	$1/T \times 10^{-3}$
2.62×10^{-5}	− 16.33	− 10.55	323	3.096
3.53×10^{-5}	− 16.06	− 10.25	333	3.003
6.52×10^{-5}	− 15.47	− 9.64	343	2.915
10.73×10^{-5}	− 15.01	− 9.14	353	2.833
12.64×10^{-5}	− 14.87	− 8.98	363	2.755
ln(k/T) vs 1/T			ln(k) vs 1/T	
Intercept	− 1.92 ± 1.34		Intercept	4.88 ± 1.35
Slope	− 4666.75 ± 459.04		Slope	− 4994.91 ± 461.78

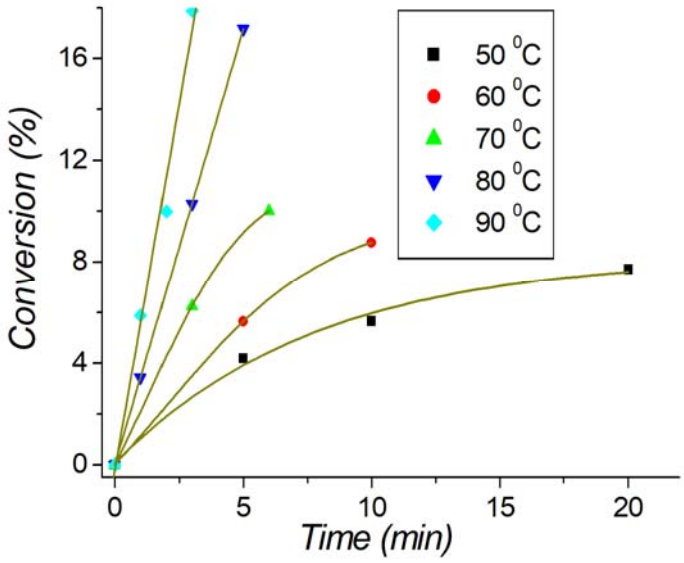

Figure S11. Plot of conversion (%) vs time (min) at different temperatures (50-90 ºC)in the reaction of *N*,*N*–diethyl–2,2,2–trifluoroacetamide and HBpin catalyzed by complex **Th1**.

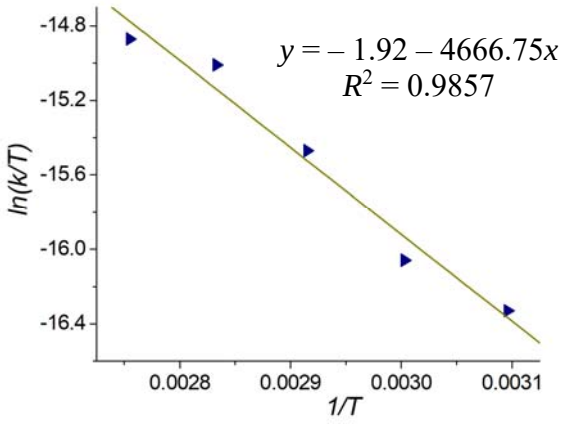

Figure S12. Eyring plot of ln(*k*/T) vs 1/T for hydroboration of *N*,*N*–diethyl–2,2,2–trifluoroacetamide by catalyst **Th1**.

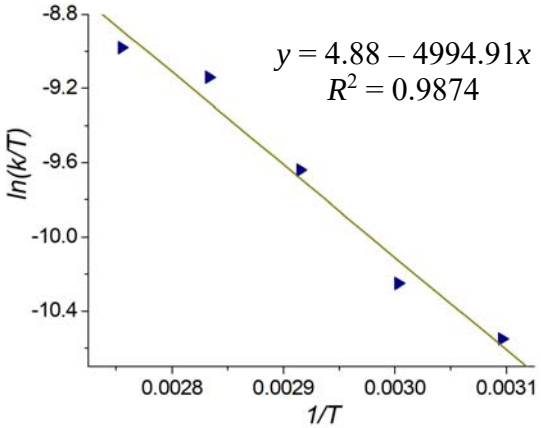

Figure S13. Arrhenius plot of ln(*k*) vs 1/T for hydroboration of *N*,*N*–diethyl–2,2,2–trifluoroacetamide by catalyst **Th1**.

2.3. Hydroboration of secondary amide: In a J. Young NMR tube, typical amount of precatalyst **Th1** (0.94 ~ 7.51 μmol), *N*-methylacetamide (0.047 ~ 0.188 mmol), HBpin (0.094 ~ 1.50 mmol), and total volume was made up to 0.6 mL with C_6D_6 in the glove box and then the tube was sealed. The NMR tube was taken out of the glove box and freeze it in an ice bath until the ^{1}H NMR experiment began at 70° C. All the experiments were done by changing either one substrate or the catalyst while keeping the other reagents constant, and the data was collected up to 10–15% conversion. The product concentrations were measured by the area ratio of starting material and product from the in situ formed reaction mixture. Reaction rates were determined by least-square fit of the initial product concentration versus time, and the plots were shown in Figures S14–S21. Activation parameters including enthalpy ($\Delta H^{\neq}$), entropy ($\Delta S^{\neq}$) and activation energy (E_a) were calculated from kinetic data using Eyring and Arrhenius plots. In a typical sample, the J. Young tube was loaded with desired amount of catalyst **Th1** (0.188 μmol), *N*-methylacetamide (0.188 mmol), HBpin (0.564 mmol) and sealed. Then the sample was inserted into Bruker Advance 300 spectrometer which had been previously set to the desired temperature (50 °C, 60 °C, 70 °C, 80 °C, 90 °C). The data was collected up to 10–15% conversion. Reaction rates were determined by the least square fit of initial product concentration versus time, and Eyring and Arrhenius plots were shown in Figures S22–S24. Enthalpy ($\Delta H^{\neq}$), entropy ($\Delta S^{\neq}$) and activation energy (E_a) were calculated from the slope and intercept of the least-square fit.

N-methylacetamide (0.1878 mmol) HBpin (0.5637 mmol)			
Rate (mmol/sec) × 10^{-5}	**Th1** (mmol) × 10^{-3}	ln(Rate)	ln(**Th1**)
0.6323	0.9393	− 11.97	− 6.97
1.4844	1.878	− 11.12	− 6.28
2.994	3.757	− 10.42	− 5.58
3.925	5.6357	− 10.14	− 5.18
6.201	7.514	− 9.69	− 4.89
		Slope	1.0539

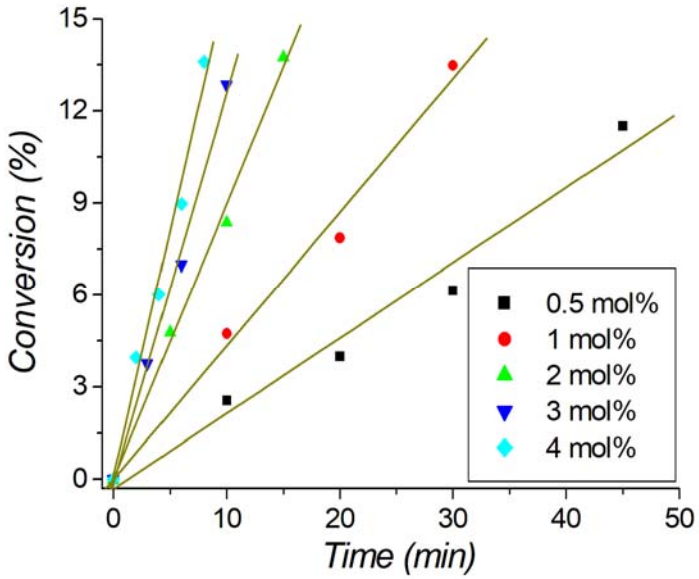

Figure S14. Plot of conversion (%) vs time (min) at different **Th1** concentrations in the reaction of *N*-methylacetamide and HBpin catalyzed by complex **Th1** at 70 ºC.

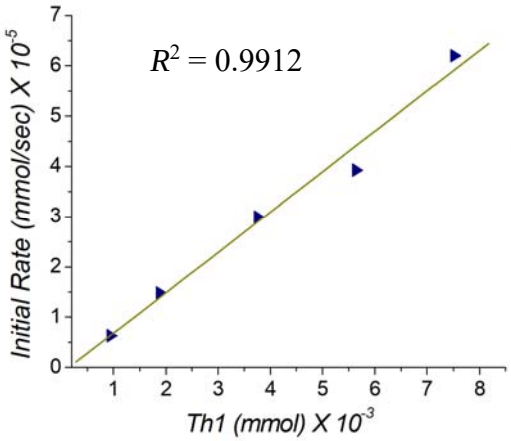

Figure S15. Plot of Initial rate *vs.* [**Th1**] in the reaction of *N*-methylacetamide and HBpin catalyzed by complex **Th1** at 70 ºC.

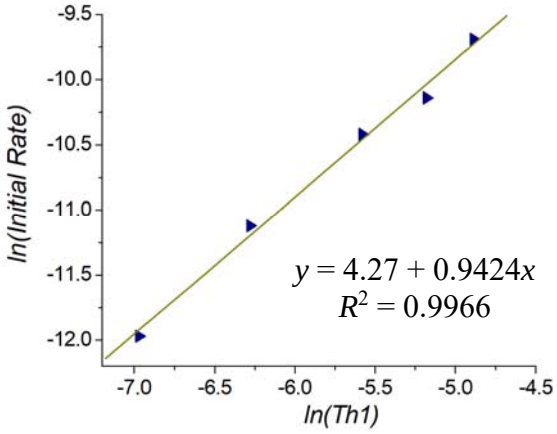

Figure S16. Plot of ln[Initial Rate] *vs.* ln[**Th1**].

Th1 (0.00235 mmol) N-methylacetamide (0.4 mmol)			
Rate (mmol/sec) × 10^{-5}	HBpin (mmol)	ln(Rate)	ln(HBpin)
1.43	0.08	− 11.16	− 2.53
2.76	0.16	− 10.49	− 1.83
3.35	0.20	− 10.30	− 1.61
4.64	0.28	− 9.97	− 1.27
5.77	0.35	− 9.76	− 1.05
		Slope	

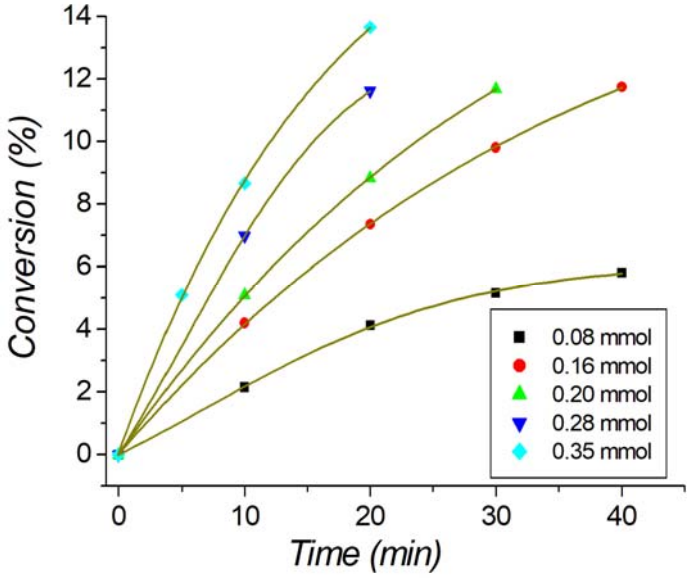

Figure S17. Plot of conversion (%) vs time (min) at different HBpin concentrations in the reaction of *N*-methylacetamide and HBpin catalyzed by complex **Th1** at 70 ºC.

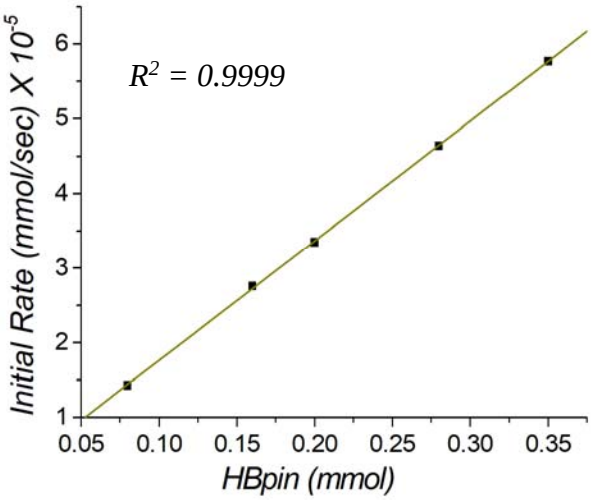

Figure S18. Plot of Initial rate *vs*. [HBpin] in the reaction of *N*-methylacetamide and HBpin catalyzed by complex **Th1** at 70 ºC.

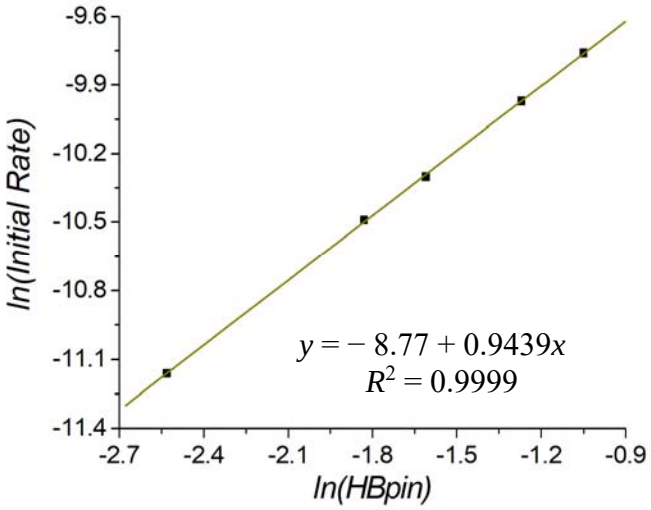

Figure S19. Plot of ln[Initial Rate] *vs*. ln[HBpin].

Th1 (0.001878 mmol) HBpin (0.8 mmol)	
Rate (mmol/sec) × 10^{-5}	*N*-methylacetamide (mmol)
12.5	0.08
11.88	0.16
14.4	0.24
12.82	0.32

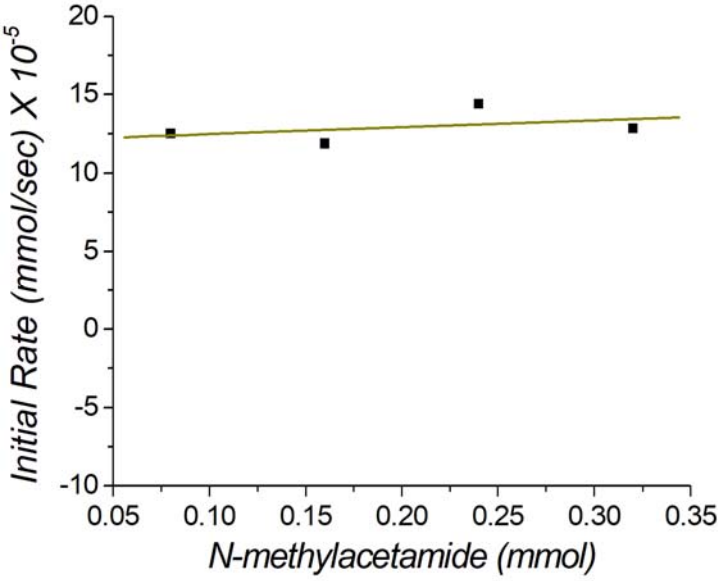

Figure S20. Plot of Initial rate *vs*. [*N*-methylacetamide] in the reaction of *N*-methylacetamide and HBpin catalyzed by complex **Th1** at 70 ºC.

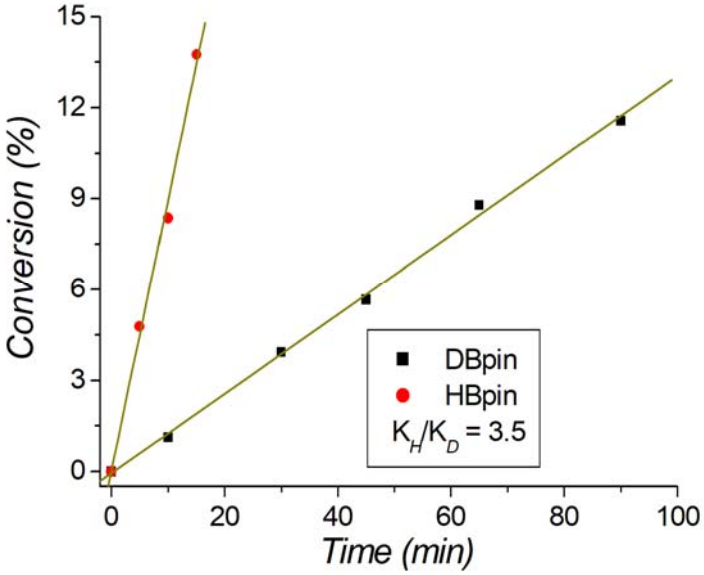

Figure S21. Plot of conversion (%) *vs*. time (min) in the reaction of *a*) *N*-methylacetamide and HBpin (3.0 equiv.) and *b*) *N*-methylacetamide and DBpin (3.0 equiv.) catalyzed by 1 mol% of complex **Th1** at 70 ºC.

N-methylacetamide (0.1878 mmol) HBpin (0.5637 mmol) **Th1** (0.001878 mmol)				
k	ln(k/T)	ln(k)	T (K)	1/T × 10^{-3}
0.2046 × 10^{-3}	− 14.27	− 8.49	323	3.096
0.4609 × 10^{-3}	− 13.49	− 7.68	333	3.003
0.80 × 10^{-3}	− 12.96	− 7.13	343	2.915
2.62 × 10^{-3}	− 11.81	− 5.94	353	2.833
4.667 × 10^{-3}	− 11.27	− 5.37	363	2.755
ln(k/T) vs 1/T			ln(k) vs 1/T	
Intercept	13.67 ± 1.08		Intercept	20.53 ± 1.10
Slope	− 9037.99 ± 370.39		Slope	− 9390.60 ± 375.87

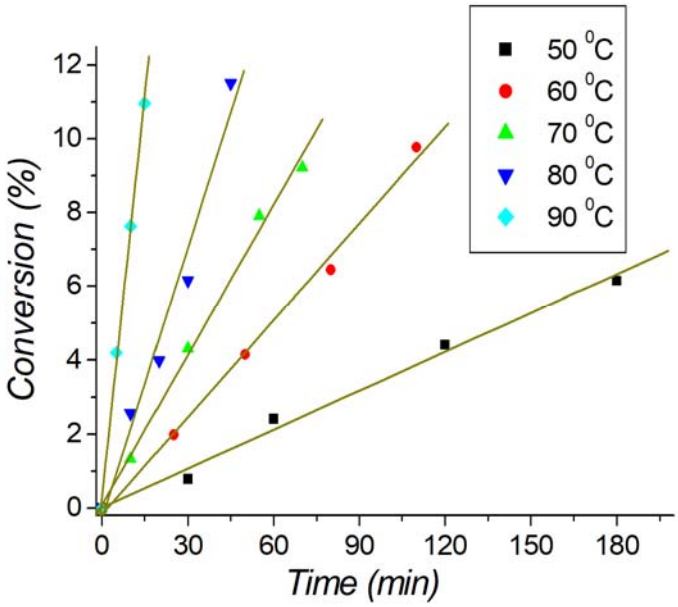

Figure S22. Plot of conversion (%) vs time (min) at different temperatures (50-90 °C) in the reaction of *N*-methylacetamide and HBpin catalyzed by complex **Th1**.

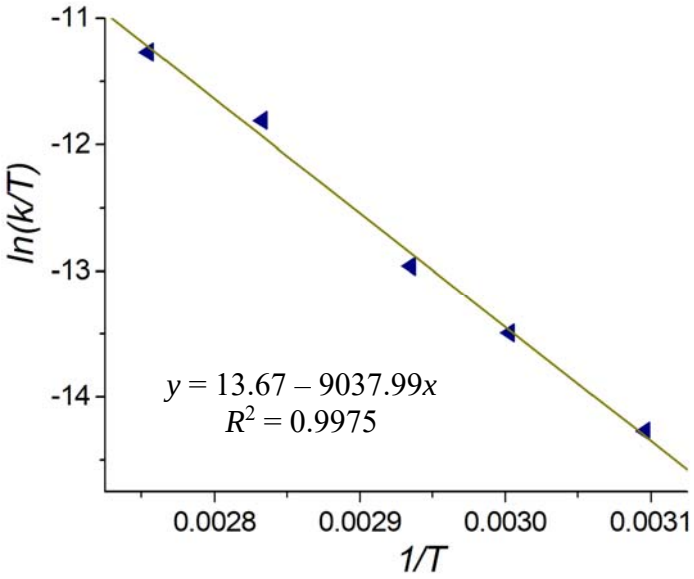

Figure S23. Eyring plot of ln(*k*/T) vs 1/T for hydroboration of *N*-methylacetamide by catalyst **Th1**.

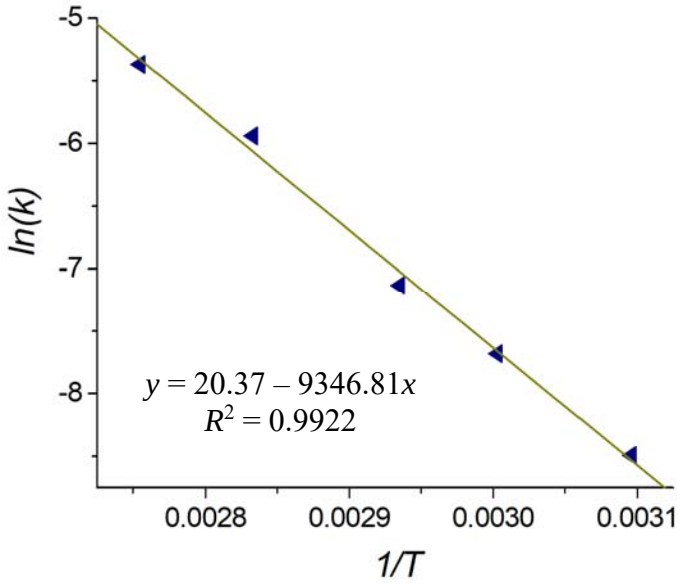

Figure S24. Arrhenius plot of ln(*k*) vs 1/T for hydroboration of *N*-methylacetamide by catalyst **Th1**.

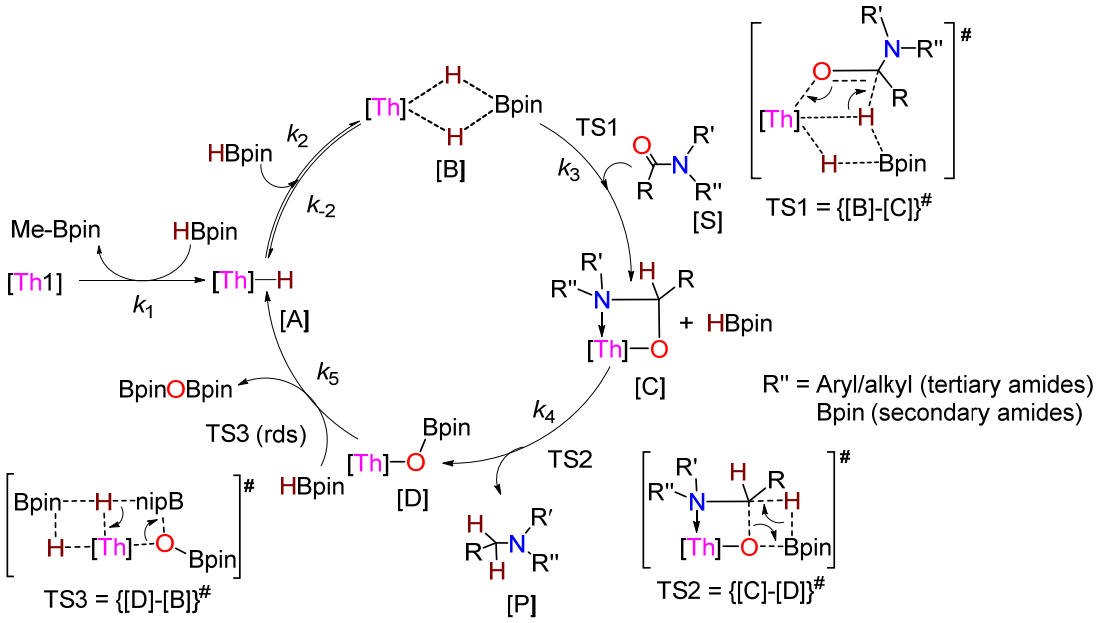

Scheme S1a

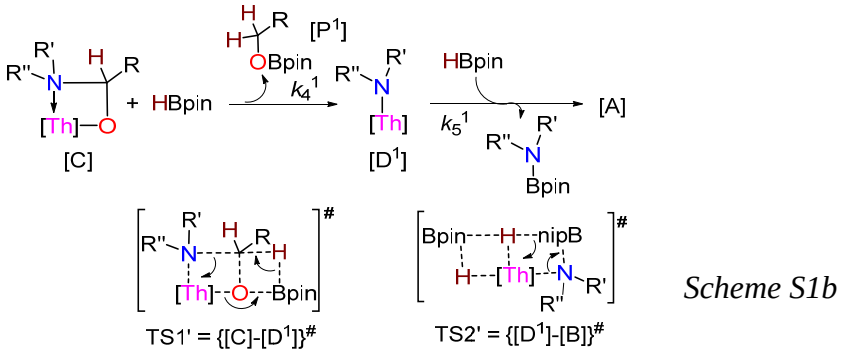

Scheme S1b

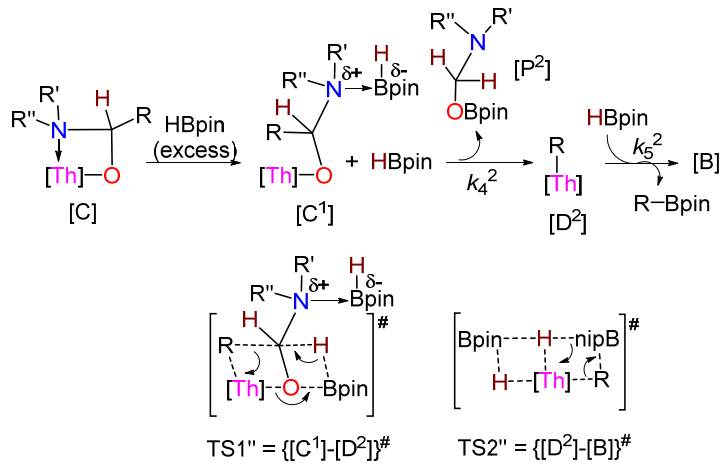

Scheme S1c

Scheme S1. Proposed mechanism of hydroboration of through a) C-O breakage pathway, b) C-N breakage pathway and c) C-C breakage pathway.

2.2. The Rate Kinetic Law for Amide Hydroboration.

According to proposed mechanism (Scheme S1), the step involving Th−O/H−B σ-bond metathesis is the rate-determining step (k_5) based on the experimental results. Therefore, we can assume a steady-state approximation giving the following rate equations:

$$\partial p/\partial t = k_5\,[D]\,[HBpin]^2 \quad (1)$$

$$\partial[D]/\partial t = -\,k_5\,[D]\,[HBpin]^2 + k_4\,[C]\,[HBpin] = 0$$

$$k_4\,[C]\,[HBpin] = k_5\,[D]\,[HBpin]^2 \quad (2)$$

$$\partial[C]/\partial t = k_3\,[B]\,[S] - k_4\,[C]\,[HBpin] = 0$$

$$[C]\,[HBpin] = k_3\,[B]\,[S] / k_4 \quad (3)$$

By substitution of eq^n (3) into eq^n (2) we get the following rate equation:

$$k_5\,[D]\,[HBpin]^2 = k_3\,[B]\,[S] \quad (4)$$

$$\partial[B]/\partial t = k_2\,[A]\,[HBpin] - k_{-2}\,[B] - k_3\,[B]\,[S] + k_5\,[D]\,[HBpin]^2 = 0 \ldots.(5)$$

$$k_2 >>>> k_{-2}$$

$$k_2\,[A]\,[HBpin] - k_3\,[B]\,[S] + k_5\,[D]\,[HBpin]^2 = 0 \quad (6)$$

$$k_2\,[A]\,[HBpin] + k_5\,[D]\,[HBpin]^2 = k_3\,[B]\,[S] \quad (7)$$

$$k_2 >>>> k_5$$

$$k_2\,[A]\,[HBpin] = k_3\,[B]\,[S] \quad (8)$$

By substitution of eq^n (8) into eq^n (4) we get the following rate equation:

$$k_5\,[D]\,[HBpin]^2 = k_2\,[A]\,[HBpin] \quad (9)$$

$$\partial p/\partial t = k_2\,[A]\,[HBpin] \quad (12)$$

$$\partial[A]/\partial t = k_1\,[Th1]\,[HBpin]^2 - k_2\,[A]\,[HBpin] = 0$$

$$k_2\,[A]\,[HBpin] = k_1\,[Th1]\,[HBpin] \quad (13)$$

By substitution of eq^n (13) into eq^n (12) we get the following rate equation:

$$\partial p/\partial t = k_1\,[Th1]\,[HBpin] \quad (14)$$

3. Stoichiometric studies

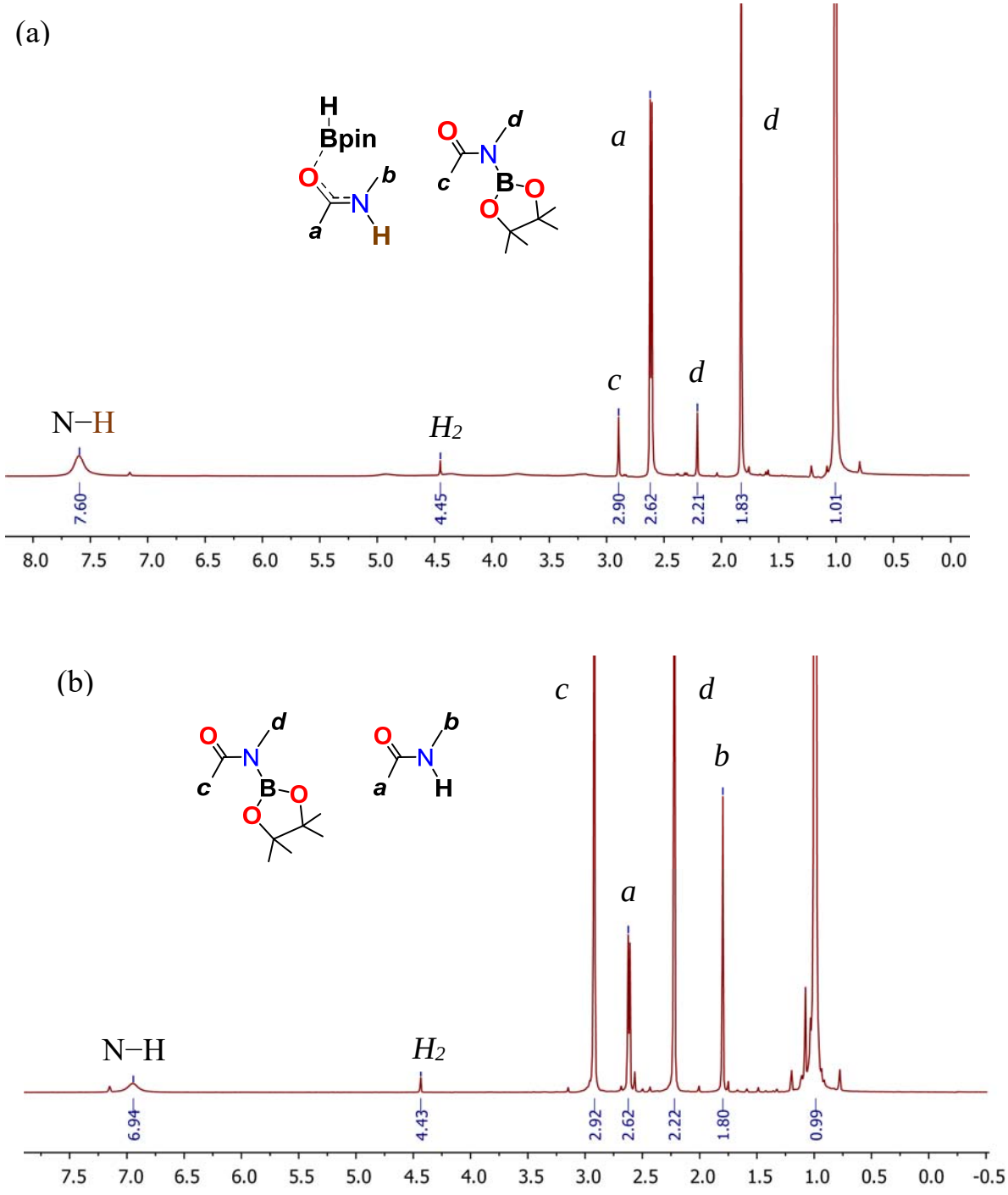

Figures S25. ^{1}H NMR of *a*) $CH_3CONHCH_3$ + HBpin (1 equiv.) in C_6D_6 after 6 h at room temperature and *b*) $CH_3CONHCH_3$ + HBpin (1 equiv.) in C_6D_6 after 12 h at 70 °C.

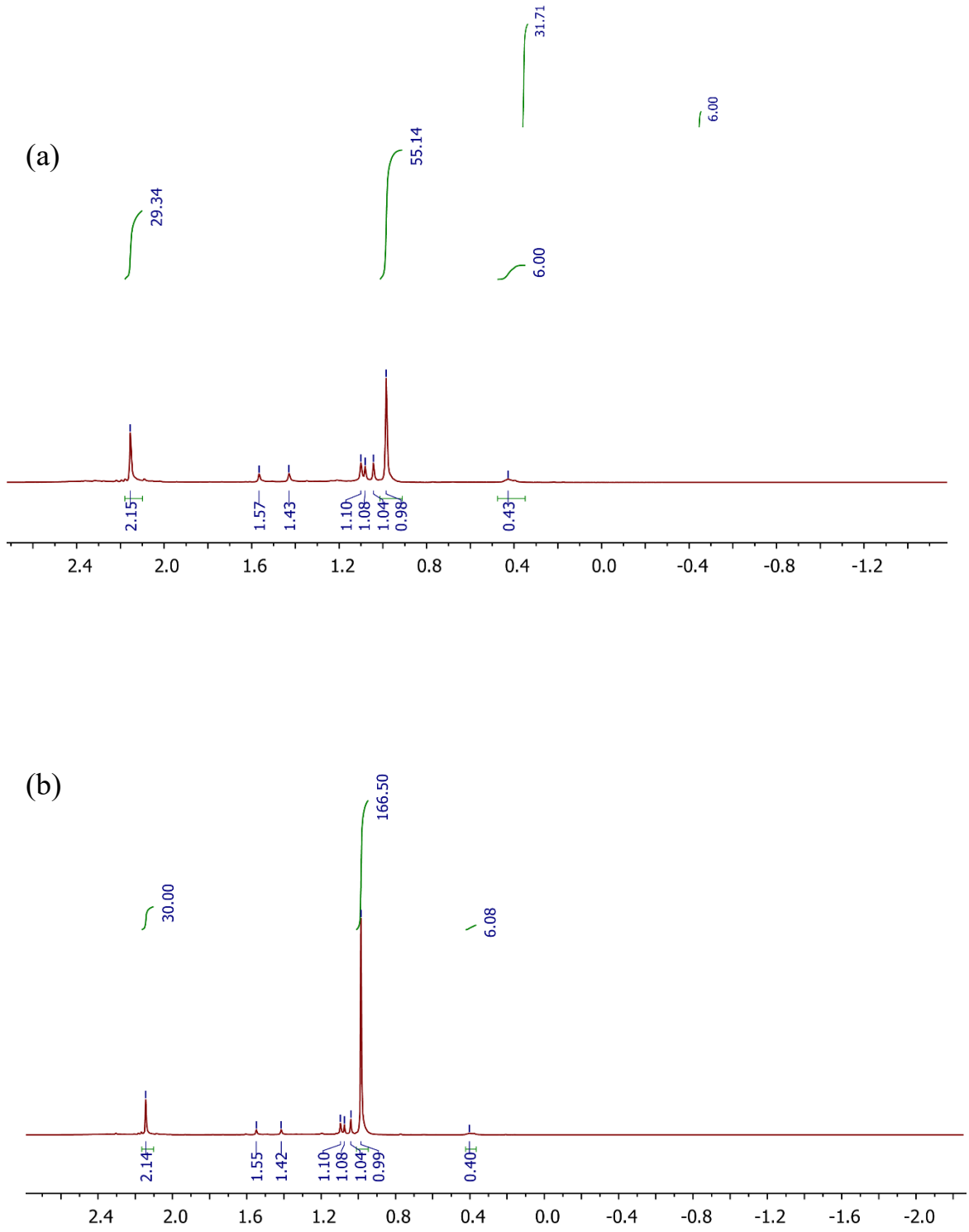

Figures S27. ^{1}H NMR of *a*) **Th1** + HBpin (5 equiv.) and *b*) **Th1** + HBpin (10 equiv.) at 25 ^{o}C in C_6D_6.

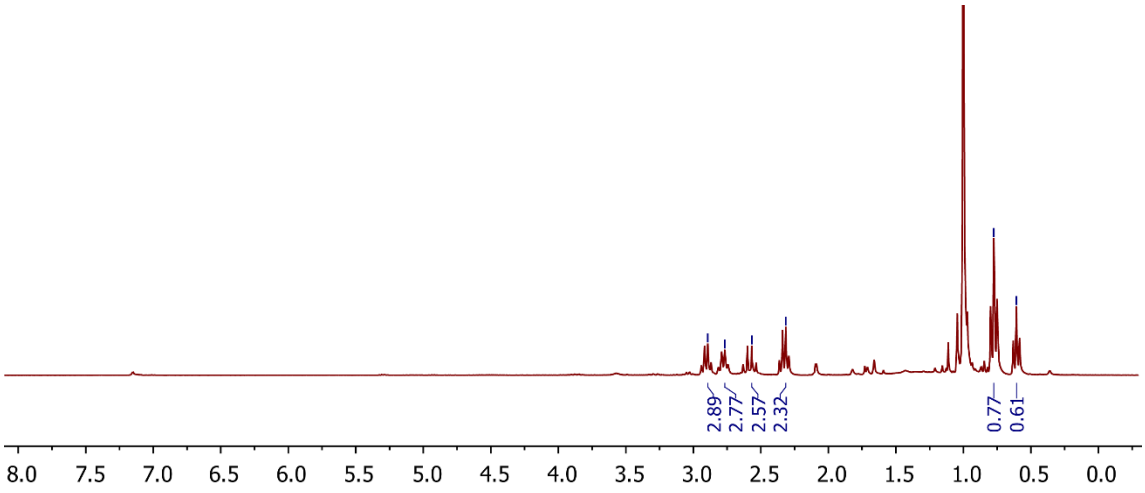

Figures S28. ^{1}H NMR of reaction mixtures of N,N–diethyl–2,2,2–trifluoroacetamide + HBpin (1 equiv.) catalysed by **Th1** (3 mol%) at 70 ºC in C_6D_6.

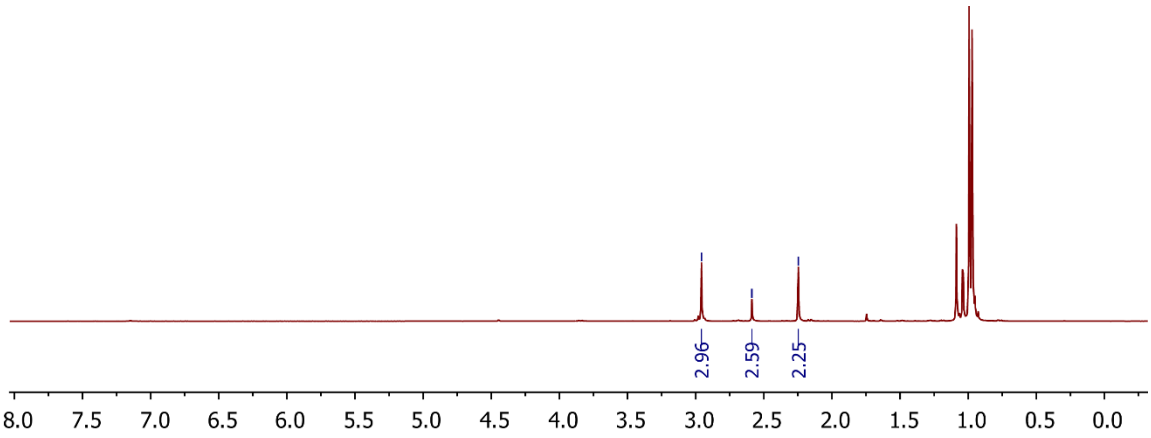

Figures S29. ^{1}H NMR of reaction mixtures of N–methylacetamide + HBpin (1 equiv.) catalyst **Th1** at 70 ºC in C_6D_6.

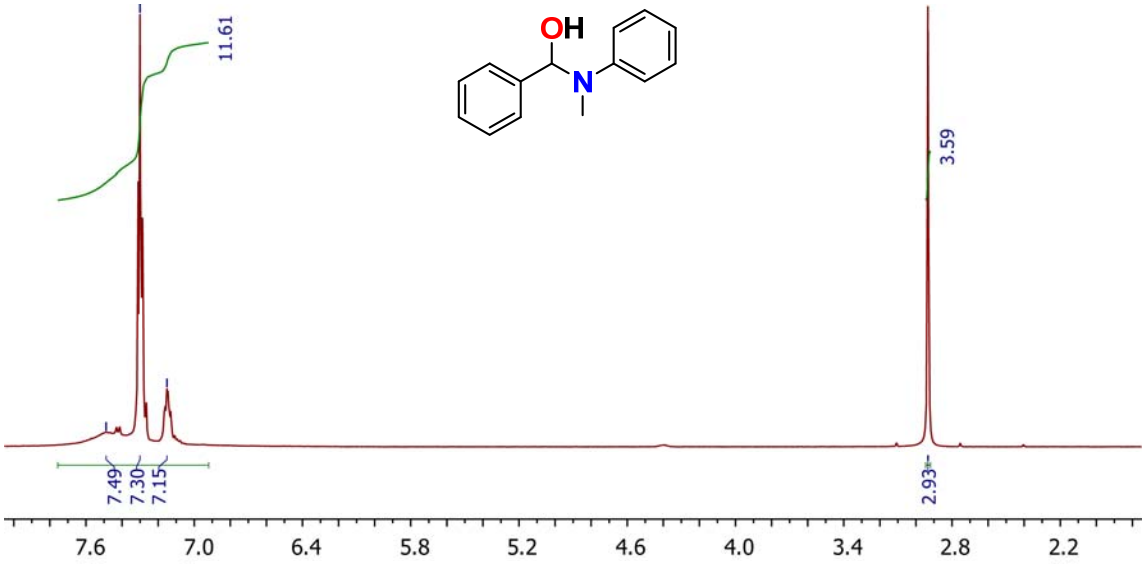

Figure S30. ^{1}H NMR of hemiaminal compound in $CDCl_3$.

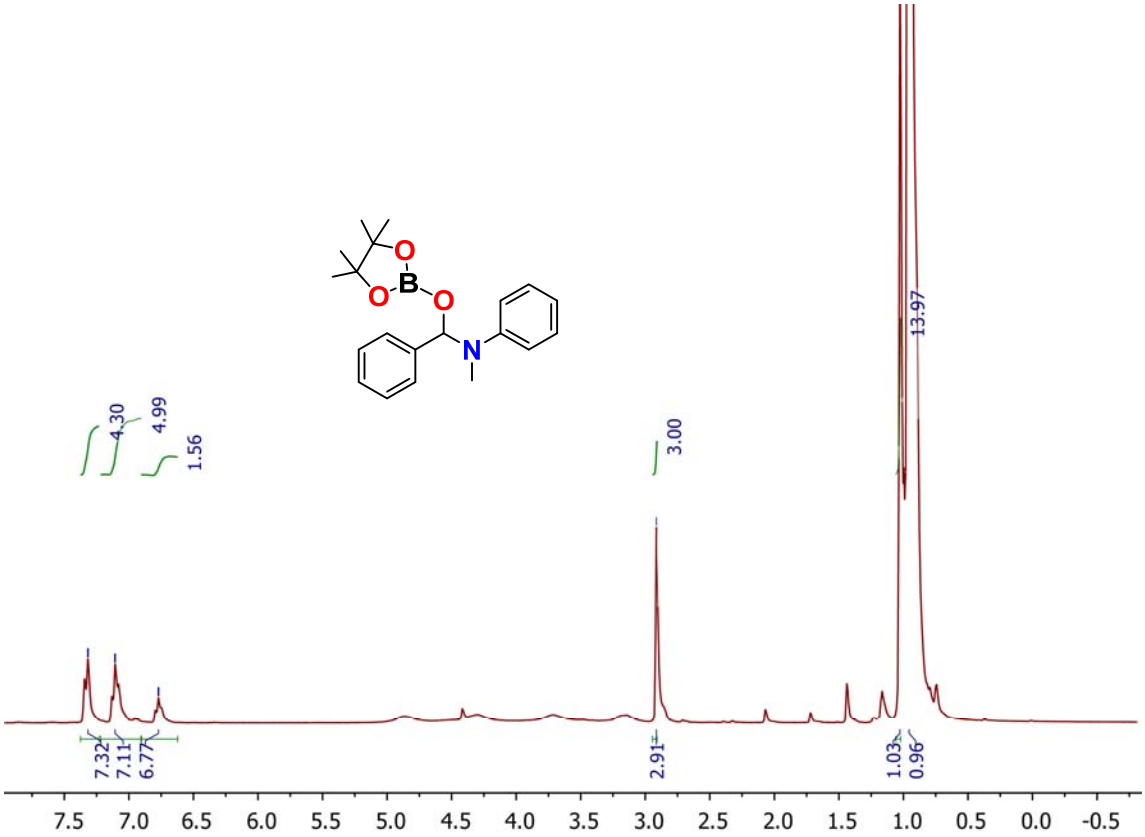

Figure S31. ^{1}H NMR of {hemiaminal + HBpin (10 equiv.)} in $CDCl_3$ at 70 ºC after 24 h.

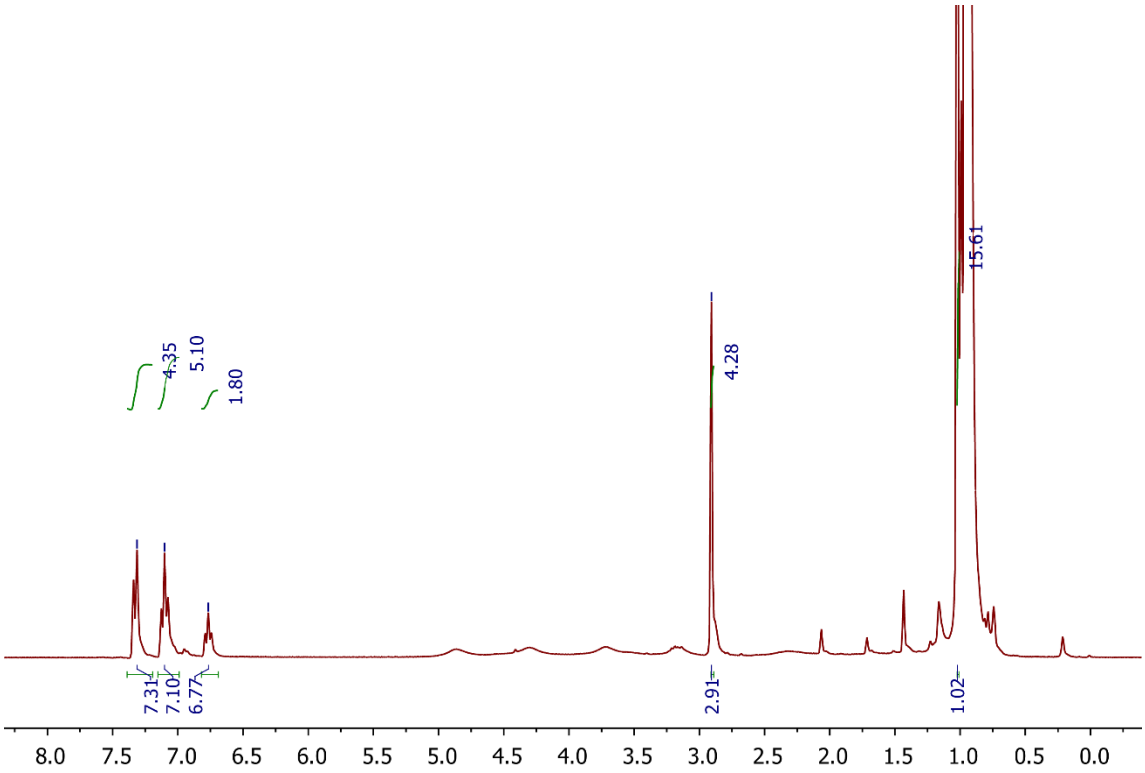

Figure S32. ^{1}H NMR of {hemiaminal + HBpin (10 equiv.)} in C_6D_6 at 70 °C after 24 h in presence of **Th1** (5 mol%).

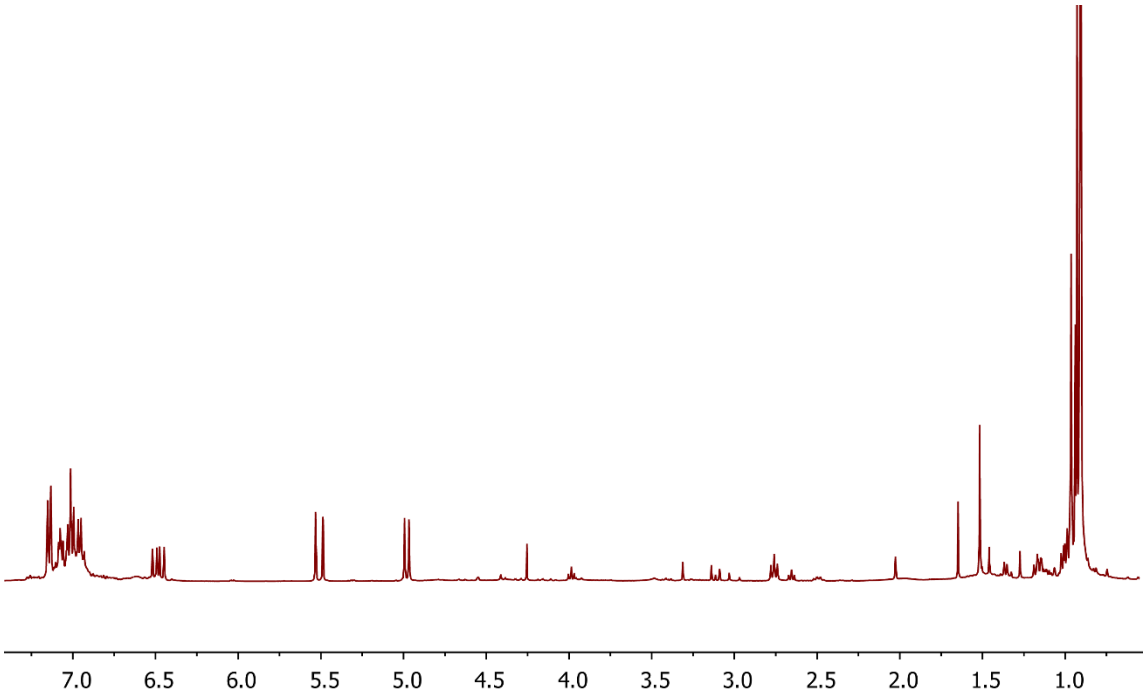

Figure S33. ^{1}H NMR of styrene hydroboration reaction using HBpin (5 equiv.) and 5 mol% of **Th1** in C_6D_6 at 70 °C after 24 h.

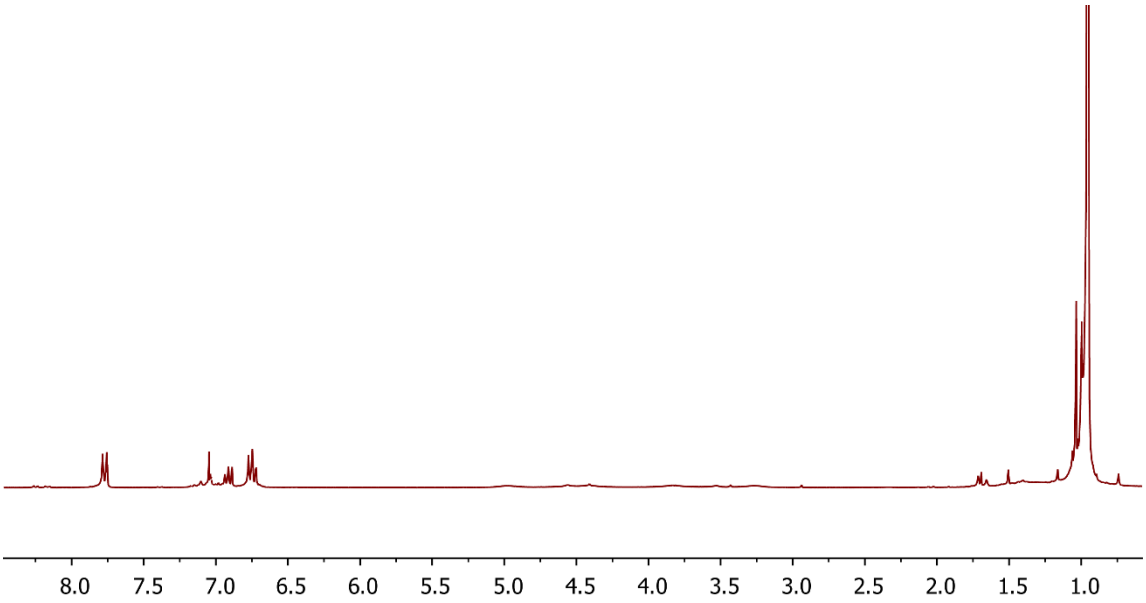

Figure S34. ^{1}H NMR of nitrobenzene hydroboration reaction using HBpin (5 equiv.) and 5 mol% of **Th1** in C_6D_6 at 70 ºC after 24 h.

4. IR studies

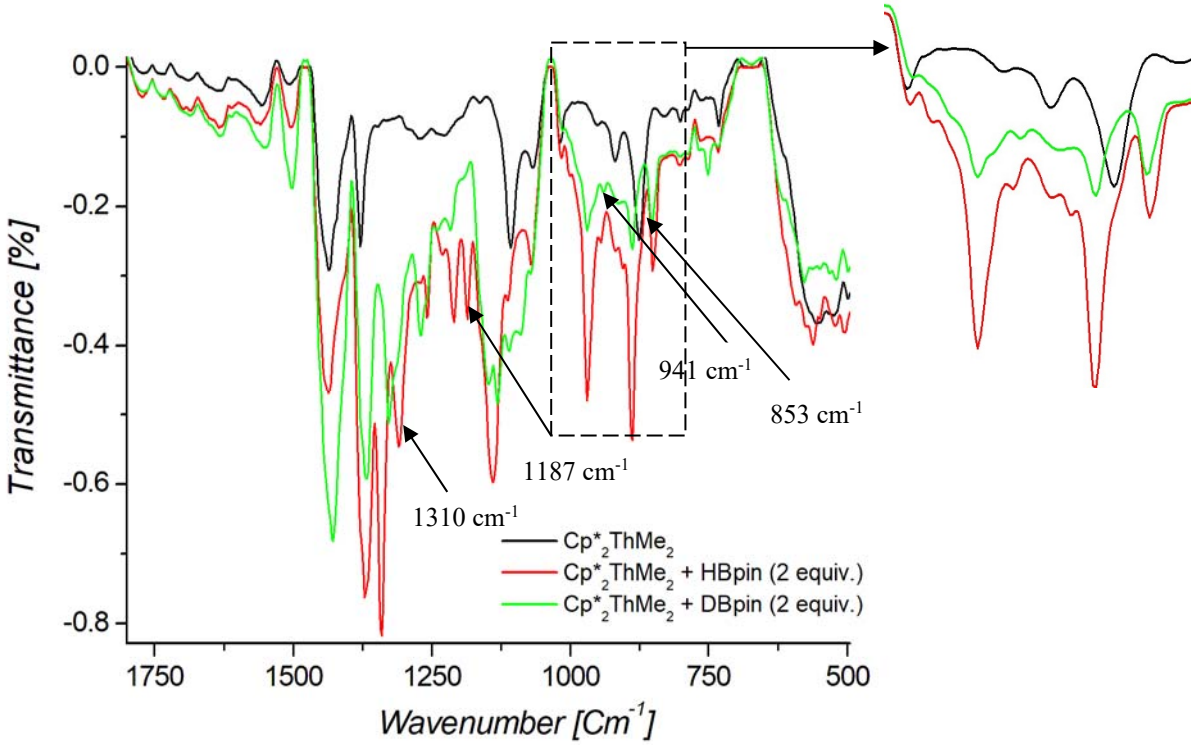

Figures S35 IR spectra of *a*) **Th1** ($Cp^*_2ThMe_2$) (black), *b*) **Th1** + HBpin (2 equiv.) (red) and *c*) **Th1** + DBpin (2 equiv.) (green) at 25 ºC in C_6H_6.

5.1. General procedure for amide hydroboration reaction

A J. Young NMR tube was loaded with *i*) aliphatic secondary amides (1 mmol), HBpin (3 mmol), **Th1** (0.01 mmol), or, *ii*) other secondary amides (1 mmol), HBpin (3 mmol), **Th1** (0.03 mmol), or, *iii*) tertiary amides (1 mmol), HBpin (2 mmol), **Th1** (0.03 mmol), or, *iv*) primary amides (1 mmol), HBpin (5 mmol), **Th1** (0.01 mmol) and the reaction was immediately diluted to 600 µL with C_6D_6. Samples were taken out of the glove box and the reaction progress was monitored by ^1H NMR spectroscopy. The crude mixtures were analyzed using ^1H NMR, ^{13}C NMR, and mass spectroscopy. The values for *2aa*,[6a] *2bb*,[6a] *2dd*,[6c] *2oo*,[6b] *2pp*,[6a] *2qq*,[6a] *2rr*,[6c] *2ss*,[6d] *2tt*,[6e] *2uu*,[6c] *2vv*,[6f] *2ww*,[6g] and *2xx*[6h] were compared to previous literature.

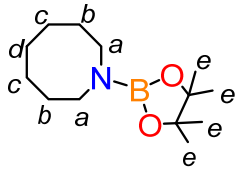

***2cc*, Entry 3, Table 2**. ^1H NMR (400 MHz, C_6D_6, 294 K): δ 3.11 (t, J = 4 Hz, 4H), 1.53 (m, 6H), 1.44 (m, 4H), 1.10 (s, 12H) ppm, $^{13}C\{^1H\}$ NMR (100 MHz, C_6D_6, 294 K): δ 81.5, 46.9, 31.3, 27.2, 24.5 ppm, $^{11}B\{^1H\}$ NMR (128.38 MHz, C_6D_6, 294 K): δ 24.42 ppm. HRMS: m/z, 240.22 $[M+H]^+$.

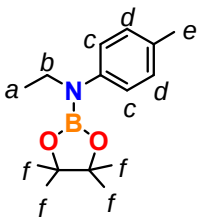

***2ff*, Entry 6, Table 2**. ^1H NMR (400 MHz, C_6D_6, 294 K): δ 7.31 (d, J = 8 Hz, 2H), 7.00 (d, J = 8 Hz, 2H), 3.59 (q, J = 8 Hz, 2H), 2.12 (s, 3H), 1.12 (t, J = 8 Hz, 3H), 1.08 (s, 12H) ppm, $^{13}C\{^1H\}$ NMR (100 MHz, C_6D_6, 294 K): δ 143.5, 130.6, 129.2, 121.8, 82.1, 41.9, 24.6, 20.3, 15.3 ppm, $^{11}B\{^1H\}$ NMR (128.38 MHz, C_6D_6, 294 K): δ 28.47 ppm. HRMS: m/z, 262.19 $[M+H]^+$.

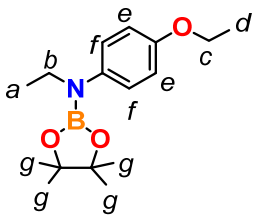

***2gg*, Entry 7, Table 2**. ^1H NMR (400 MHz, C_6D_6, 294 K): δ 7.26 (d, J = 8 Hz, 2H), 6.80 (d, J = 8 Hz, 2H), 3.60 (m, 4H), 1.11 (m, 3H), 1.09 (s, 12H), 1.04 (m, 3H) ppm, $^{13}C\{^1H\}$ NMR (100 MHz, C_6D_6, 294 K): δ 154.7, 139.0, 123.8, 114.6, 82.1, 63.1, 42.5, 24.4, 15.4, 14.6 ppm, $^{11}B\{^1H\}$ NMR (128.38 MHz, C_6D_6, 294 K): δ 28.46 ppm. HRMS: m/z, 292.21 $[M+H]^+$.

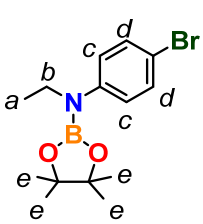

***2hh*, Entry 8, Table 2.** ^1H NMR (400 MHz, C_6D_6, 294 K): δ 7.24 (d, J = 8 Hz, 2H), 7.08 (d, J = 8 Hz, 2H), 3.41 (q, J = 8 Hz, 2H), 1.04 (s, 12H), 1.00 (t, J = 8 Hz, 3H) ppm, $^{13}C\{^1H\}$ NMR (100 MHz, C_6D_6, 294 K): δ 145.1, 131.4, 122.4, 113.7, 82.4, 41.3, 24.3, 14.8 ppm, $^{11}B\{^1H\}$ NMR (128.38 MHz, C_6D_6, 294 K): δ 28.45 ppm. HRMS: m/z, 326.09 $[M+H]^+$.

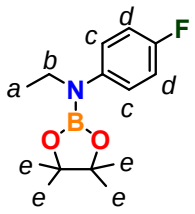

***2ii*, Entry 9, Table 2**. ^{1}H NMR (400 MHz, C_6D_6, 294 K): δ 7.18-7.16 (m, 2H), 6.85 (t, J = 8 Hz, 2H), 3.48 (q, J = 8 Hz, 2H), 1.08 (s, 12H), 1.04 (m, 3H) ppm, ^{13}C{^{1}H} NMR (100 MHz, C_6D_6, 294 K): δ 159.6, 157.1, 142.0, 122.87 (d, J = 28 Hz), 114.86 (d, J = 84 Hz), 82.3, 42.0, 24.6, 15.3 ppm, ^{11}B{^{1}H} NMR (128.38 MHz, C_6D_6, 294 K): δ 28.45 ppm. HRMS: m/z, 266.19 $[M+H]^+$.

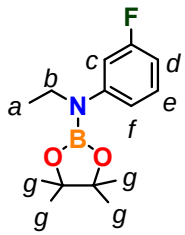

***2jj*, Entry 10, Table 2**. ^{1}H NMR (400 MHz, C_6D_6, 294 K): δ 7.29 (d, J = 12 Hz, 1H), 7.07 (d, J = 8 Hz, 1H), 6.94 (q, J = 8 Hz, 1H), 6.55 (t, J = 8 Hz, 1H), 3.44 (q, J = 8 Hz, 2H), 1.04-1.01 (m, 15H) ppm, ^{13}C{^{1}H} NMR (100 MHz, C_6D_6, 294 K): δ 164.8, 162.4, 148.0 (d, J = 40 Hz), 129.5 (d, J = 40 Hz), 115.3 (d, J = 8 Hz), 107.4 (dd, J = 76 Hz, J = 24 Hz), 82.5, 41.1, 24.2, 14.8 ppm, ^{11}B{^{1}H} NMR (128.38 MHz, C_6D_6, 294 K): δ 28.46 ppm. HRMS: m/z, 266.17 $[M+H]^+$.

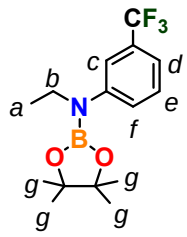

***2kk*, Entry 11, Table 2**. ^{1}H NMR (400 MHz, C_6D_6, 294 K): δ 7.77 (s, 1H), 7.38 (d, J = 8 Hz, 1H), 7.07-6.99 (m, 2H), 3.42 (q, J = 8 Hz, 2H), 1.05 (bs, 3H), 1.04 (s, 12H) ppm, ^{13}C{^{1}H} NMR (100 MHz, C_6D_6, 294 K): δ 146.7, 130.7 (q, J = 124 Hz), 129.1, 123.2, 117.3 (q, J = 16 Hz), 116.7, (q, J = 16 Hz), 82.5, 41.09, 24.5, 14.6. ppm, ^{11}B{^{1}H} NMR (128.38 MHz, C_6D_6, 294 K): 28.44 ppm. HRMS: m/z, 316.18 $[M+H]^+$.

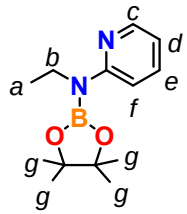

***2ll*, Entry 12, Table 2**. ^{1}H NMR (400 MHz, C_6D_6, 294 K): δ 8.29 (d, J = 4 Hz, 1H), 7.87 (d, J = 8 Hz, 1H), 7.22-7.17 (m, 1H), 6.48-6.45 (m, 1H), 4.11 (q, 2H), 1.37 (t, J = 8 Hz, 3H), 1.07 (s, 12H) ppm, ^{13}C{^{1}H} NMR (100 MHz, C_6D_6, 294 K): δ 157.7, 147.4, 136.3, 115.5, 114.6, 82.5, 39.1, 24.3, 15.8 ppm, ^{11}B{^{1}H} NMR (128.38 MHz, C_6D_6, 294 K): 25.16 ppm. HRMS: m/z, 249.18 $[M+H]^+$.

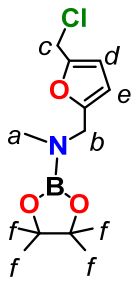

***2mm*, Entry 13, Table 2**. ^{1}H NMR (400 MHz, C_6D_6, 294 K): δ 6.79 (d, J = 4 Hz, 1H), 5.88 (d, J = 4 Hz, 1H), 4.02 (s, 3H), 3.07 (s, 4H), 1.00 (s, 12H) ppm, ^{13}C{^{1}H} NMR (100 MHz, C_6D_6, 294 K): δ 150.9, 150.0, 115.7, 111.1, 82.5, 36.7, 31.1, 24.2 ppm, ^{11}B{^{1}H} NMR (128.38 MHz, C_6D_6, 294 K): δ 28.45 ppm. HRMS: m/z, 286.18 $[M+H]^+$.

5.2. Synthetic procedure for amino-pinacol borane to amine

Following the previousy described procedure the resulted amine-borane adducts, obtained in the gram-scale reaction, have been reacted with SiO_2 and methanol and left for stirring at 60 °C for 8 h. The resulted mixture was filtered and the filtrate and other volatiles was dried in vacuum. After that the residue was subjected to neutral-Al_2O_3 chromatography and the amines were isolated by using ethyl acetate/hexane as eluent. ^{1}H NMR and ^{13}C NMR spectrum of already reported amines

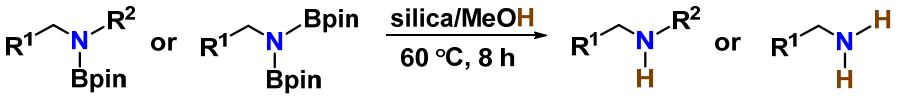

Scheme S2. Synthesis of amine-borane adduct to amine.

are compared with the previous literature (*2cc*-Bpin,[6i] *2dd*-Bpin[6c], *2ff*-Bpin,[6j] *2hh*-Bpin,[6j] *2ii*-Bpin,[6k] *2jj*-Bpin,[6l] *2ll*-Bpin,[6m] *2oo*-Bpin,[6n] *2ww*-Bpin,[6o]). ^{1}H NMR and ^{13}C NMR spectrum of new amine compounds are provided below and in Figures S77-92.

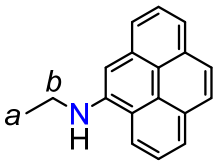

***2ee-Bpin*, Entry 3, Table 2**. ^{1}H NMR (400 MHz, C_6D_6, 294 K): δ 8.06-7.98 (m, 5H), 7.90 (t, J = 8 Hz, 2H), 7.76 (d, J = 8 Hz, 1H), 7.36 (d, J = 8 Hz, 1H), 4.94 (br, NH), 3.50 (q, J = 8 Hz, 2H), 1.48 (t, J = 8 Hz, 3H) ppm, ^{13}C{^{1}H} NMR (100 MHz, C_6D_6, 294 K): δ 132.4, 131.7, 127.8, 126.4, 126.0, 125.9, 125.87, 125.7, 123.9, 123.3, 119.4, 116.6, 39.3, 14.9 ppm, HRMS: m/z, 246.12 $[M+H]^+$.

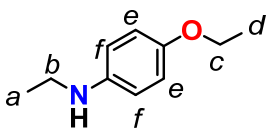

***2gg-Bpin*, Entry 7, Table 2**. ^{1}H NMR (400 MHz, C_6D_6, 294 K): δ 6.78 (d, J = 8 Hz, 2H), 6.58 (d, J = 8 Hz, 2H), 3.96 (q, J = 8 Hz, 2H), 3.11 (q, J = 8 Hz, 2H), 1.37 (t, J = 8 Hz, 3H), 1.24 (t, J = 8 Hz, 3H) ppm, ^{13}C{^{1}H} NMR (100 MHz, C_6D_6, 294 K): δ 151.4, 142.8, 115.8, 114.1, 64.2, 39.5, 15.1 ppm. HRMS: m/z, 166.12 $[M+H]^+$.

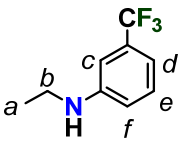

***2kk-Bpin*, Entry 11, Table 2**. ^{1}H NMR (400 MHz, C_6D_6, 294 K): δ 7.78 (s, 1H), 7.73 (d, J = 8 Hz, 1H), 7.44 (d, J = 8Hz, 1H), 7.36 (d, J = 8 Hz, 1H), 7.32 (br, NH, 1H), 2.20 (s, 2H), 1.16 (s, 3H) ppm, ^{13}C{^{1}H} NMR (75 MHz, C_6D_6, 294 K): δ 138.2, 129.5, 122.7 (m), 120.7 (m), 118.3, 116.3 (m), 36.6, 24.5. HRMS: m/z, 190.08 $[M+H]^+$.

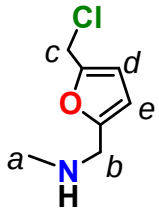

***2mm-Bpin*, Entry 13, Table 2**. ^{1}H NMR (400 MHz, C_6D_6, 294 K): δ 7.01 (d, J = 4 Hz, 1H), 6.43 (d, J = 4 Hz, 1H), 6.36 (br, NH, 1H), 4.54 (s, 2H), 2.96 (d, J = 4Hz, 3H), 2.94 (d, J = 4 Hz, 2H) ppm, ^{13}C{^{1}H} NMR (75 MHz, C_6D_6, 294 K): δ 114.7, 114.4, 111.7, 111.5, 66.3, 36.8, 25.8 ppm. HRMS: m/z, 160.05 $[M+H]^+$.

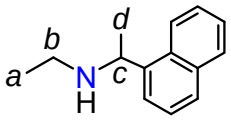

***2nn-Bpin*, Entry 3, Table 2**. ^{1}H NMR (400 MHz, C_6D_6, 294 K): δ 8.21 (d, J = 8 Hz, 1H), 7.91 (d, J = 8 Hz, 1H), 7.78 (d, J = 8 Hz, 1H), 7.70 (d, J = 8 Hz, 1H), 7.57-7.49 (m, 3H), 4.70 (q, J = 8 Hz, 1H), 2.67 (m, 2H), 1.55 (d, J = 8 Hz, 3H), 1.17 (t, J = 8 Hz, 3H) ppm, ^{13}C{^{1}H} NMR (100 MHz, C_6D_6, 294 K): δ 140.3, 132.9, 130.3, 127.9, 126.0, 124.7, 124.6, 124.2, 121.8, 121.5, 52.36, 41.11, 22.51, 14.46 ppm. HRMS: m/z, 200.14. $[M+H]^+$.

5.3. General procedure for amide hydroboration reaction

Inside the glovebox, a sealable tube was loaded with acetanilide (1 g, 7.39 mmol), HBpin (3.22 mL, 22.19 mmol), **Th1** (118 mg, 0.22 mmol) and the reaction was immediately diluted to 10 mL with drt toluene. The tube was taken out of the glove box and the reaction mixture was heated at 70 ºC. After 24 h the reaction mixture was cooled down to room temperature and the solvent was evaporated under high vacuum. Afterthat, the procedure described to synthesis amine from amino-pinacol borane adduct was followed. the pure amine product was seperated by neutral-Al_2O_3 chromatography and the using ethyl acetate/hexane as eluent. ^{1}H NMR and ^{13}C NMR spectrum of new amine compounds are provided below and in Figures S77-78.

5.4. Calculation of product conversion (%)

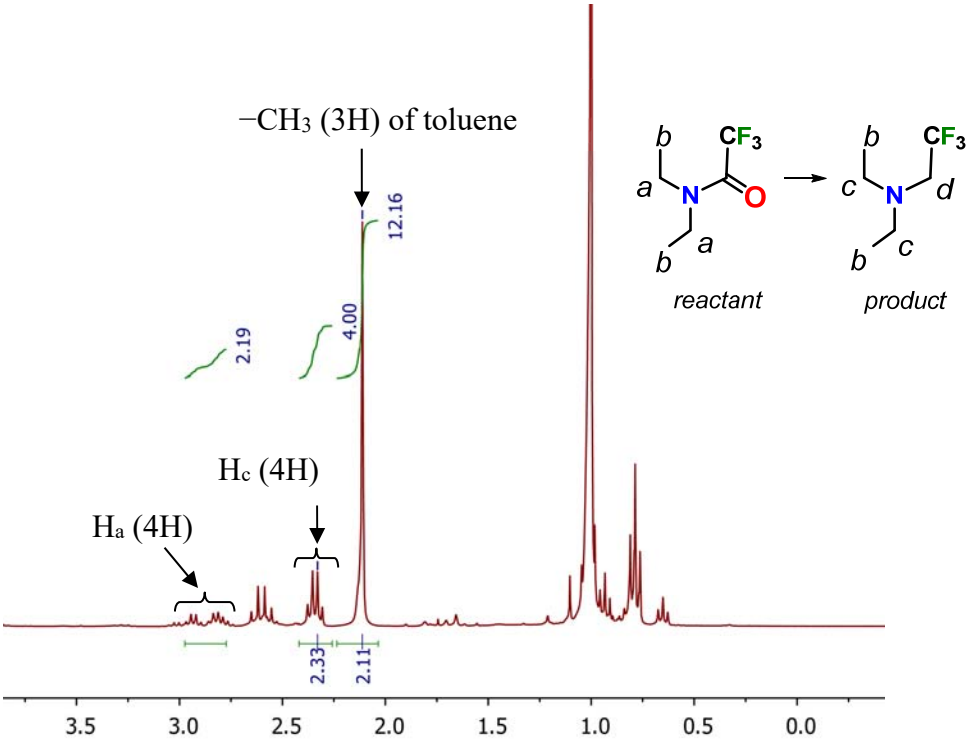

Figure S36. ^{1}H NMR of the reaction mixture of *2s* + HBpin (2 equiv.) at 70 ^{0}C after 12 h in C_6D_6.

Conversion (%) calculation with respect to unreacted reactant

Integral area of H_a (reactant) = 2.19, Integral area of H_c (product) = 4 (2.33 ppm)

% of Conversion = mmol of product/mmol of total reactant x 100%

= mmol of product formed/(mmol of product + mmol unreacted reactant) x 100%

= integral area of product signal/(integral area of product signal + integral area of unreacted reactant signal) x 100%

= 4/(4 + 2.19) x 100%

= 65%

Conversion (%) calculation with internal standards

0.1878 mmol *N*,*N*–diethyl–2,2,2–trifluoroacetamide, 0.3757 mmol HBpin and 0.5116 mmol toluene as internal standard were loaded up in a J. Young NMR tube and left for heating at 70 ^{0}C. The conversion was measured after 12 h.

Integral area of $-CH_3$ (3H) of toluene = 12.16 (2.11 ppm), So, for 4Hs we are supposed to get integral area 16.21 if 0.5116 mmol prosuct is formed. But, integral area of product signal H_c (4H) = 4 (2.33 ppm). So product is formed = 4/16.21 x 0.5116 = 0.1262 mmol

% of conversion = 0.1262/0.1878 x 100% = 67%.

5.5 NMR specta amine-borane adducts in reaction mixtures

***2aa*, Entry 1, Table 2**

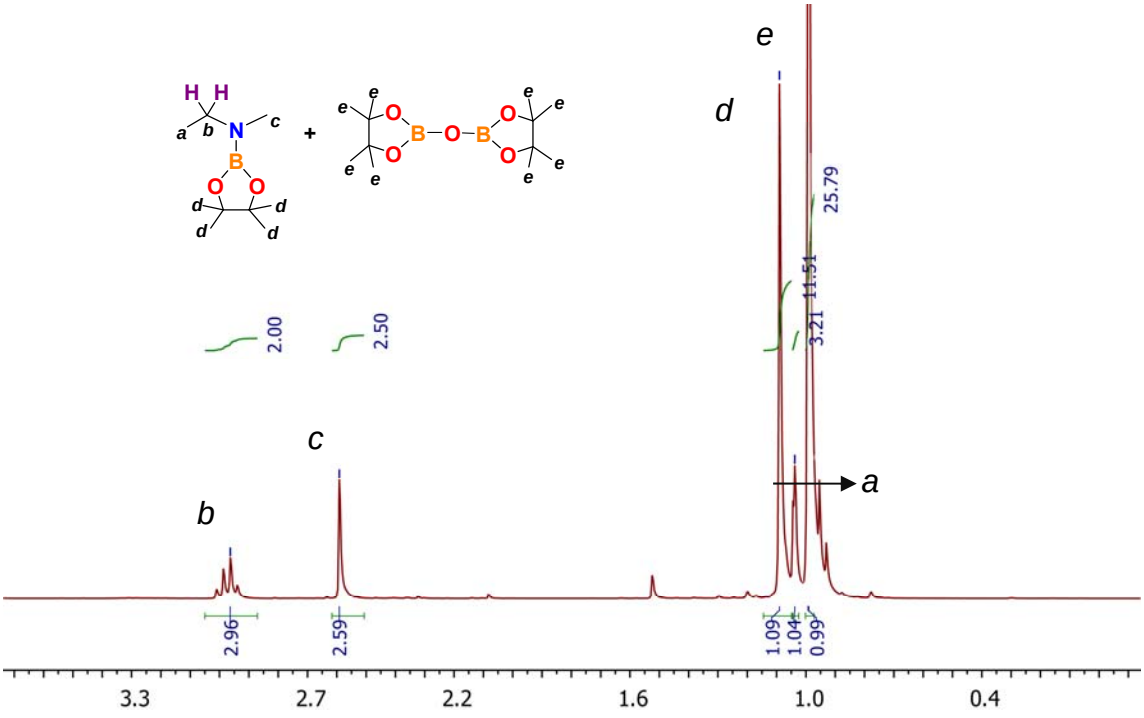

Figure S37. ^{1}H NMR of ***2aa*** in reaction mixture in C_6D_6.

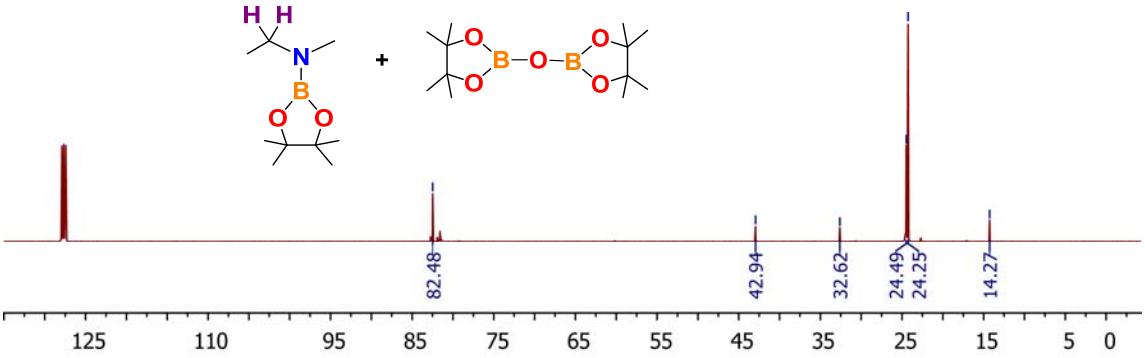

Figure S38. ^{13}C NMR of ***2aa*** in reaction mixture in C_6D_6.

***2bb*, Entry 2, Table 2**

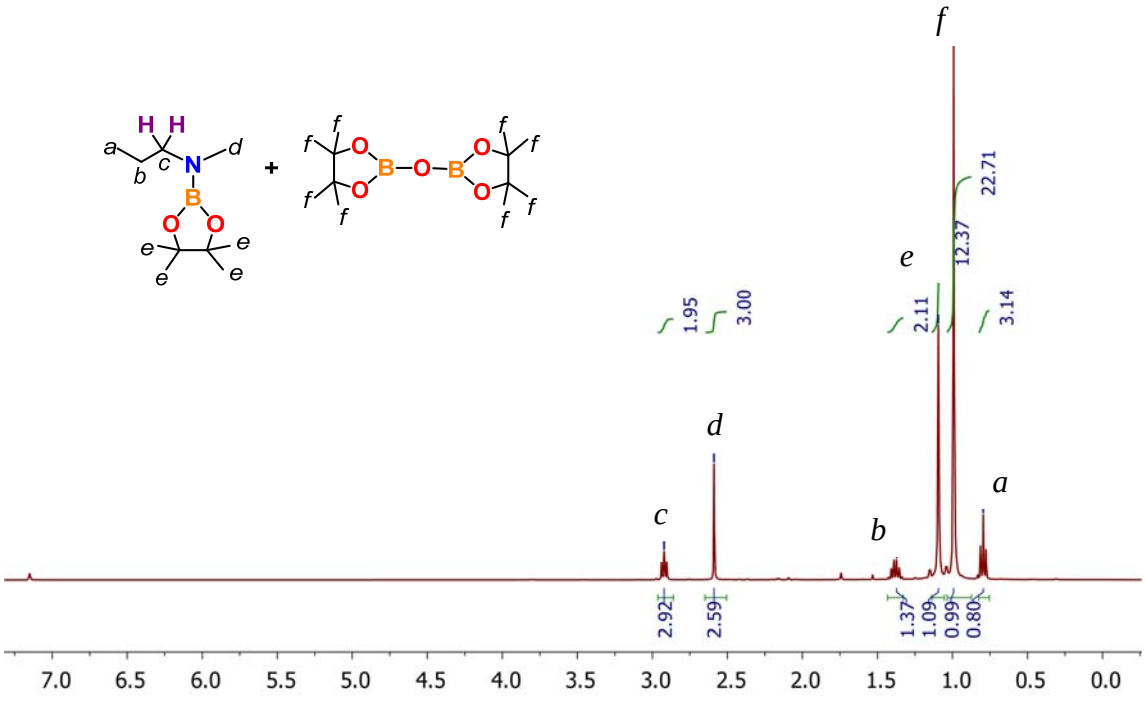

Figure S39. ^{1}H NMR of ***2bb*** in reaction mixture in C_6D_6.

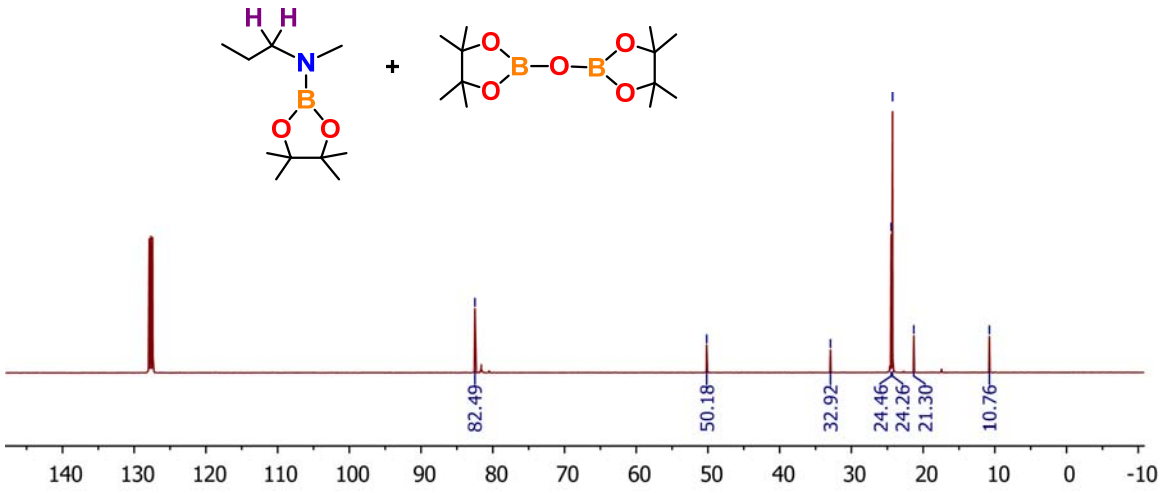

Figure S40. ^{13}C NMR of ***2bb*** in reaction mixture in C_6D_6.

***2cc*, Entry 3, Table 2**

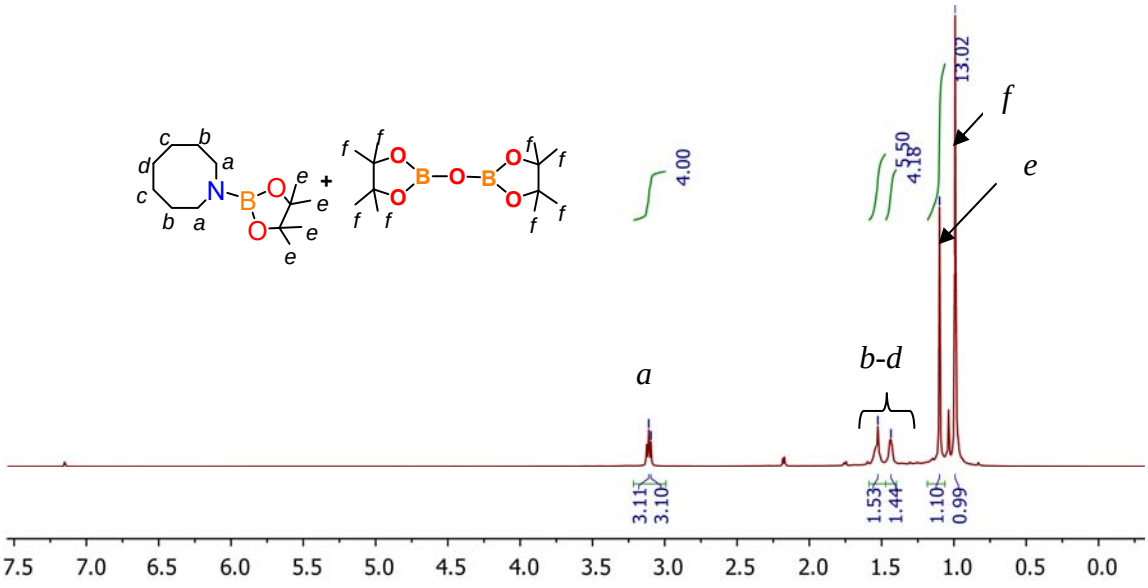

Figure S41. ^{1}H NMR of ***2cc*** in reaction mixture in C_6D_6.

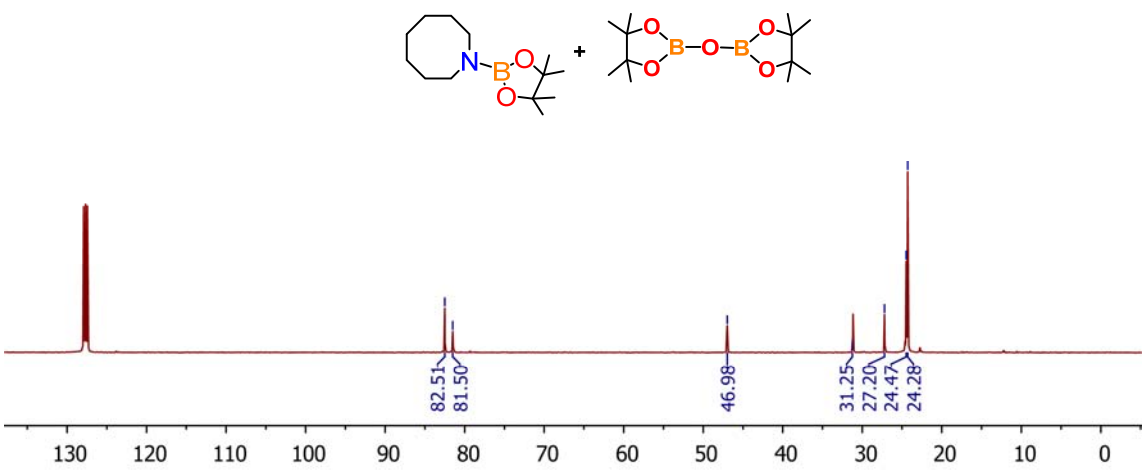

Figure S42. ^{13C} NMR of ***2cc*** in reaction mixture in C_6D_6.

***2dd*, Entry 4, Table 2**

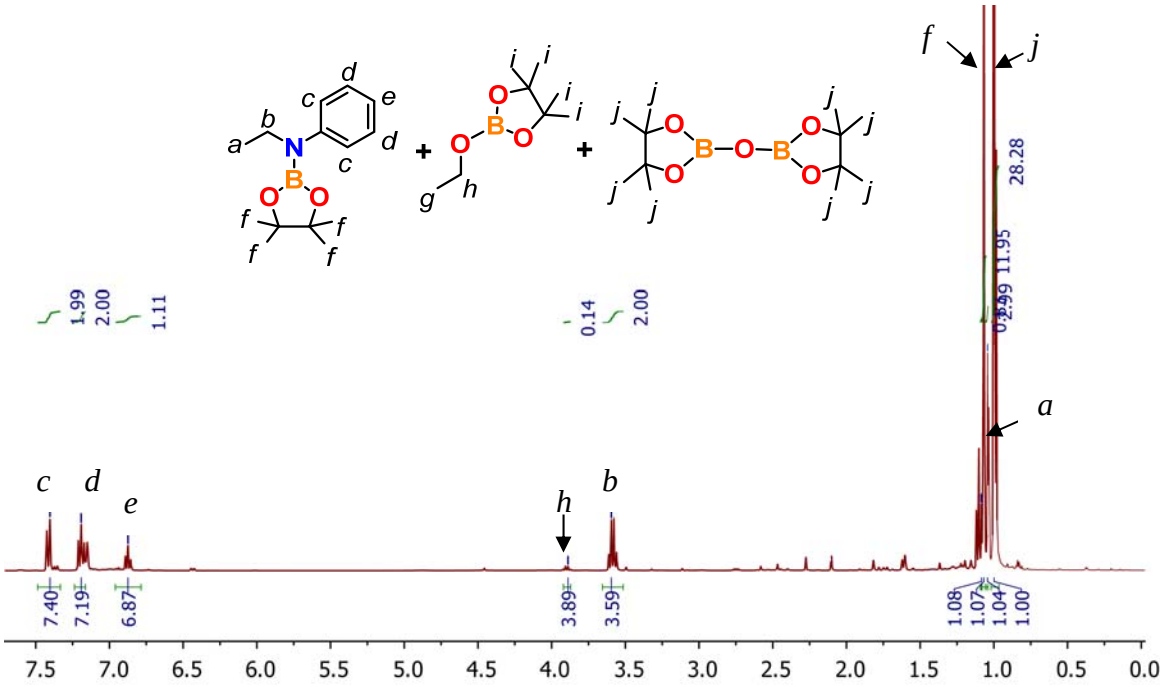

Figure S43. ^{1}H NMR of ***2dd*** in reaction mixture in C_6D_6.

Integral area of H_b = 2; Integral area of H_h = 0.14

% of C-O cleaved product = {2/(2 + 0.14)} x 100% = 94%

% of C-N cleaved product = {0.14/(2 + 0.14)} x 100% = 6%

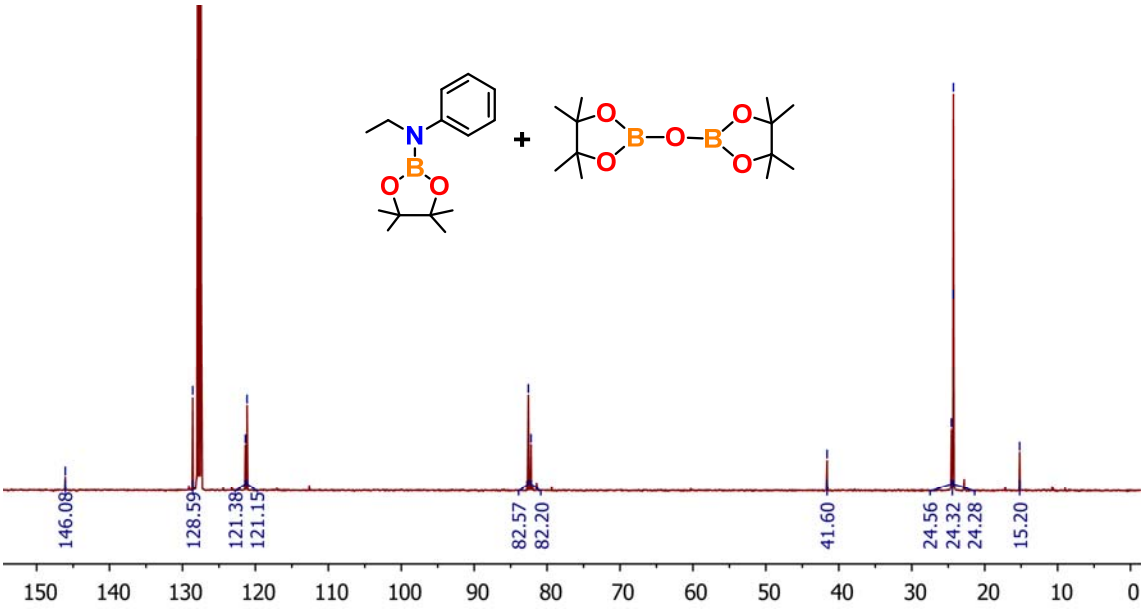

Figure S44. ^{13}C NMR of ***2dd*** in reaction mixture in C_6D_6.

***2ff*, Entry 6, Table 2**

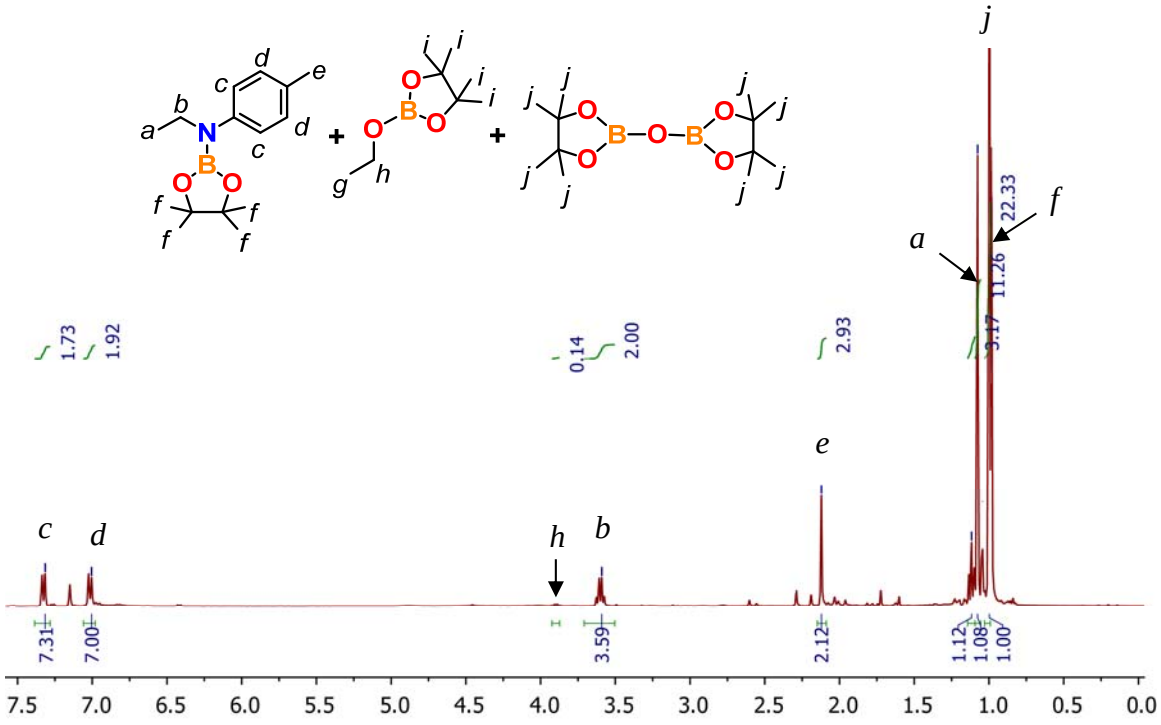

Figure S45. ^{1}H NMR of ***2ff*** in reaction mixture in C_6D_6.

Integral area of H_b = 2; Integral area of H_h = 0.14
% of C-O cleaved product = {2/(2 + 0.14)} x 100% = 94%
% of C-N cleaved product = {0.14/(2 + 0.14)} x 100% = 6%

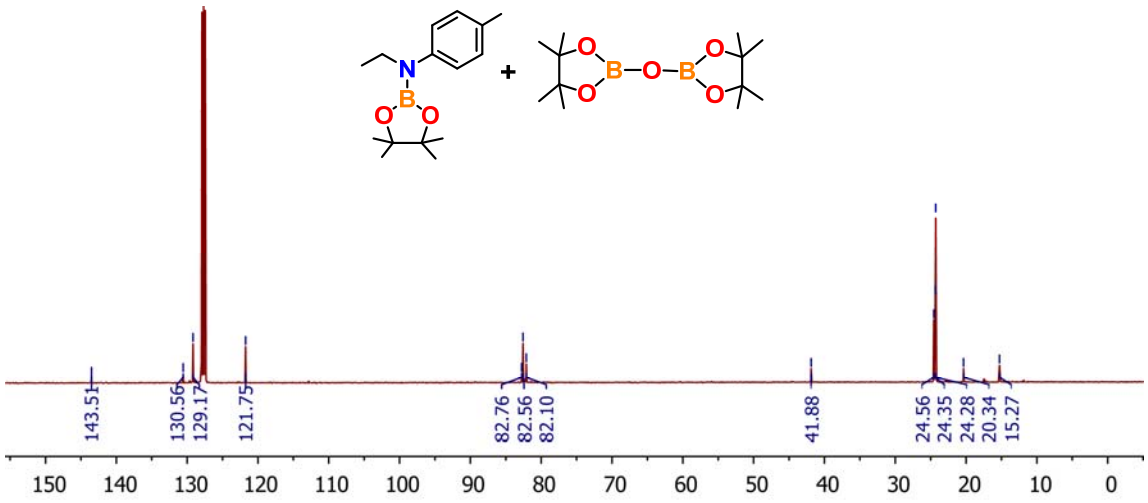

Figure S46. ^{13}C NMR of ***2ff*** in reaction mixture in C_6D_6.

***2gg*, Entry 7, Table 2**.

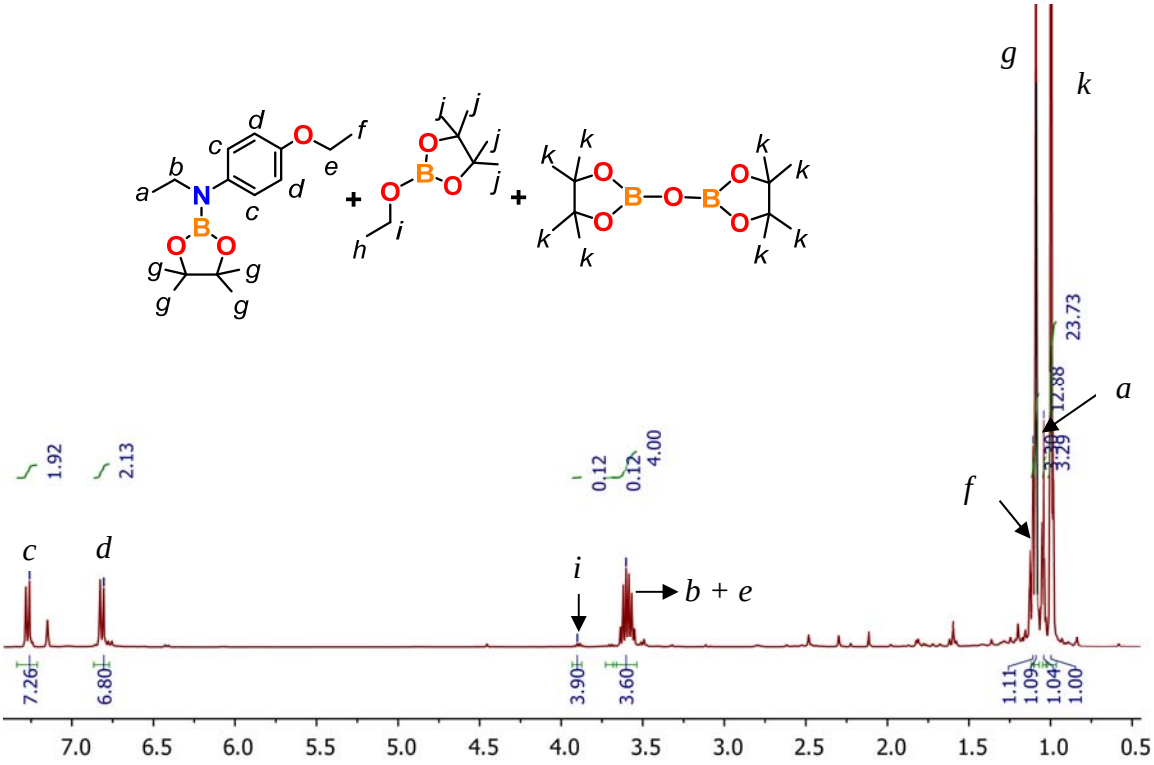

Figure S47. ^{1}H NMR of ***2gg*** in reaction mixture in C_6D_6.

Integral area of H_b = 4; Integral area of H_i = 0.24
% of C-O cleaved product = {4/(2 + 0.24)} x 100% = 95%
% of C-N cleaved product = {0.24/(2 + 0.24)} x 100% = 5%

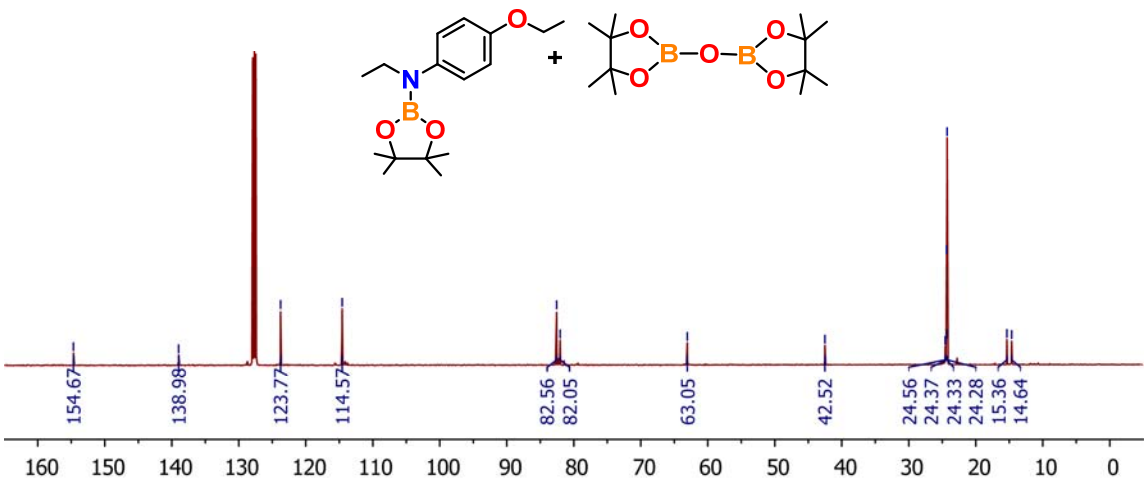

Figure S48. ^{13}C NMR of ***2gg*** in reaction mixture in C_6D_6.

***2hh*, Entry 8, Table 2**

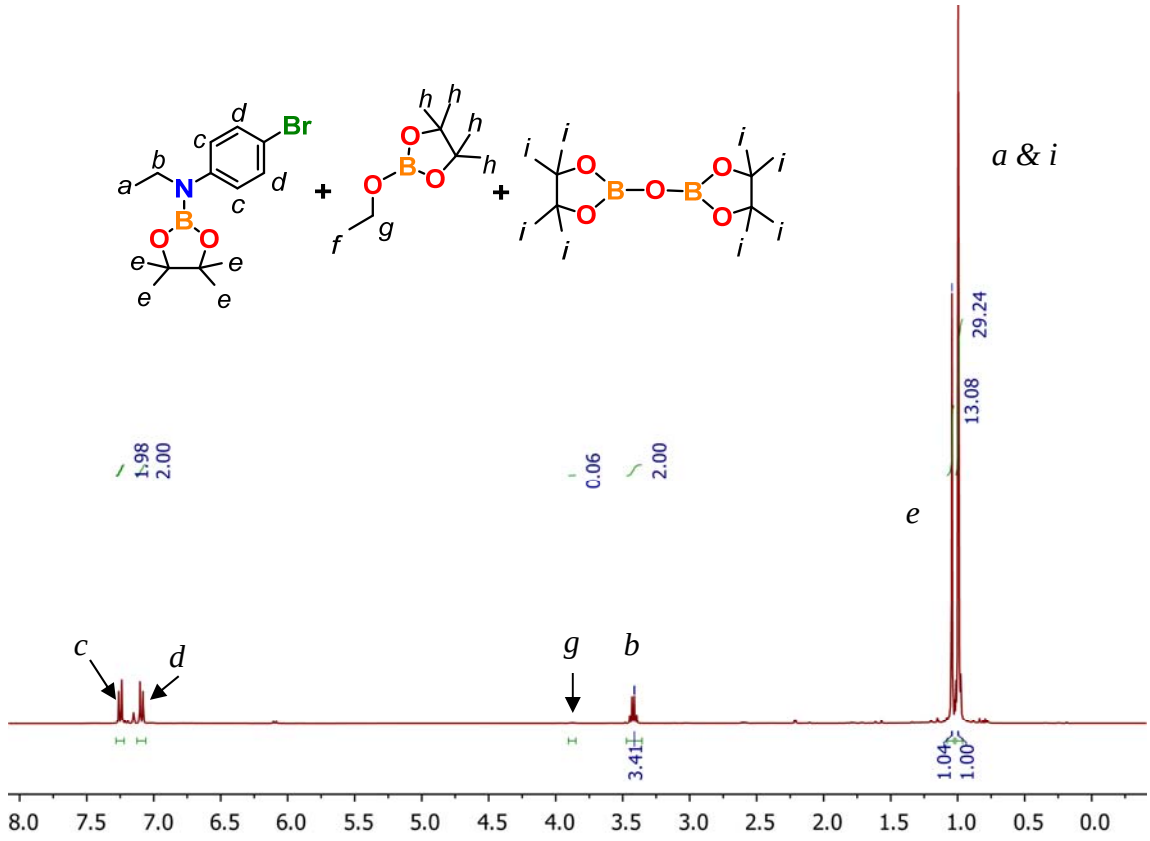

Figure S49. ^{1}H NMR of ***2hh*** in reaction mixture in C_6D_6.

Integral area of H_b = 2; Integral area of H_g = 0.06
% of C-O cleaved product = {2/(2 + 0.06)} x 100% = 97%
% of C-N cleaved product = {0.06/(2 + 0.06)} x 100% = 3%

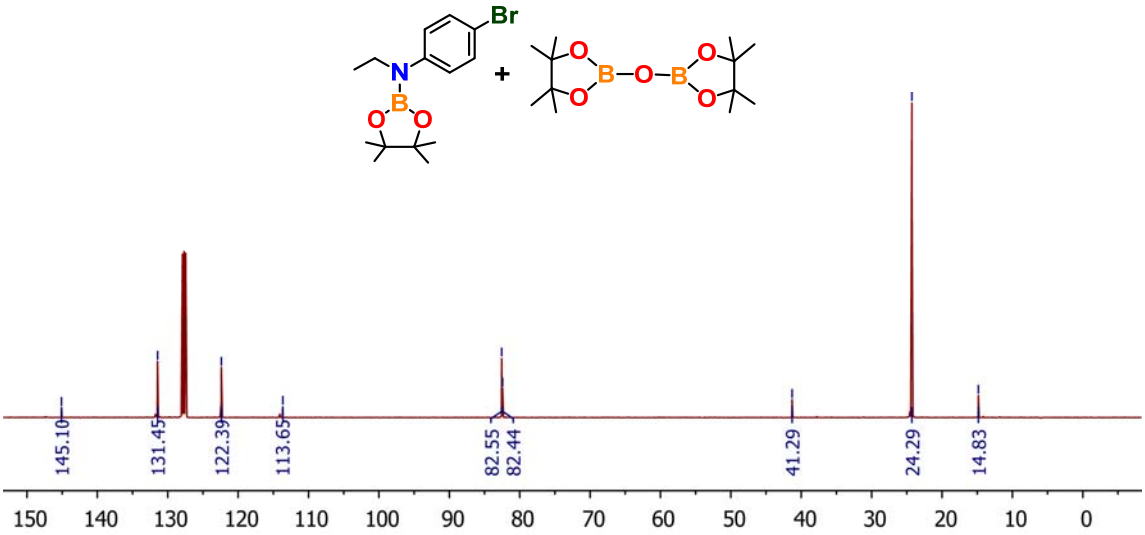

Figure S50. ^{13}C NMR of ***2hh*** in reaction mixture in C_6D_6.

***2ii*, Entry 9, Table 2**

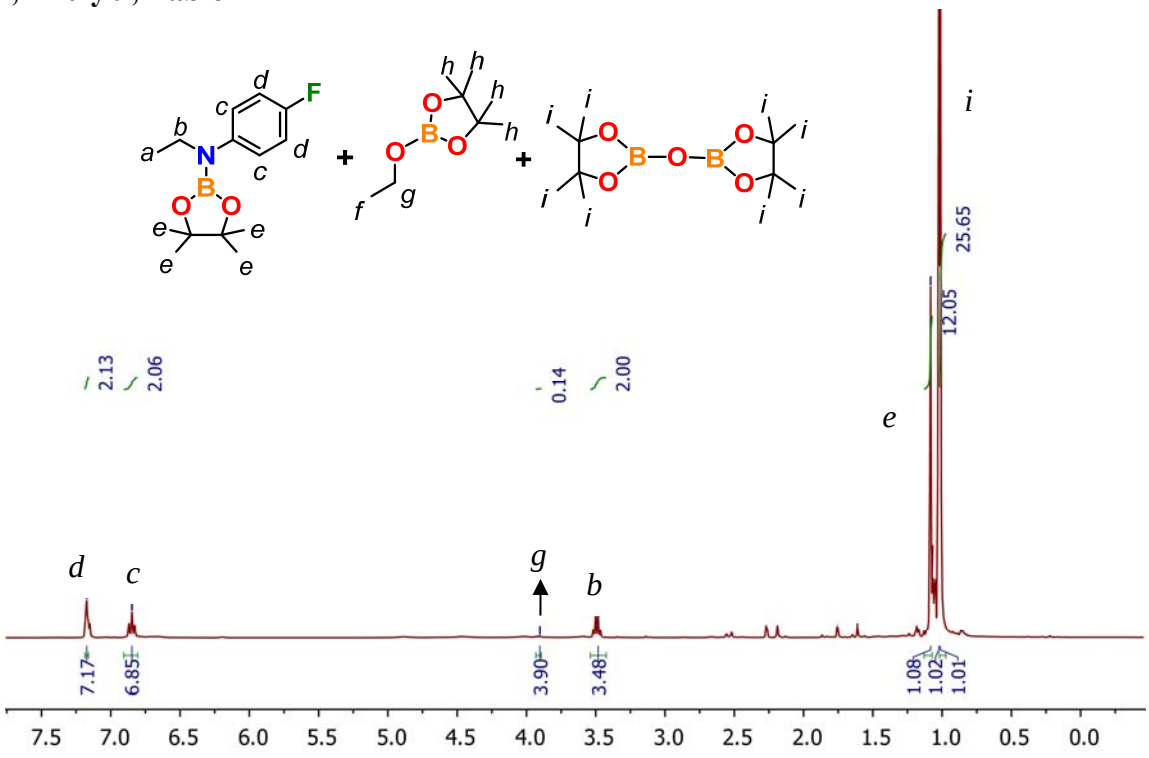

Figure S51. ^{1}H NMR of ***2ii*** in reaction mixture in C_6D_6.

Integral area of H_b = 2; Integral area of H_g = 0.14

% of C-O cleaved product = {2/(2 + 0.14)} x 100% = 94%

% of C-N cleaved product = {0.14/(2 + 0.14)} x 100% = 6%

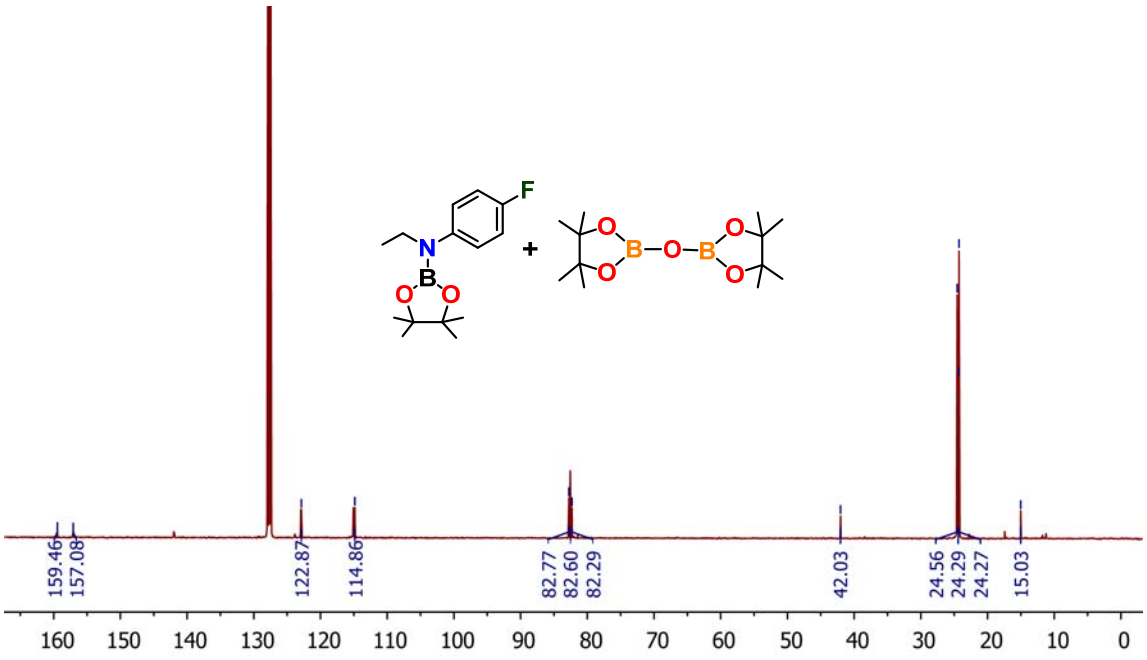

Figure S52. ^{13}C NMR of ***2ii*** in reaction mixture in C_6D_6.

***2jj*, Entry 10, Table 2**

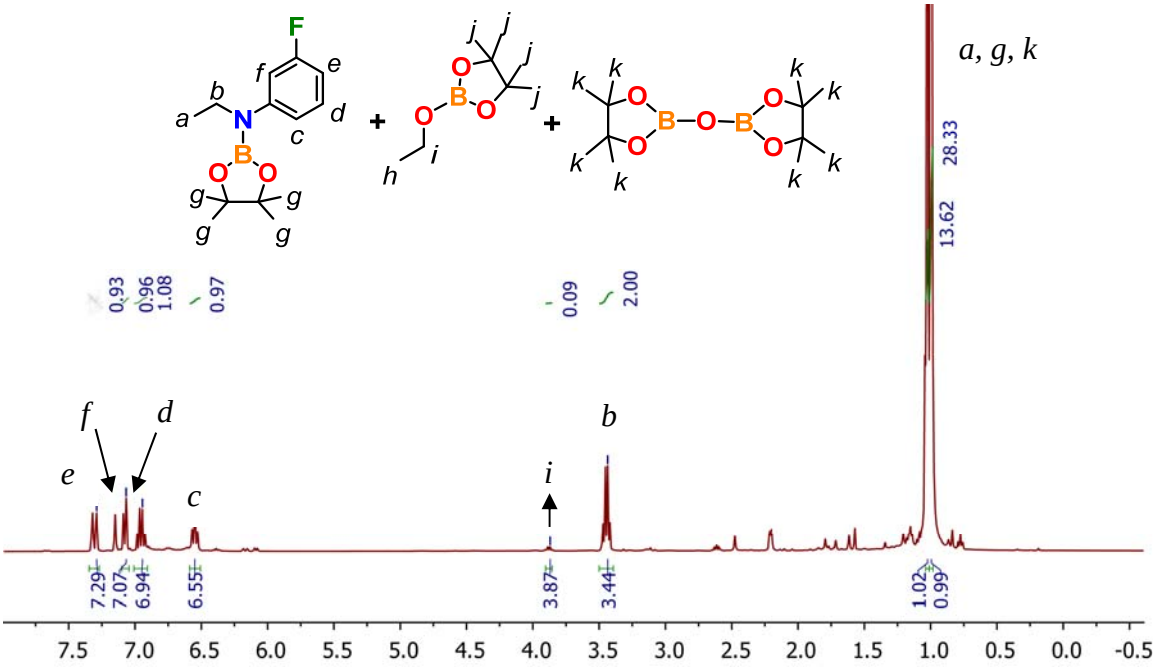

Figure S53. ^{1}H NMR of ***2jj*** in reaction mixture in C_6D_6.

Integral area of H_b = 2; Integral area of H_i = 0.09

% of C-O cleaved product = {2/(2 + 0.0.09)} x 100% = 96%

% of C-N cleaved product = {0.09/(2 + 0.09)} x 100% = 4%

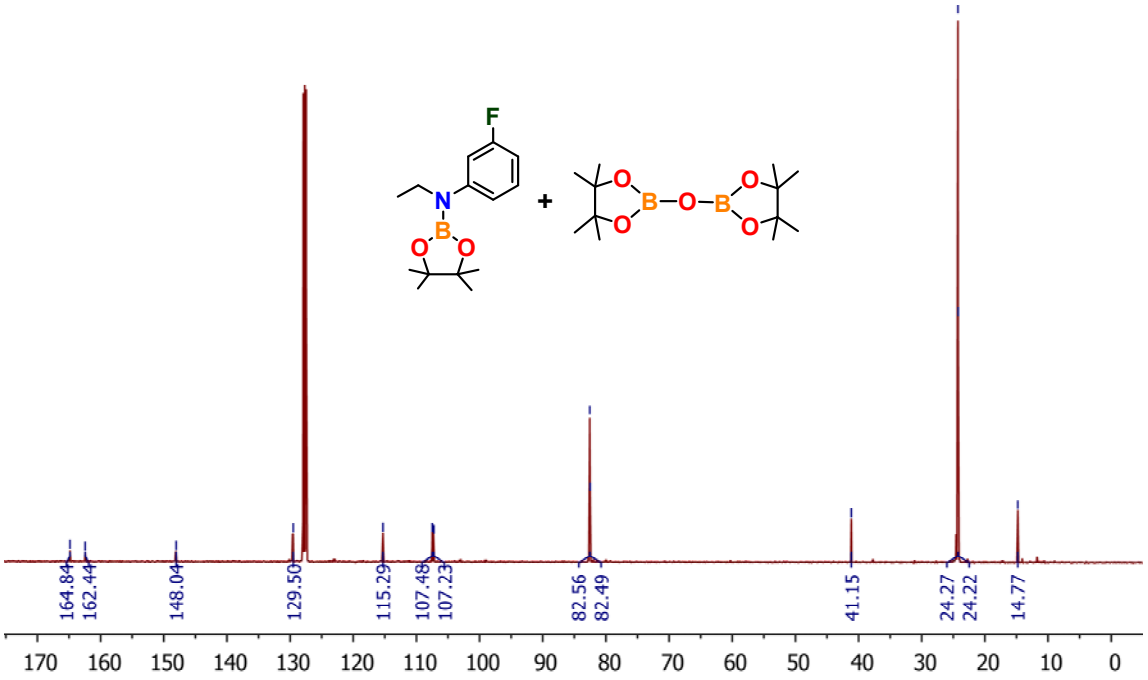

Figure S54. ^{13}C NMR of ***2jj*** in reaction mixture in C_6D_6.

***2kk*, Entry 11, Table 2**

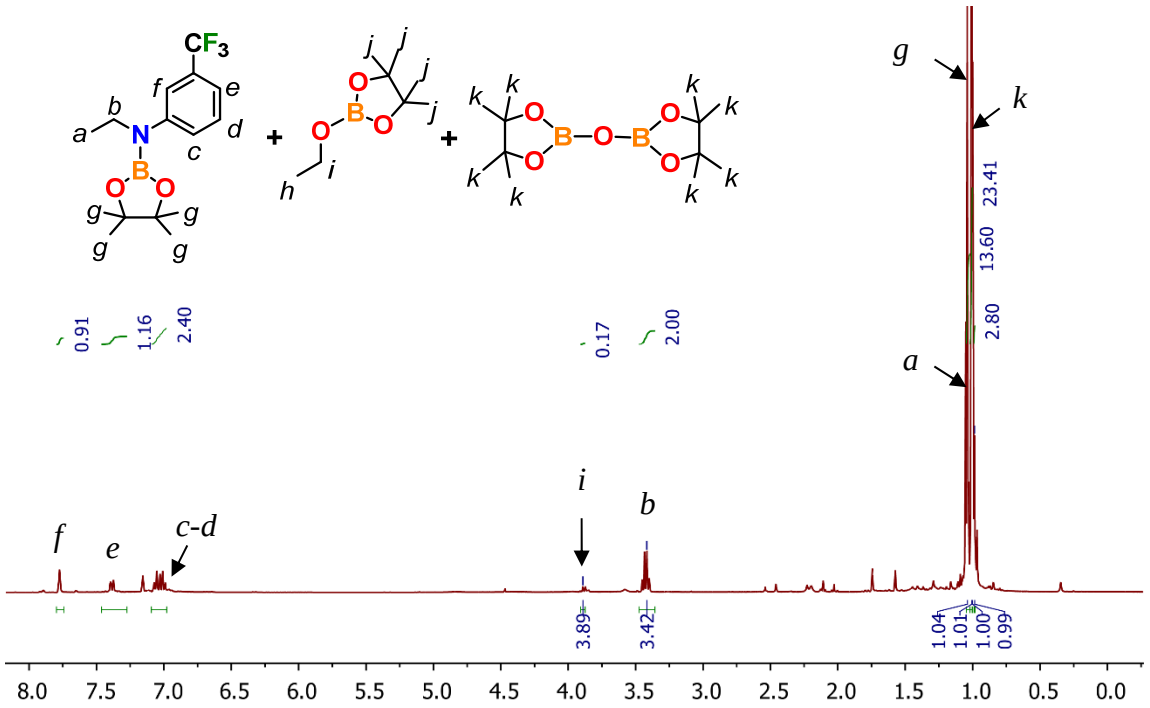

Figure S55. ^{1}H NMR of ***2kk*** in reaction mixture in C_6D_6.

Integral area of H_b = 2; Integral area of H_i = 0.17

% of C-O cleaved product = {2/(2 + 0.17)} x 100% = 92%

% of C-N cleaved product = {0.17/(2 + 0.17)} x 100% = 8%

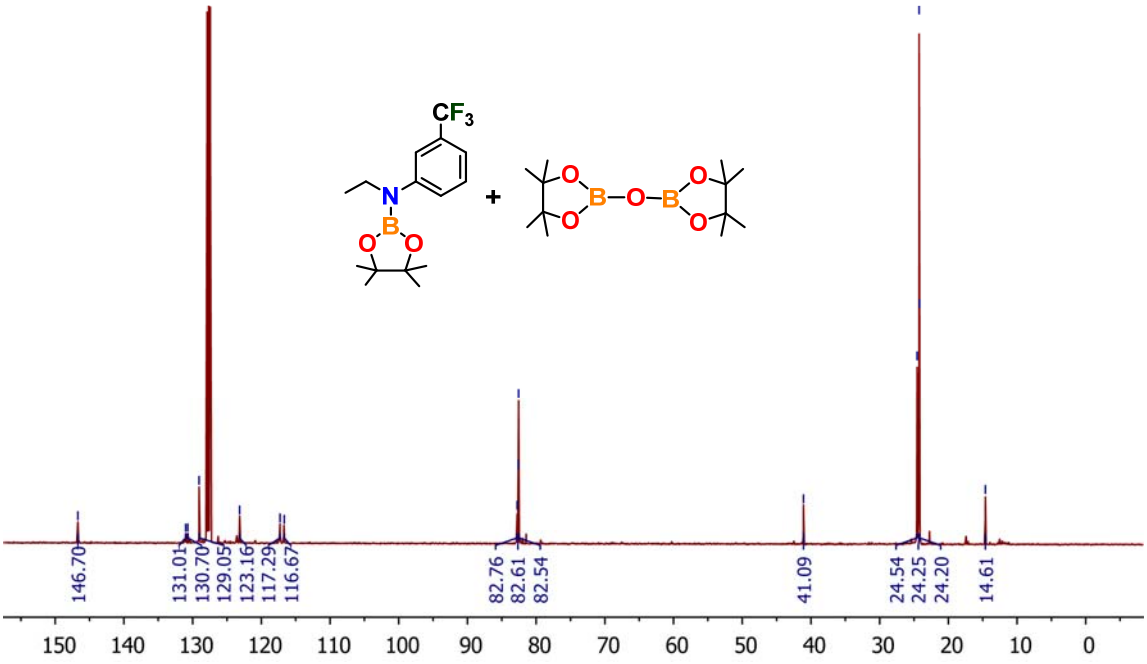

Figure S56. ^{13}C NMR of ***2kk*** in reaction mixture in C_6D_6.

***2ll*, Entry 12, Table 2**

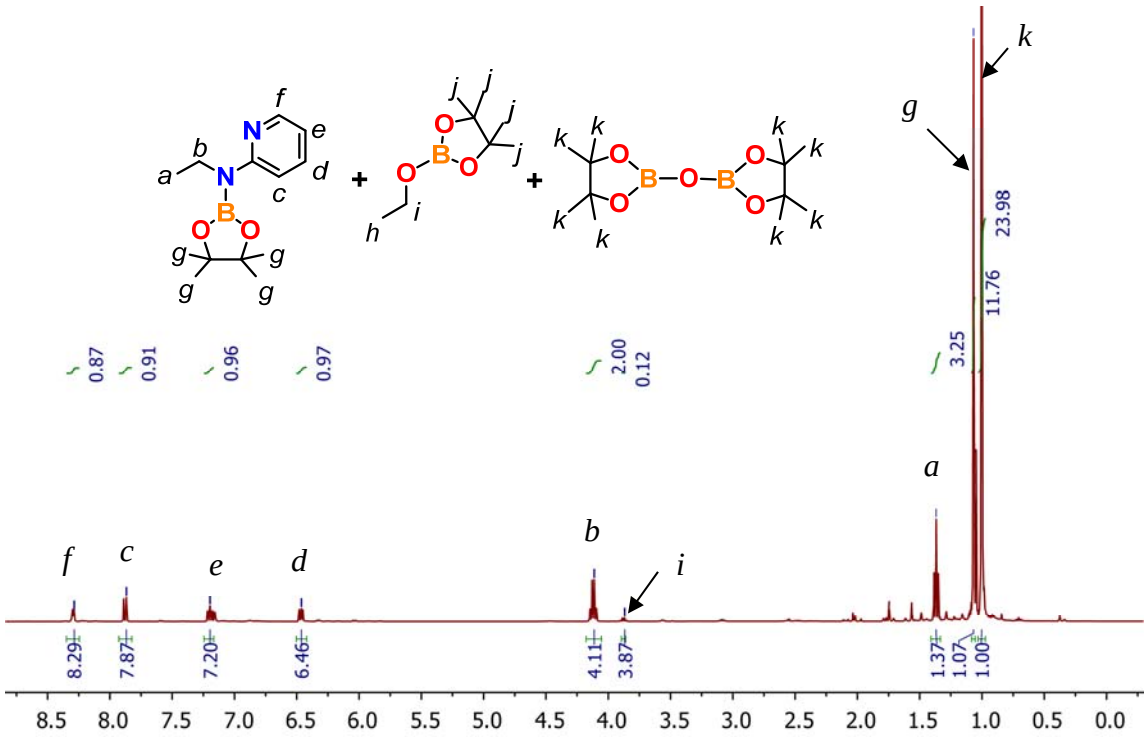

Figure S57. ^{1}H NMR of ***2ll*** in reaction mixture in C_6D_6.

Integral area of H_b = 2; Integral area of H_i = 0.12
% of C-O cleaved product = {2/(2 + 0.12)} x 100% = 96%
% of C-N cleaved product = {0.12/(2 + 0.12)} x 100% = 4%

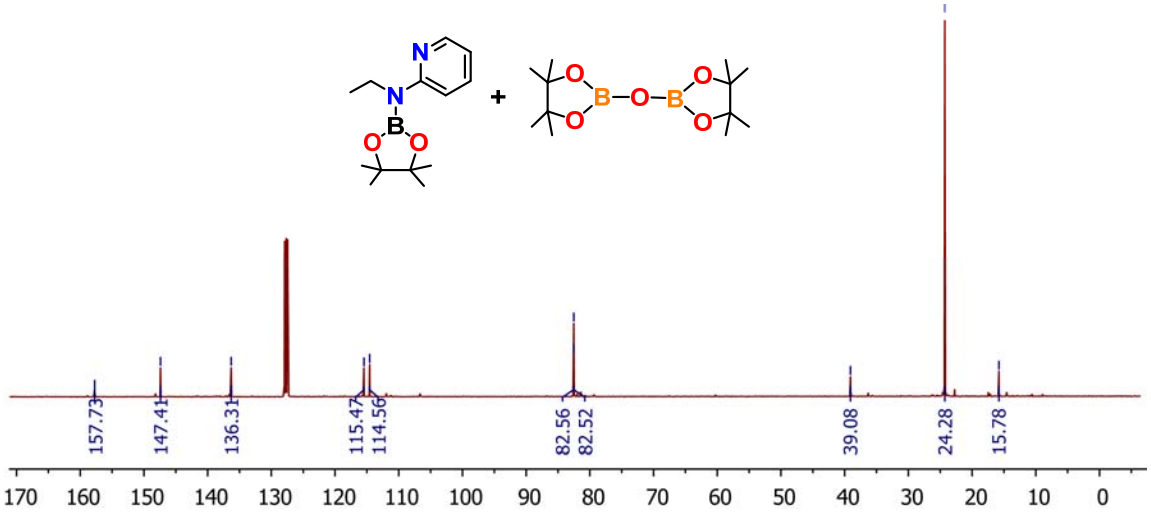

Figure S58. ^{13}C NMR of ***2ll*** in reaction mixture in C_6D_6.

***2mm*, Entry 13, Table 2**

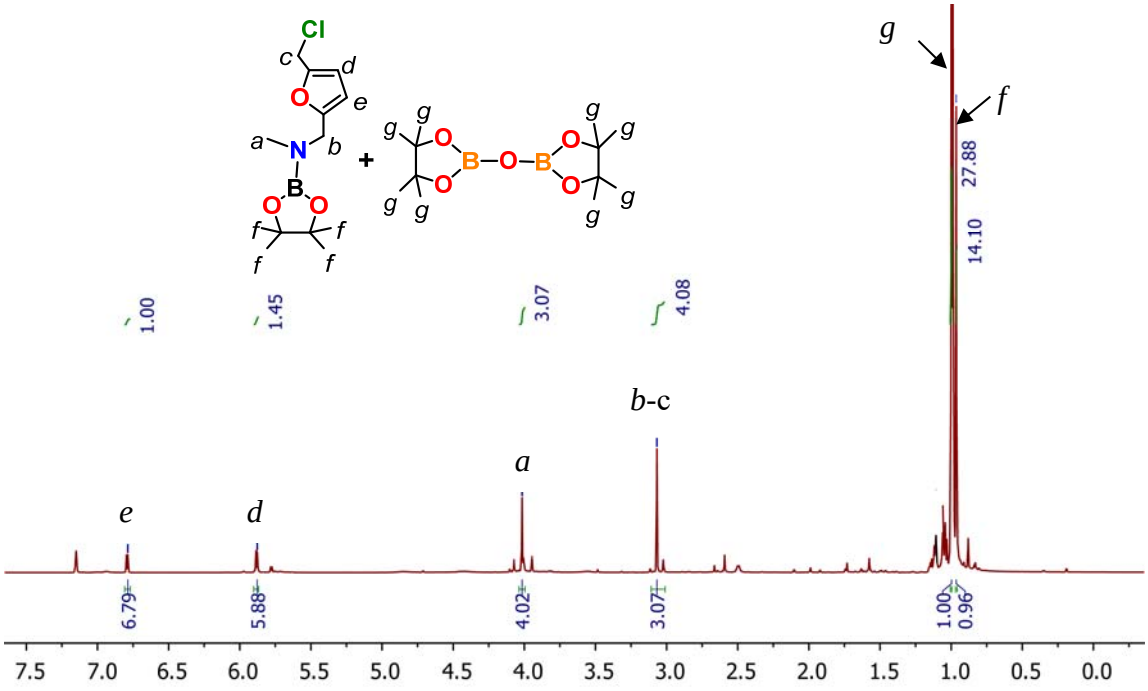

Figure S59. ^{1}H NMR of ***2mm*** in reaction mixture in C_6D_6.

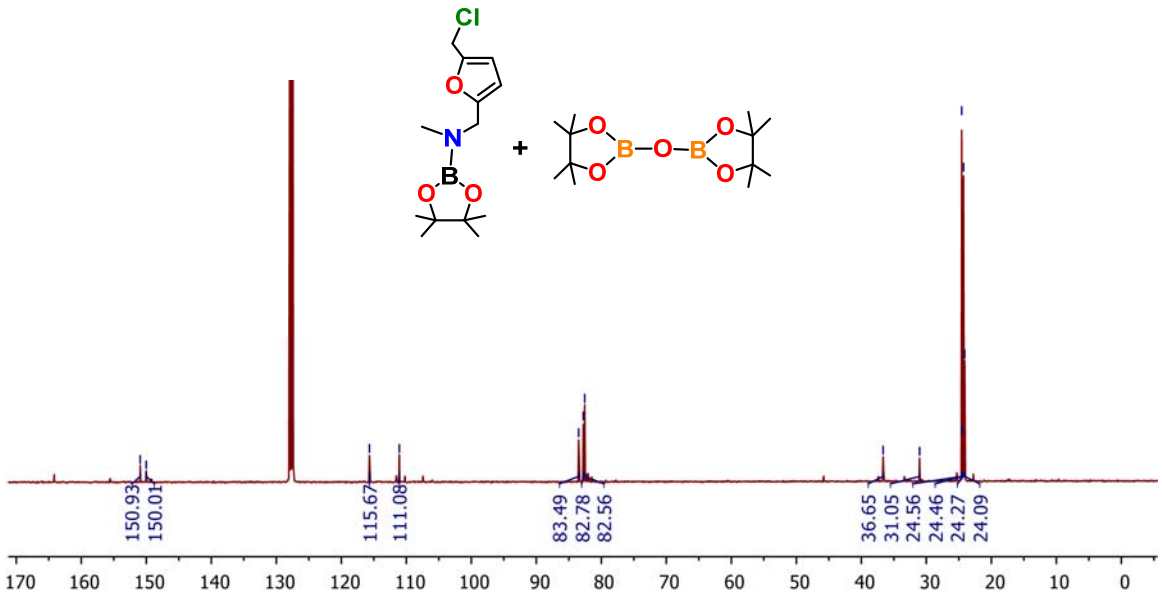

Figure S60. ^{13}C NMR of ***2mm*** in reaction mixture in C_6D_6.

***2oo*, Entry 15, Table 2**

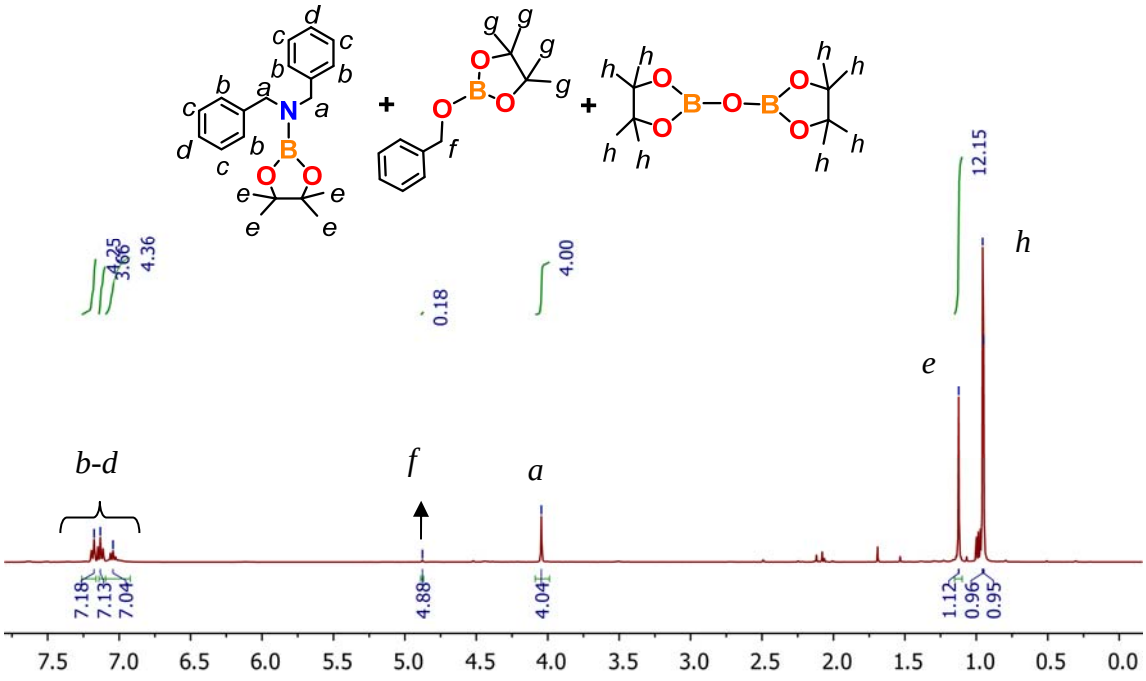

Figure S61. ^{1}H NMR of ***2oo*** in reaction mixture in C_6D_6.

Integral area of H_b = 4; Integral area of $2H_i$ = 0.36
% of C-O cleaved product = {4/(4 + 0.36)} x 100% = 93%
% of C-N cleaved product = {0.36/(4 + 0.36)} x 100% = 7%

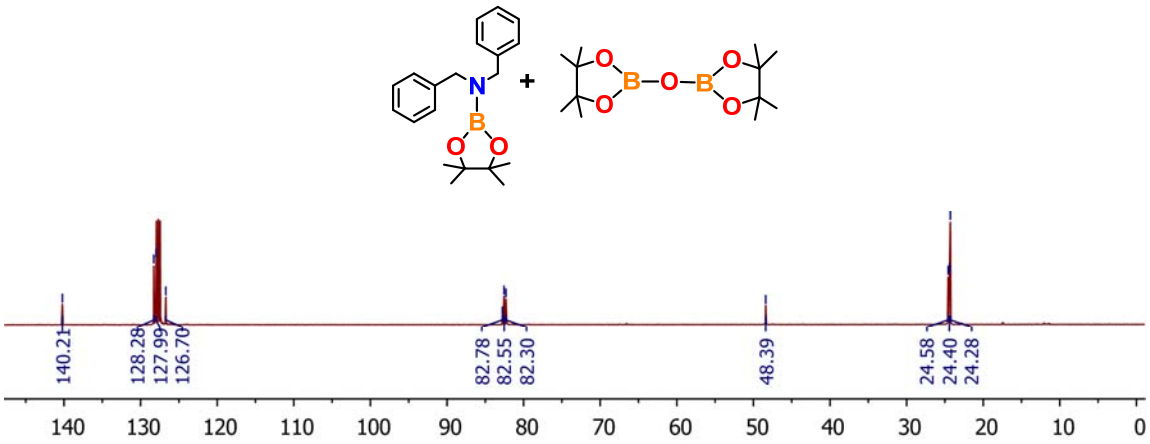

Figure S62. ^{13}C NMR of ***2oo*** in reaction mixture in C_6D_6.

***2pp*, Entry 16, Table 2**

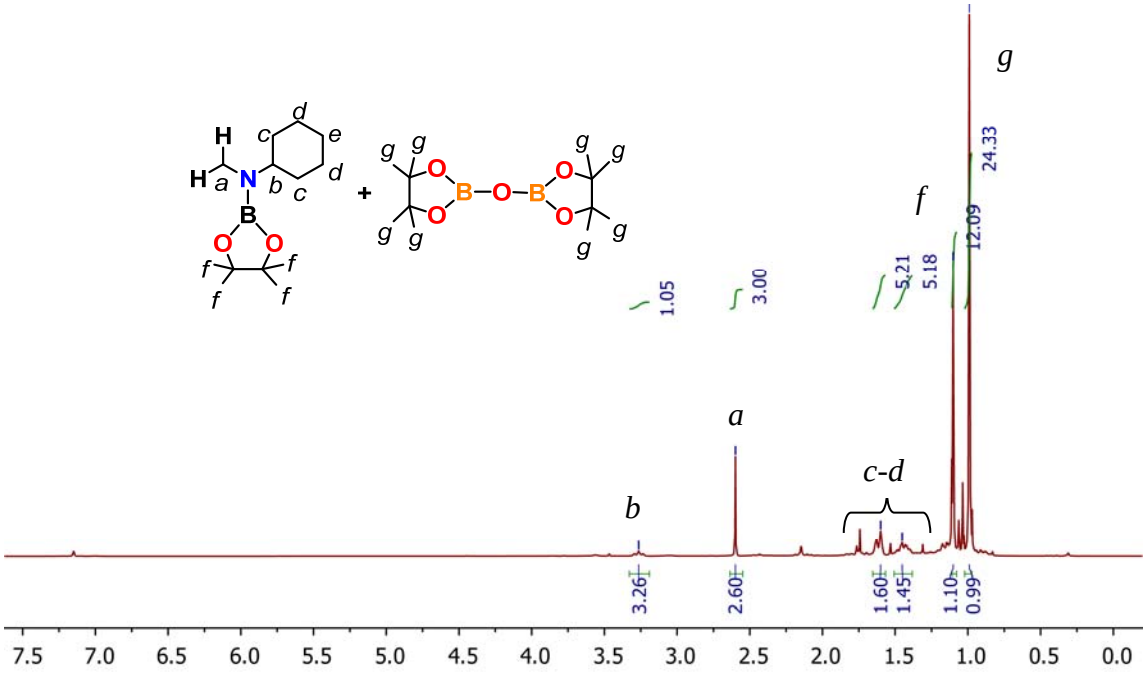

Figure S63. ^{1}H NMR of ***2pp*** in reaction mixture in C_6D_6.

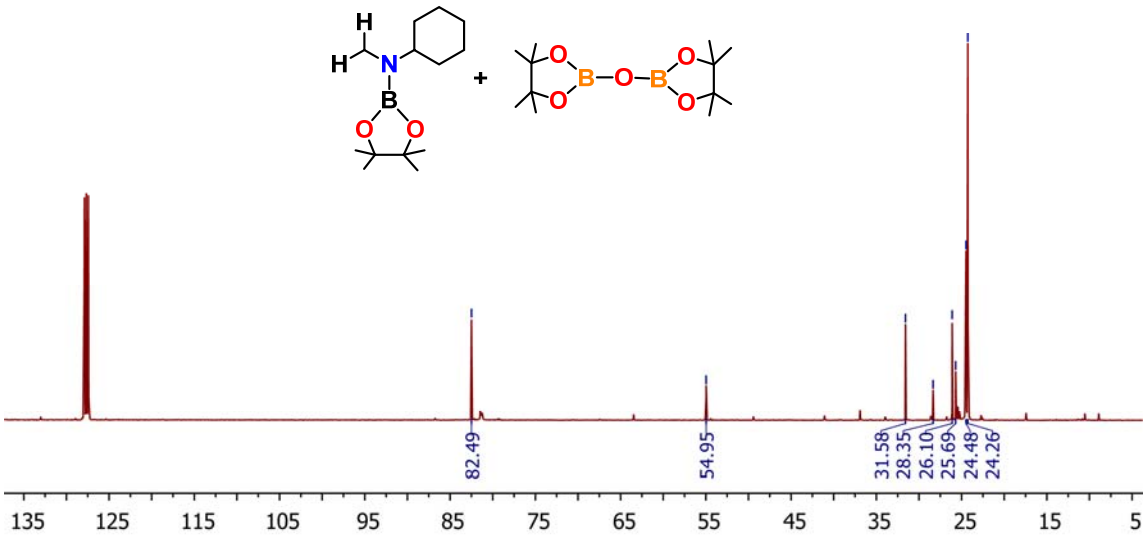

Figure S64. ^{13}C NMR of ***2pp*** in reaction mixture in C_6D_6.

***2qq*, Entry 17, Table 2**

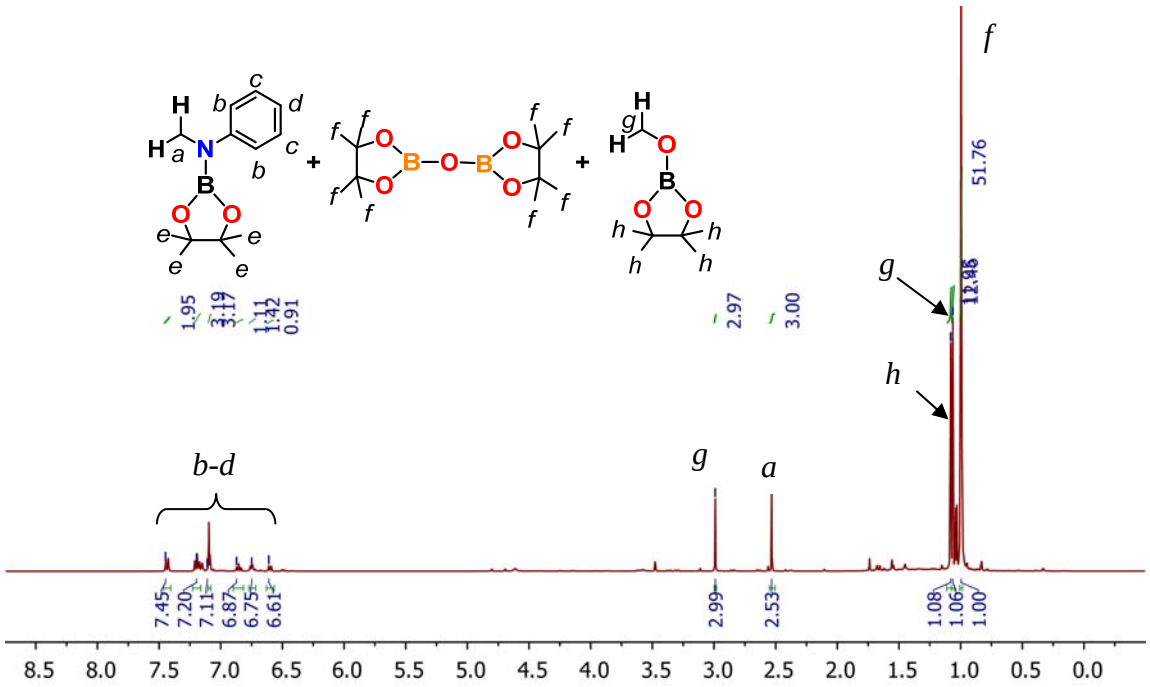

Figure S65. ^{1}H NMR of ***2qq*** in reaction mixture in C_6D_6.

Integral area of H_b = 3; Integral area of H_g = 2.97
% of C-O cleaved product = {3/(3 + 2.97)} x 100% = 50.2%
% of C-N cleaved product = {2.97/(3 + 2.97)} x 100% = 49.8%

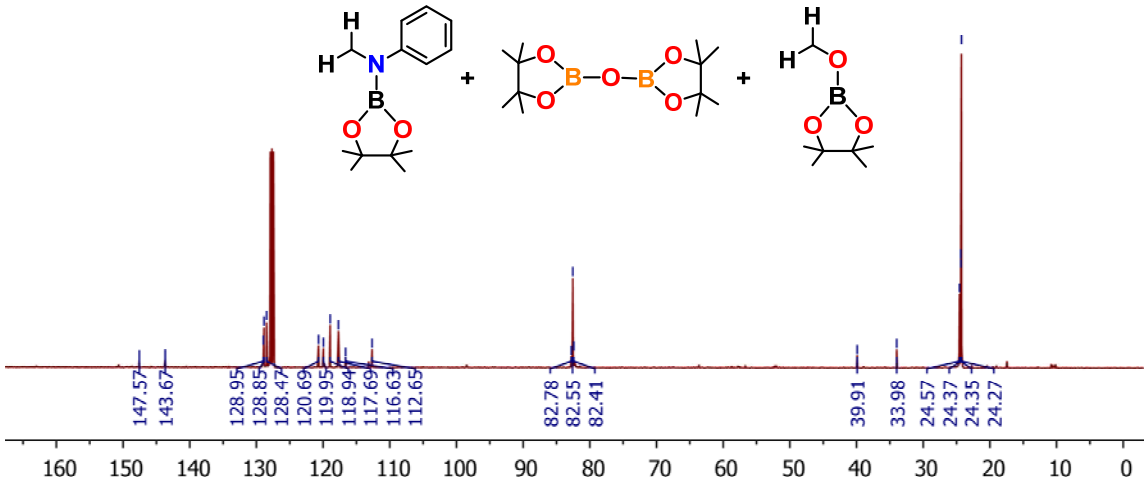

Figure S66. ^{13}C NMR of ***2qq*** in reaction mixture in C_6D_6.

***2rr*, Entry 18, Table 2**

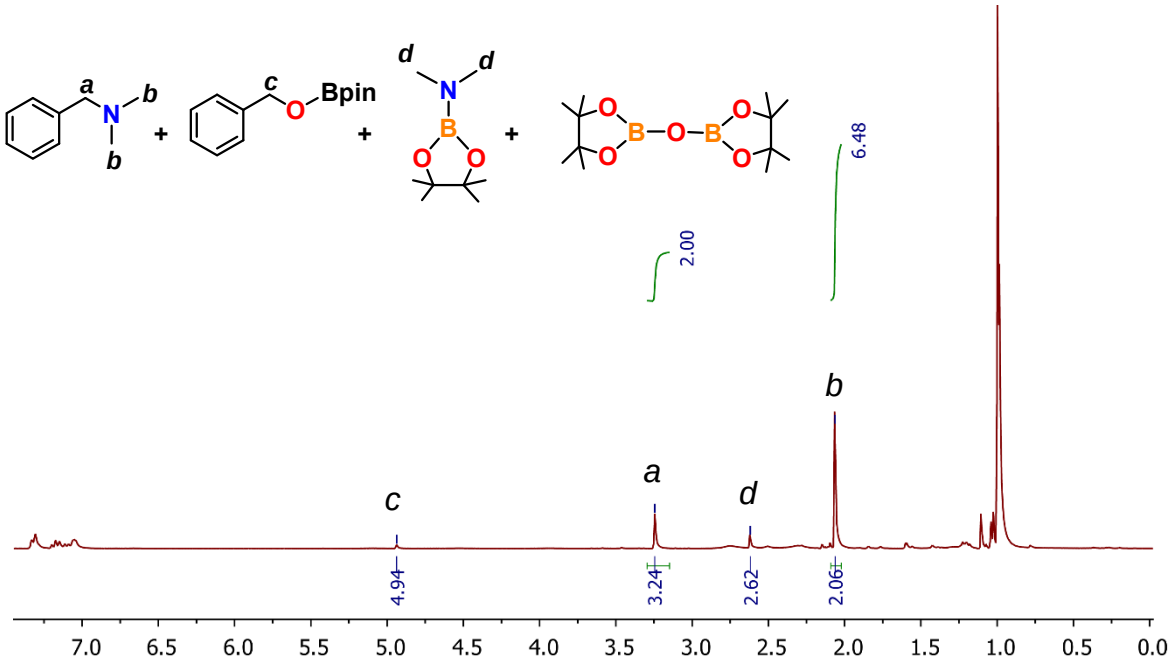

Figure S67. ^{1}H NMR of ***2rr*** in reaction mixture in C_6D_6.

Integral area of H_a = 2; Integral area of H_c = 0.09
% of C-O cleaved product = {2/(2 + 0.09)} x 100% = 95%
% of C-N cleaved product = {0.09/(2 + 0.09)} x 100% = 5%

***2ss*, Entry 19, Table 2**

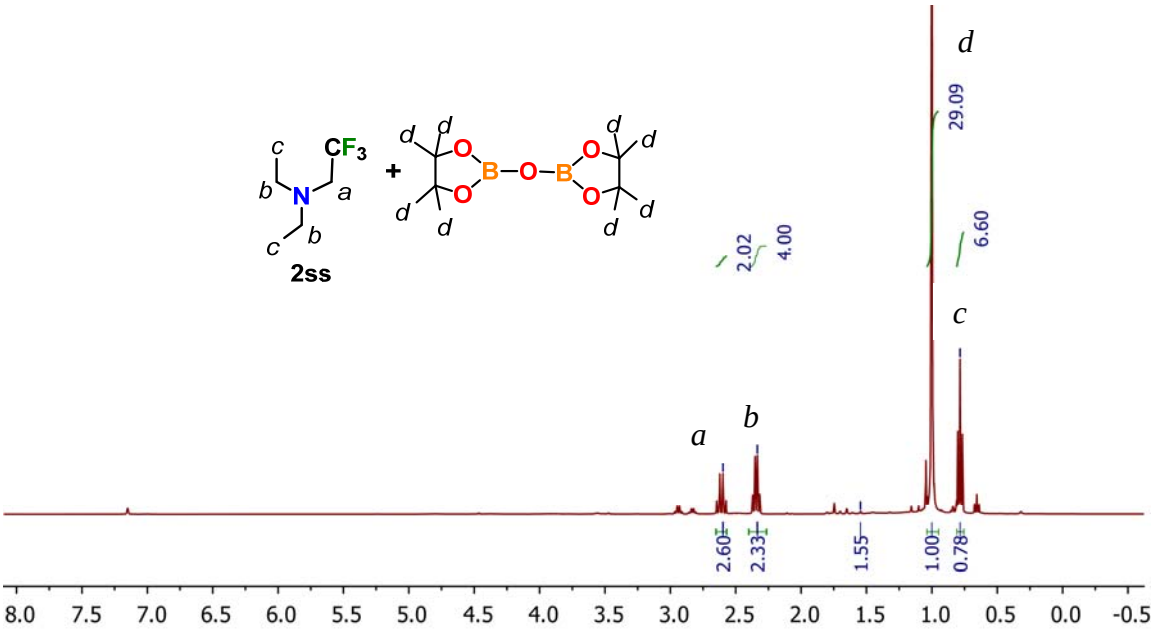

Figure S68. ^{1}H NMR of ***2ss*** in reaction mixture in C_6D_6.

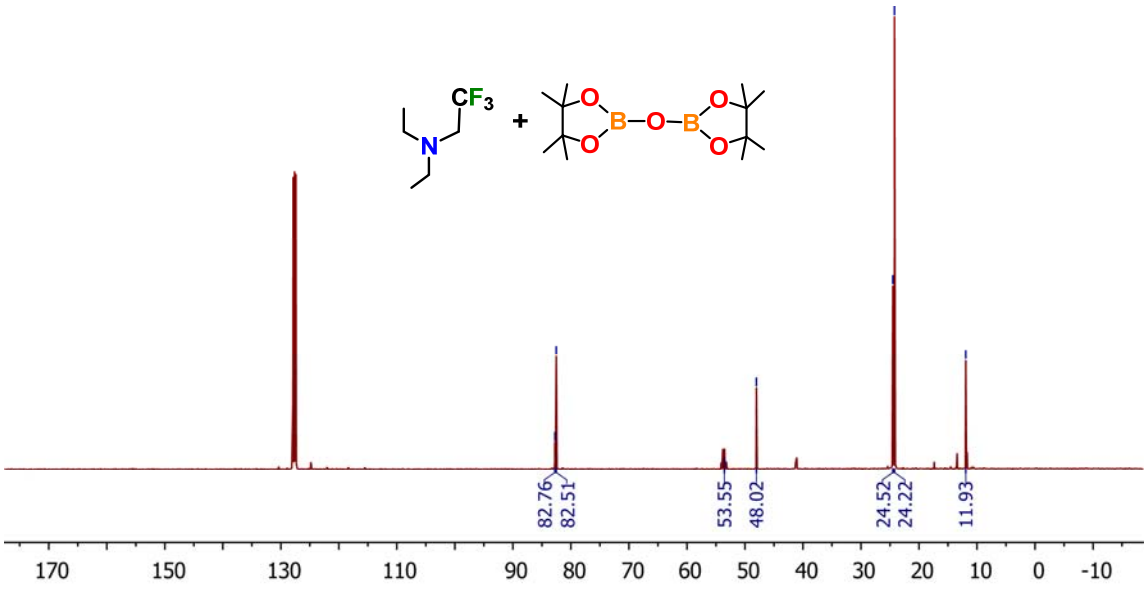

Figure S69. ^{13}C NMR of ***2ss*** in reaction mixture in C_6D_6.

***2tt*, Entry 20, Table 2**

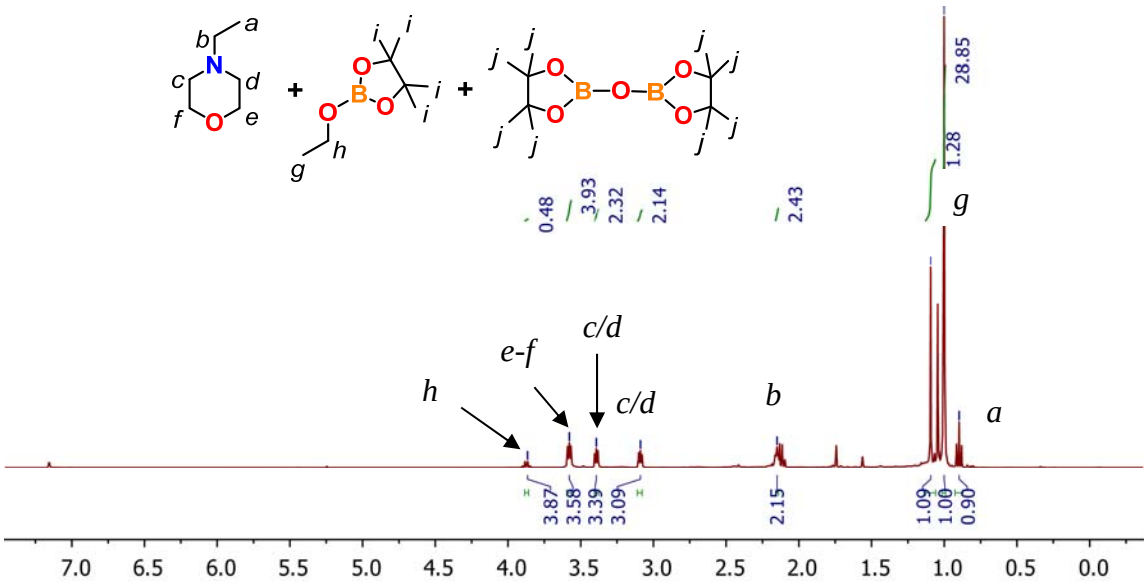

Figure S70. ^{1}H NMR of ***2tt*** in reaction mixture in C_6D_6.

Integral area of H_b = 2.43; Integral area of H_h = 0.48
% of C-O cleaved product = {2.43/(2.43 + 0.48)} x 100% = 85%
% of C-N cleaved product = {0.48/(2.43 + 0.48)} x 100% = 15%

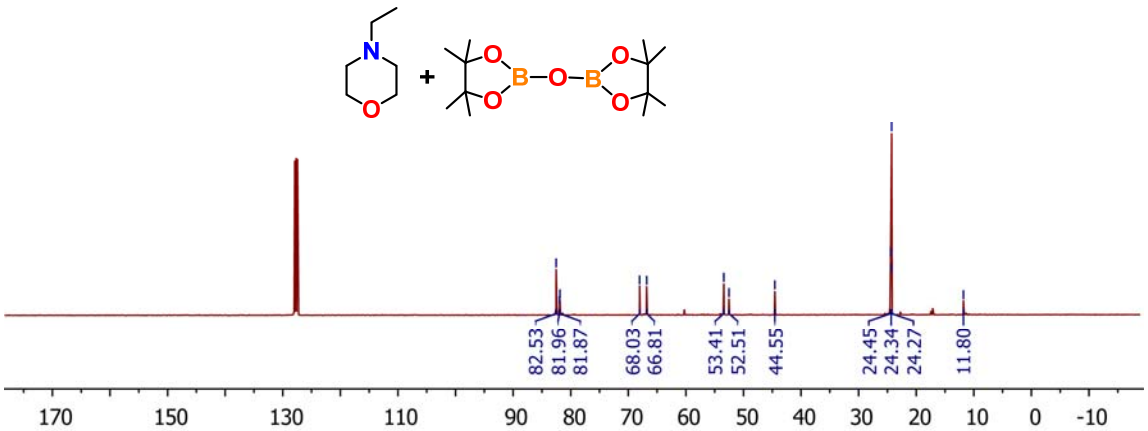

Figure S71. ^{13}C NMR of ***2tt*** in reaction mixture in C_6D_6.

***2uu*, Entry 21, Table 2**

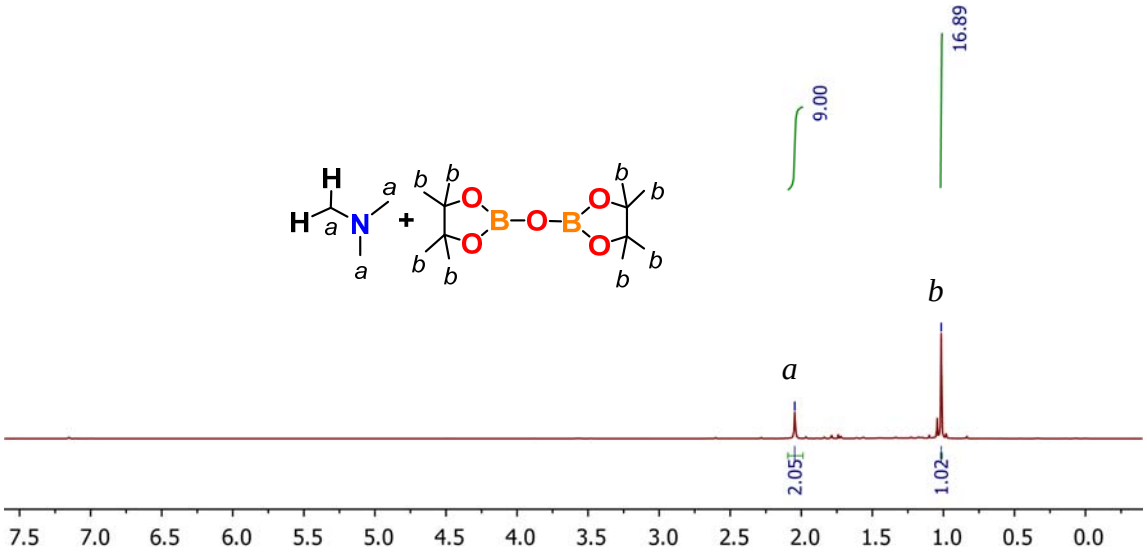

Figure S72. ^{1}H NMR of ***2uu*** in reaction mixture in C_6D_6.

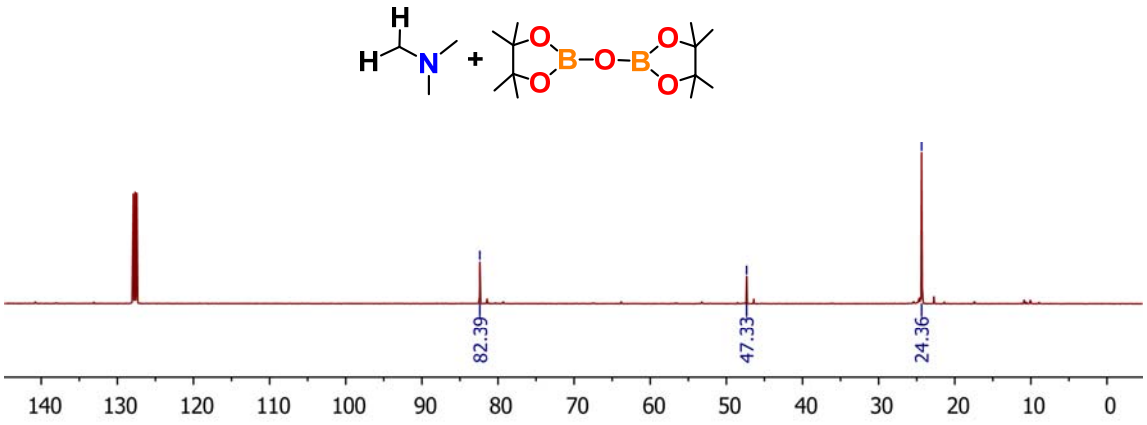

Figure S73. ^{13}C NMR of ***2uu*** in reaction mixture in C_6D_6.

2vv, Entry 22, Table 2

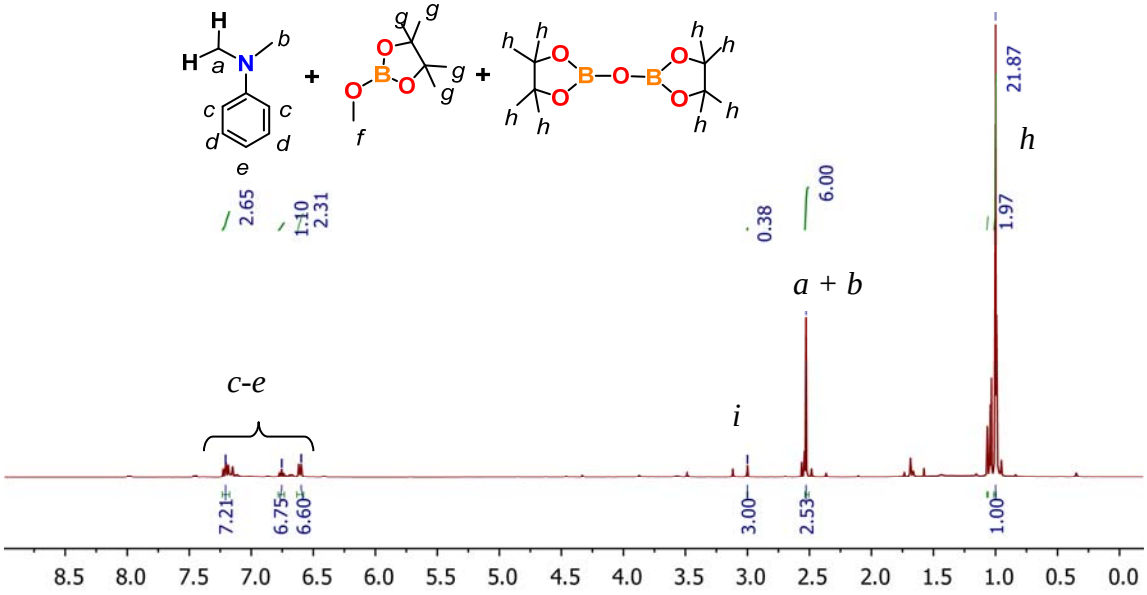

Figure S74. ^{1}H NMR of ***2vv*** in reaction mixture in C_6D_6.

Integral area of H_a = 3; Integral area of H_i = 0.38
% of C-O cleaved product = {3/(3 + 0.38)} x 100% = 90%
% of C-N cleaved product = {0.38/(3 + 0.38)} x 100% = 10%

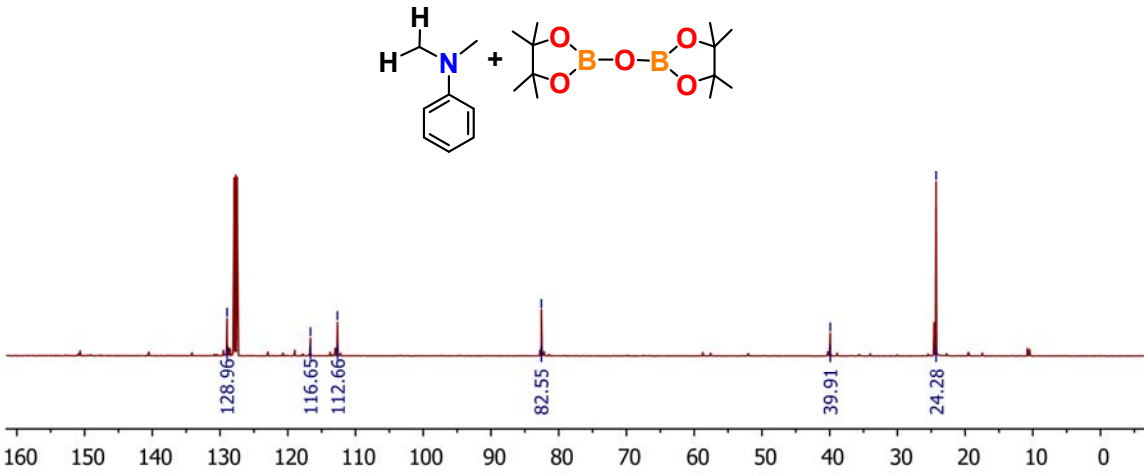

Figure S75. ^{13}C NMR of ***2vv*** in reaction mixture in C_6D_6.

2ww, Entry 23, Table 2

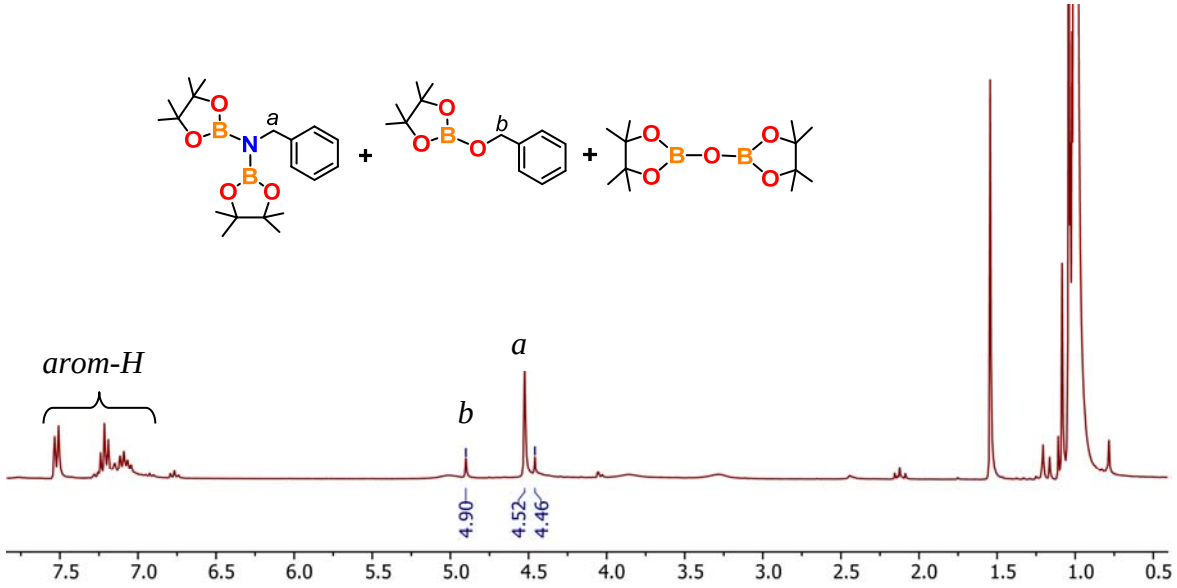

Figure S76. ^{1}H NMR of ***2ww*** in reaction mixture in C_6D_6.

Integral area of H_a = 2; Integral area of H_b = 0.2
% of C-O cleaved product = {2/(2 + 0.2)} x 100% = 90%
% of C-N cleaved product = {0.2/(2 + 0.2)} x 100% = 10%

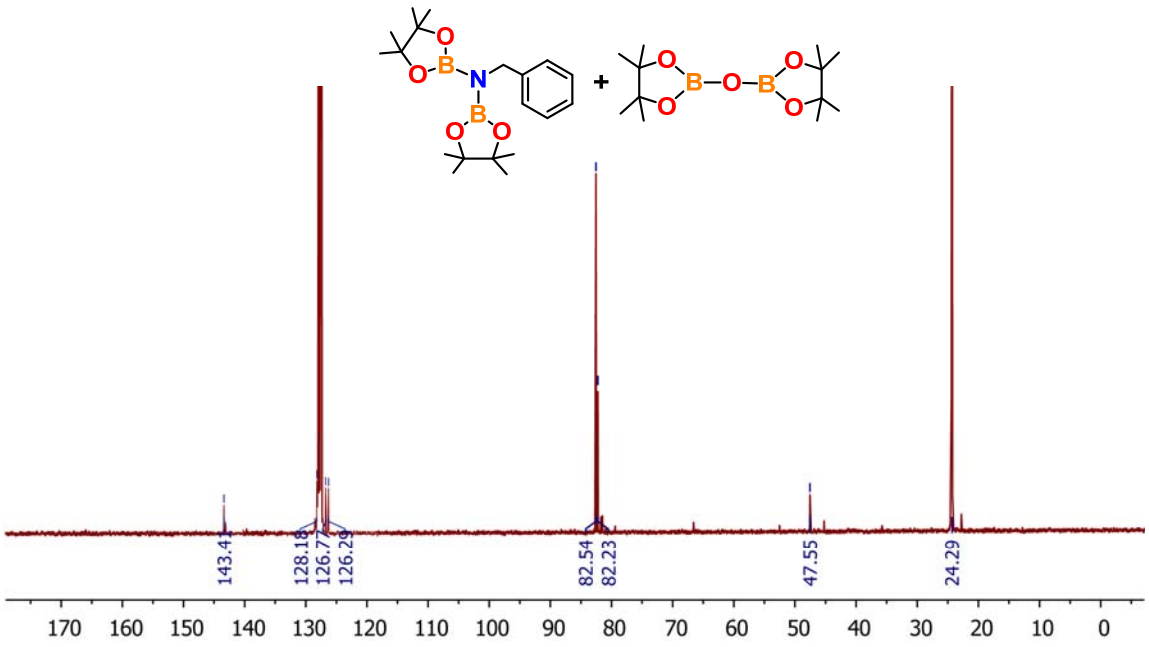

Figure S77. ^{13}C NMR of ***2ww*** in reaction mixture in C_6D_6.

2xx, Entry 24, Table 2

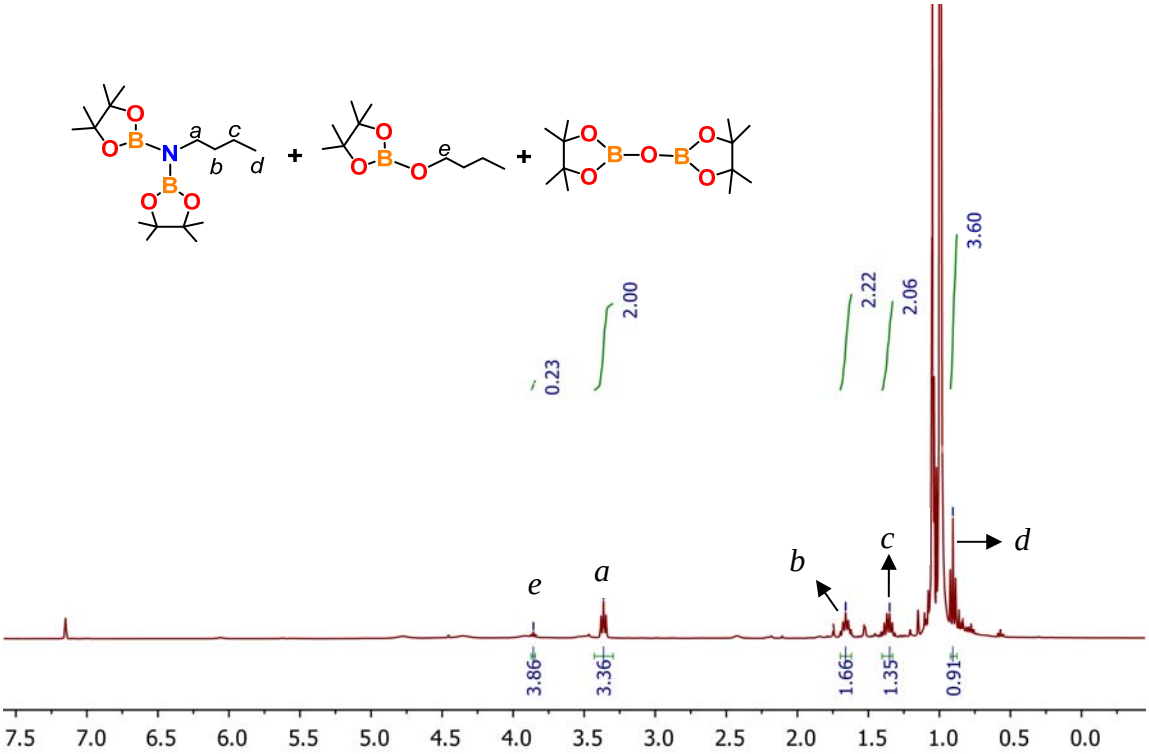

Figure S78. ^{1}H NMR of ***2xx*** in reaction mixture in C_6D_6.

Integral area of H_a = 2; Integral area of H_e = 0.2
% of C-O cleaved product = {2/(2 + 0.2)} x 100% = 90%
% of C-N cleaved product = {0.2/(2 + 0.2)} x 100% = 10%

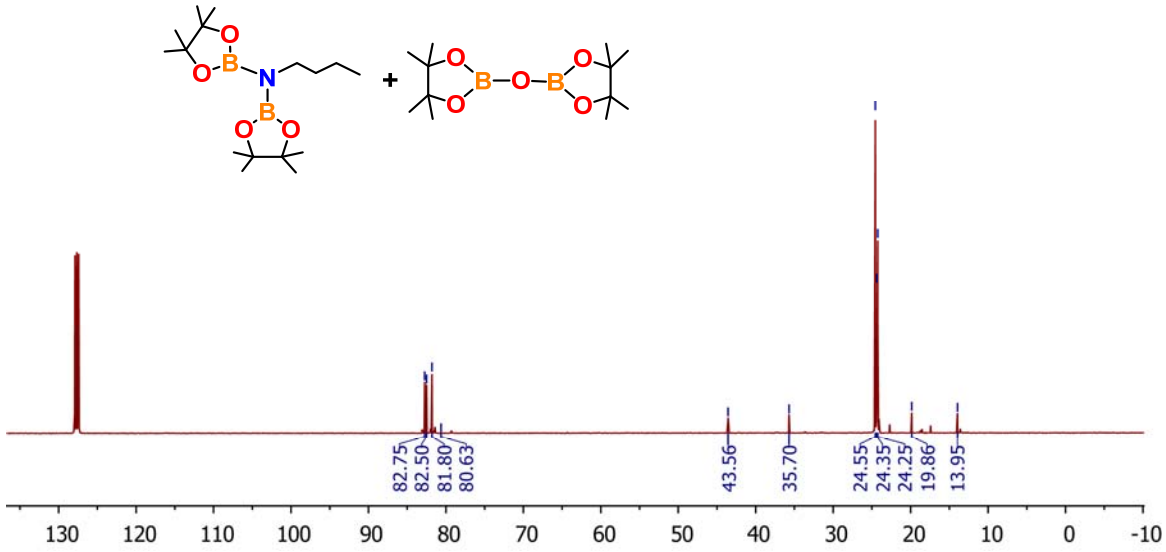

Figure S79. ^{13}C NMR of ***2xx*** in reaction mixture in C_6D_6.

5.4 NMR specta of isolates amines from amine-borane adducts

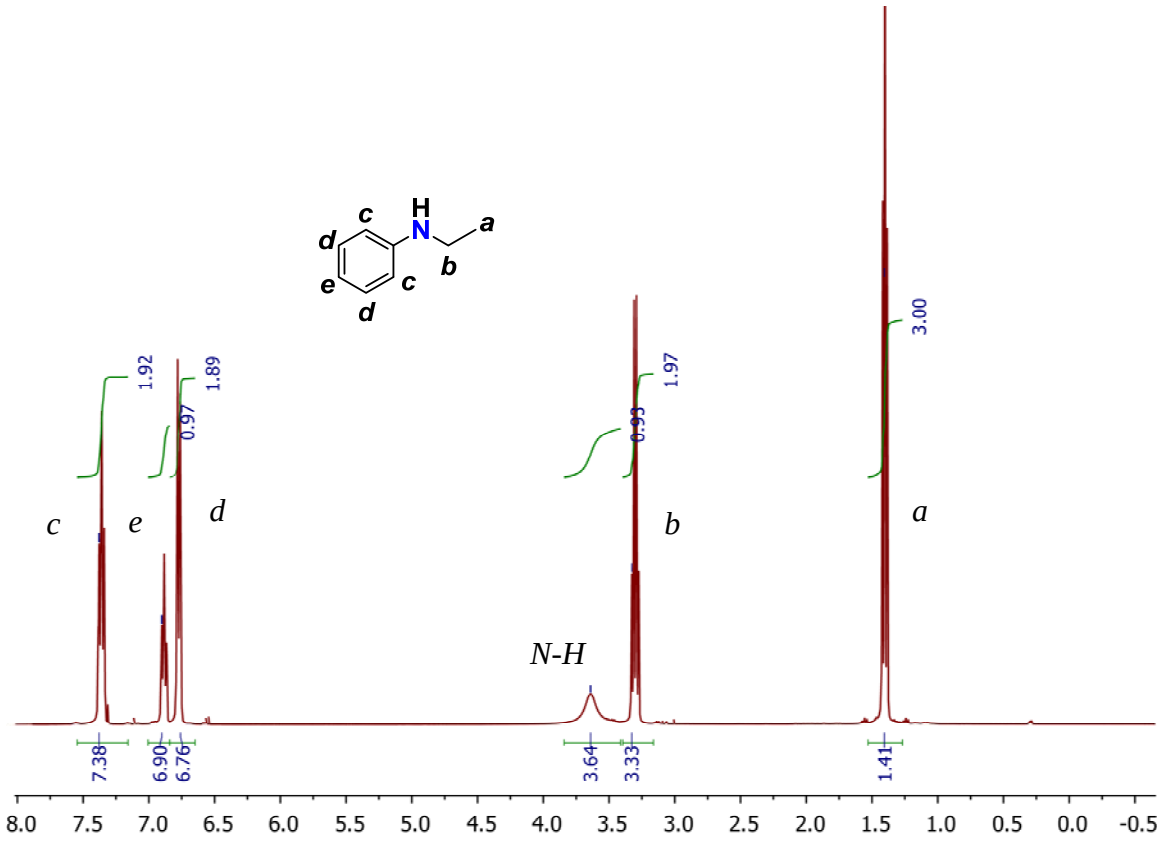

Figure S80. ^{1}H NMR of ***2dd*** in $CDCl_3$ after deprotection of amine-borane adduct.[6c]

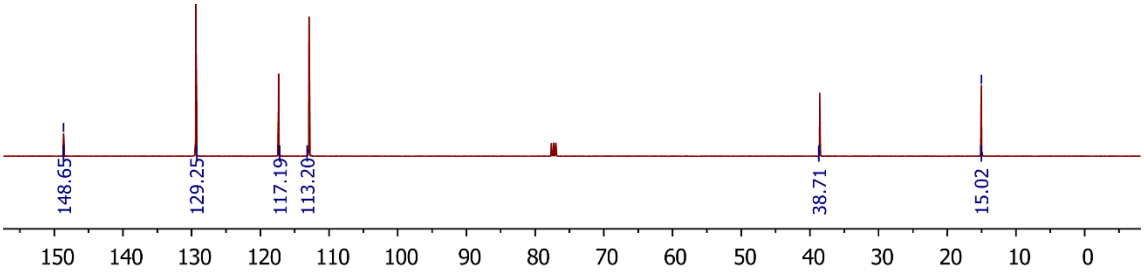

Figure S81. ^{13}C NMR of ***2dd*** in $CDCl_3$ after deprotection of amine-borane adduct.[6c]

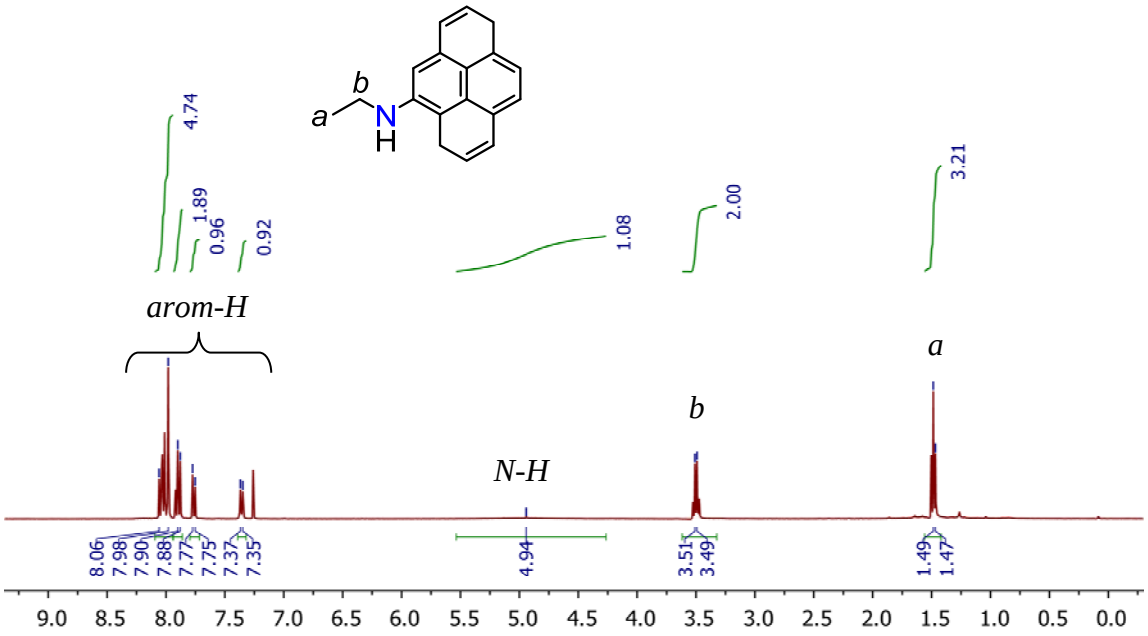

Figure S82. ^{1}H NMR of ***2ee*** in $CDCl_3$ after deprotection of amine-borane adduct.

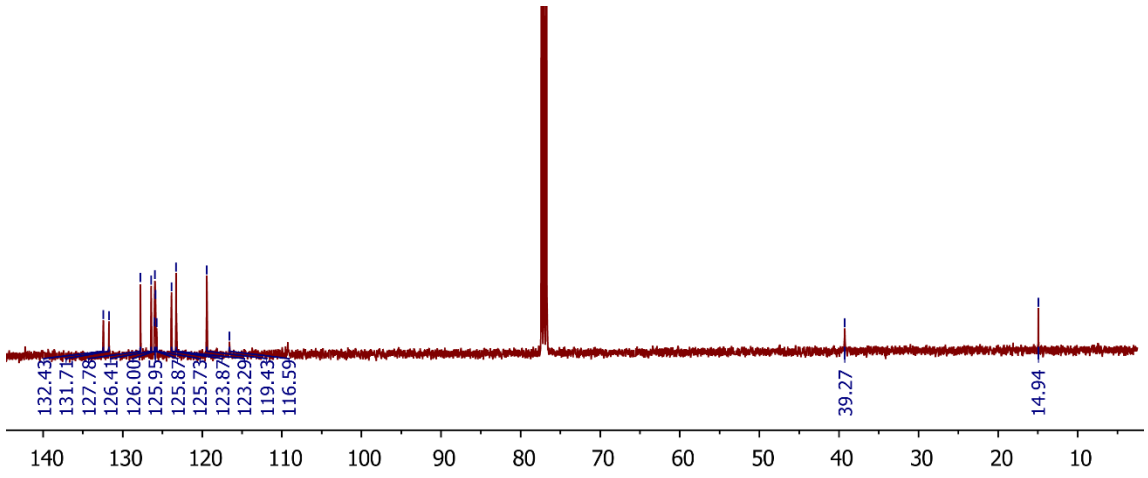

Figure S83. ^{13}C NMR of ***2ee*** in $CDCl_3$ after deprotection of amine-borane adduct.

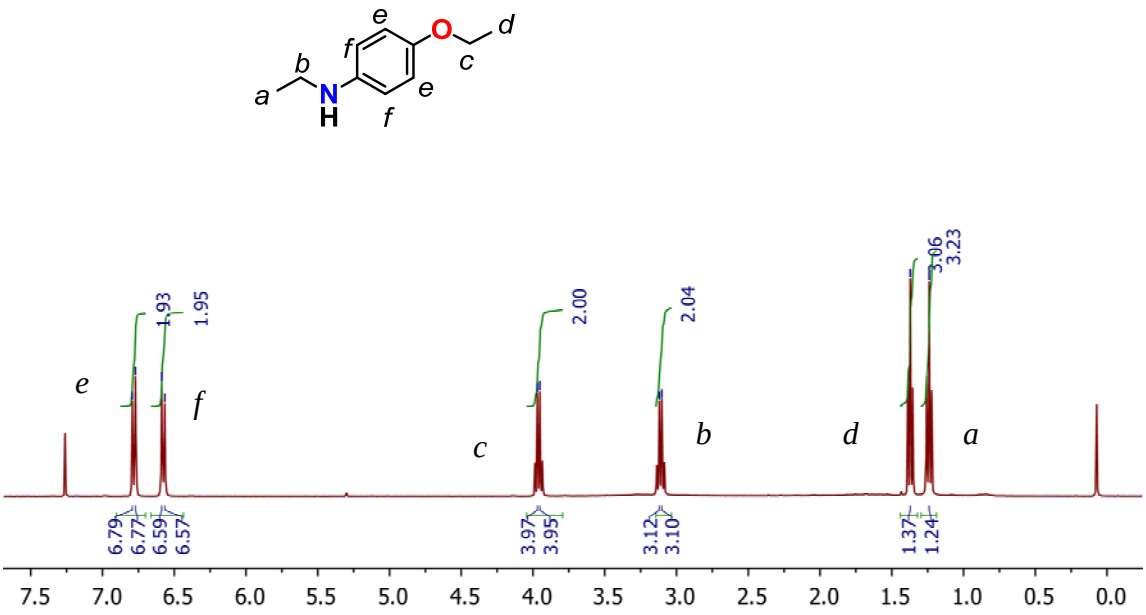

Figure S84. ^{1}H NMR of ***2gg*** in $CDCl_3$ after deprotection of amine-borane adduct.

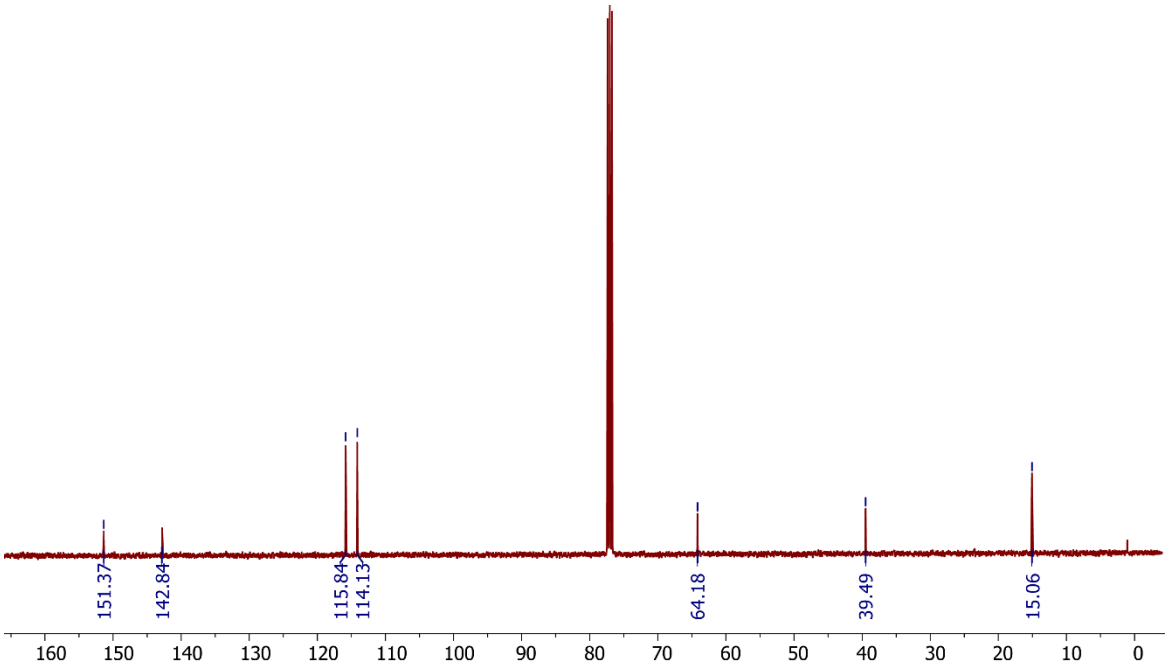

Figure S85. ^{13}C NMR of ***2gg*** in $CDCl_3$ after deprotection of amine-borane adduct.

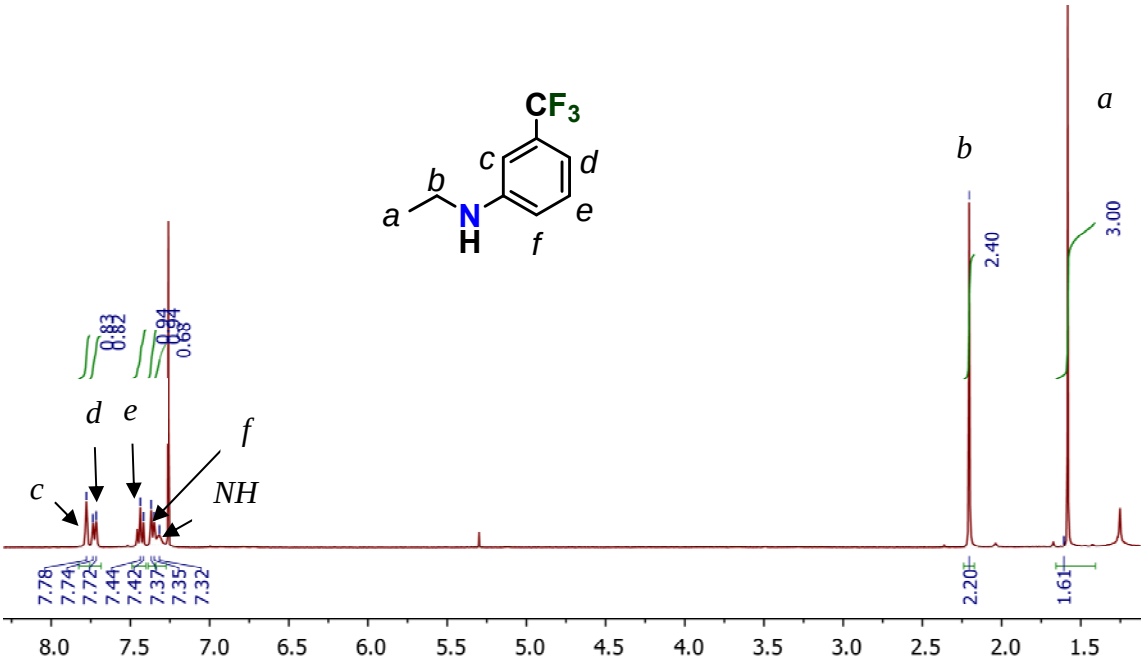

Figure S86. ^{1}H NMR of ***2kk*** in $CDCl_3$ after deprotection of amine-borane adduct.

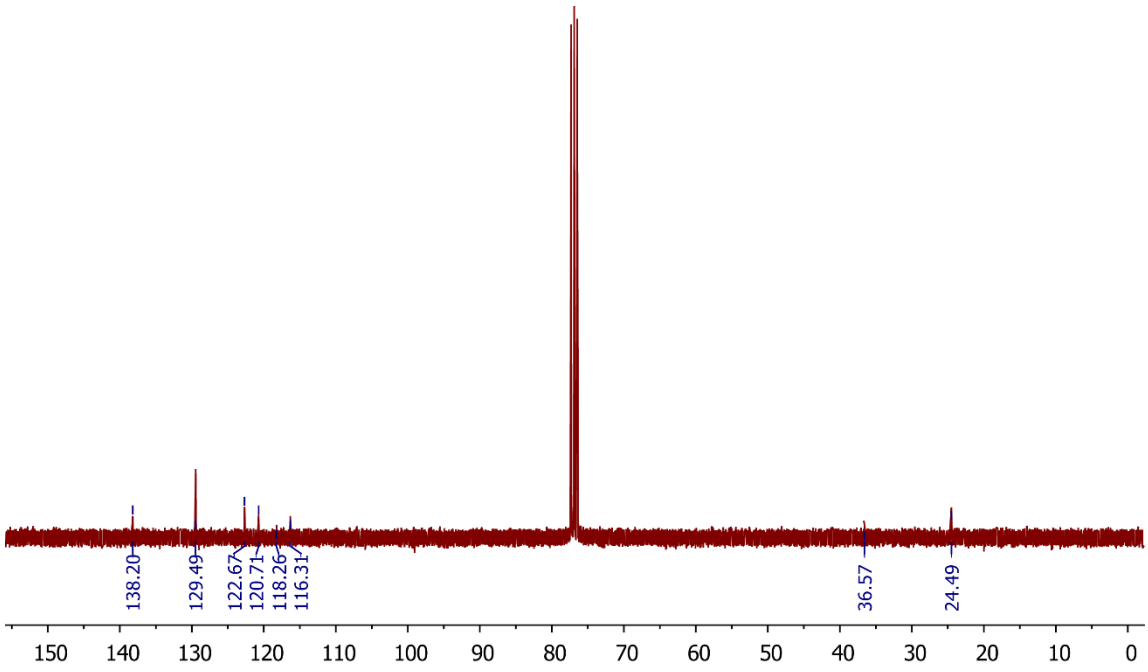

Figure S87. ^{1}H NMR of ***2kk*** in $CDCl_3$ after deprotection of amine-borane adduct.

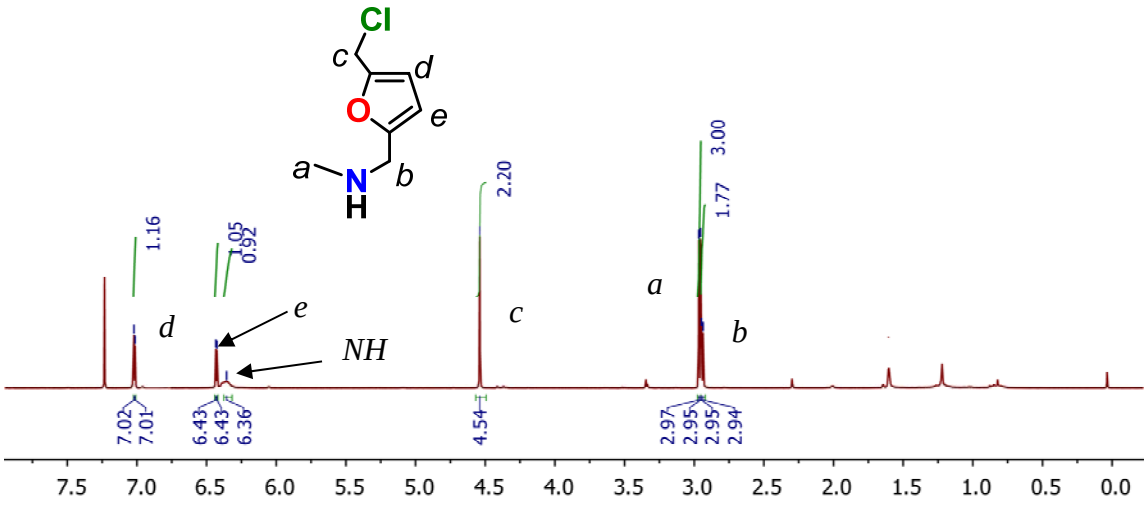

Figure S88. ^{1}H NMR of ***2mm*** in $CDCl_3$ after deprotection of amine-borane adduct.

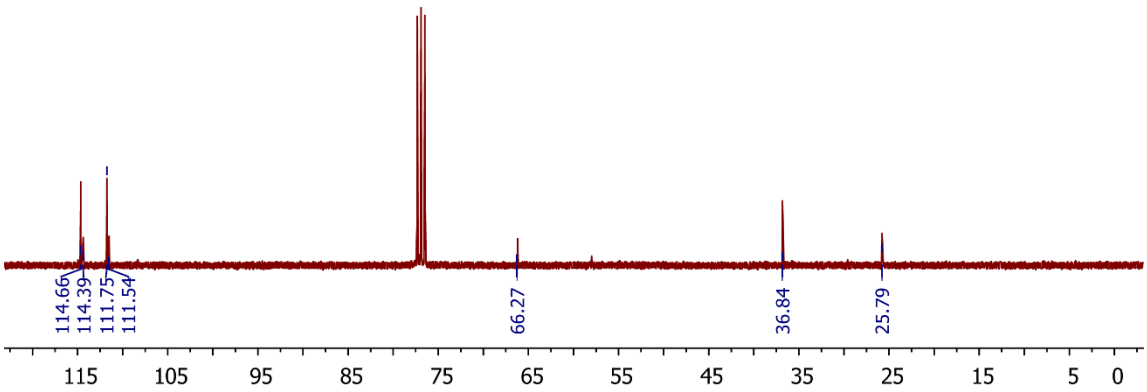

Figure S89. ^{13}C NMR of ***2mm*** in $CDCl_3$ after deprotection of amine-borane adduct.

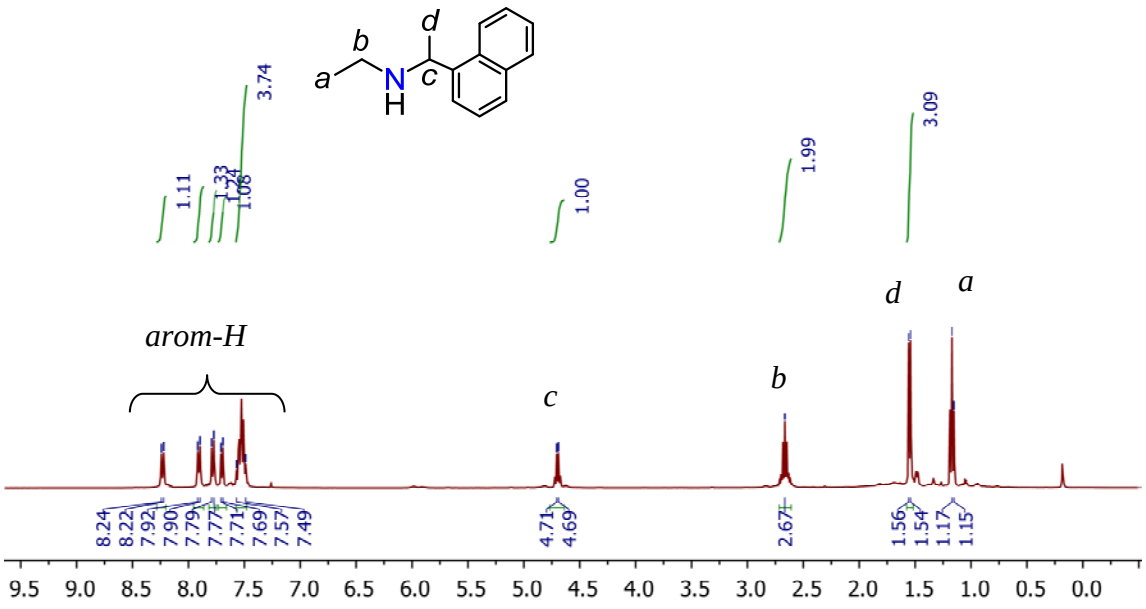

Figure S90. ^{1}H NMR of ***2nn*** in $CDCl_3$ after deprotection of amine-borane adduct.

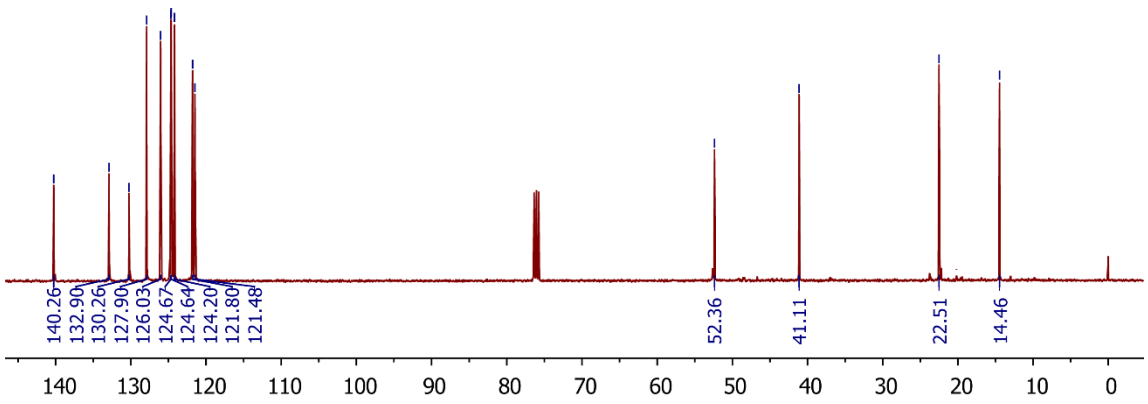

Figure S91. ^{13}C NMR of ***2nn*** in $CDCl_3$ after deprotection of amine-borane adduct.

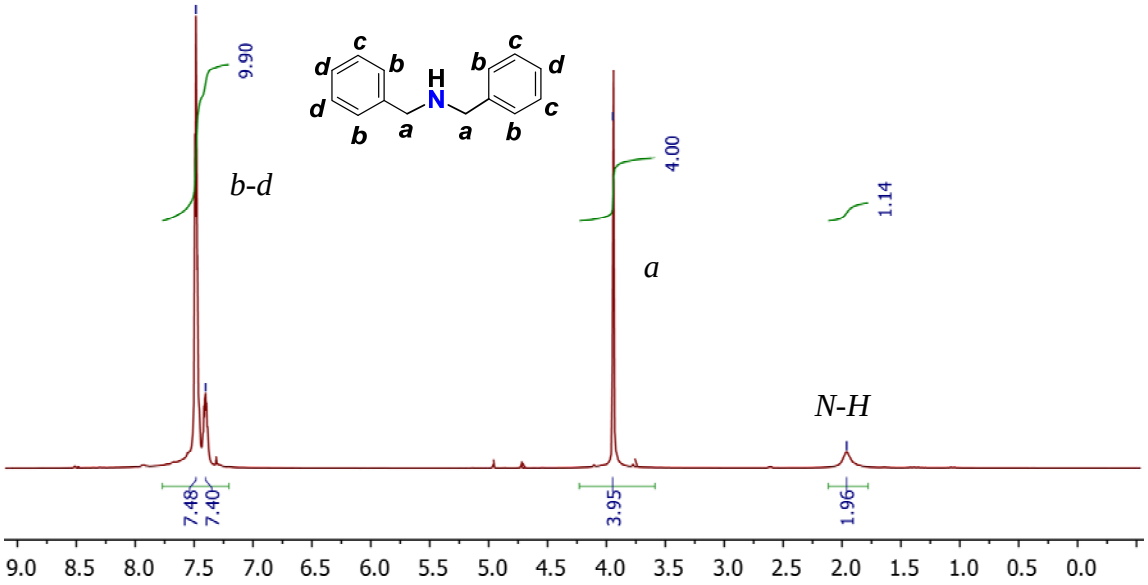

Figure S92. ^{1}H NMR of ***2oo*** in $CDCl_3$ after deprotection of amine-borane adduct.[6n]

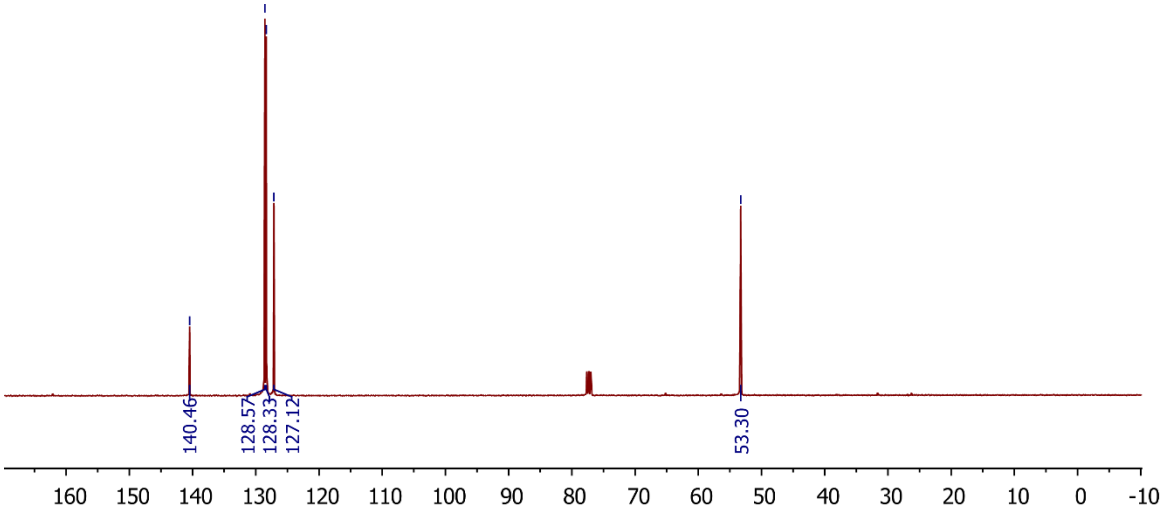

Figure S93. ^{13}C NMR of ***2oo*** in $CDCl_3$ after deprotection of amine-borane adduct.[6n]

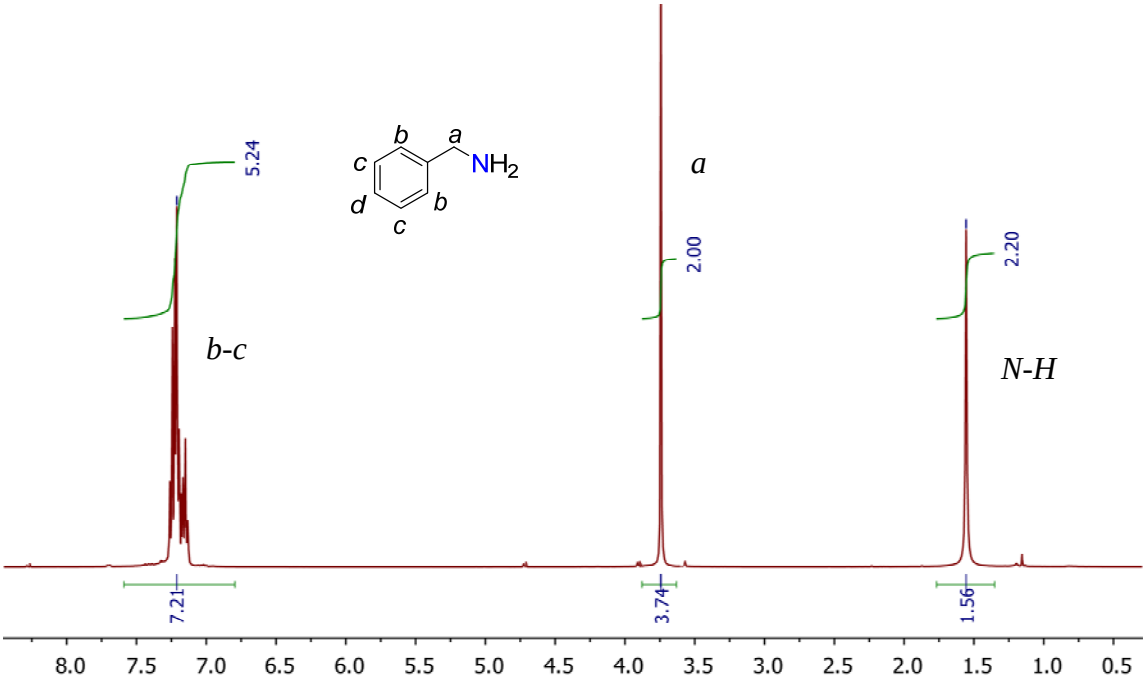

Figure S94. ^{1}H NMR of ***2ww*** in $CDCl_3$ after deprotection of amine-borane adduct.[6o]

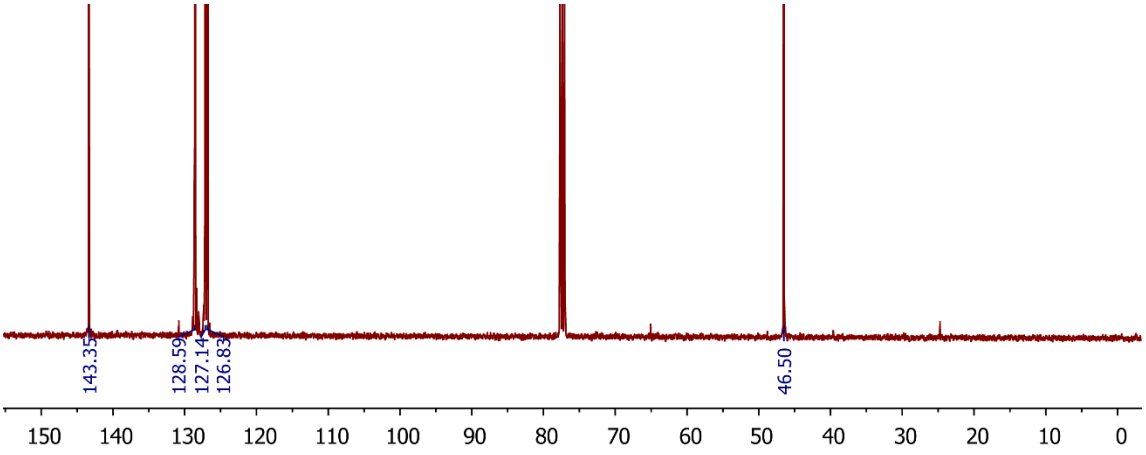

Figure S95. ^{13}C NMR of ***2ww*** in $CDCl_3$ after deprotection of amine-borane adduct.[6o]

6. Reference

1 (a) C. Liu, G. Li, S. Shi, G. Meng, R. Lalancette, R. Szostak and M. Szostak, *ACS Catal*., 2018, **8**, 9131 – 9139. (b) Y. Li, Z. Yan, G. Tu, J. Zhang and Y. Zhao, *RSC Adv*., 2018, **8**, 30374 – 30378.
2 P. J. Fagan, J. M. Manriquez, E. A. Maatta, A. M. Seyam and T. J. Marks, *J. Am. Chem. Soc*., 1981, **103**, 6650 – 6667.
3 T. Cantat, B. L. Scott and J. L. Kiplinger, *Chem. Commun*., 2010, **46**, 919 – 921.
4 S. Saha and M. S. Eisen, *ACS Catal*., 2019, **9**, 5947 – 5956.
5 J. Y. Wu, B. Moreau and T. Ritter, *J. Am. Chem. Soc.*, 2009, **131**, 12915 – 12917.
6 (a) Y. Yang, M. D. Anker, J. Fang, M. F. Mahon, L. Maron, C. Weetman and M. S. Hil, *Chem. Sci*., 2017, **8**, 3529 – 3537. (b) C. Ghosh, S. Kim, M. R. Mena, J.-H. Kim, R. Pal, C. L. Rock, T. L. Groy, M.-H. Baik and R. J. Trovitch, *J. Am. Chem. Soc.*, 2019, **141**, 15327 – 15337. (c) S. R. Tamang, A. Singh, D. Bedi, A. R. Bazkiaei, A. A. Warner, K. Glogau, C. McDonald, D. K. Unruh and M. Findlater, *Nature Catalysis,* 2020, **3**, 154 – 162. (d) K. G. Andrews, R. Faizova and R. M. Denton, *Nature Commun*., 2017, **8**, 1 − 6. (e) T. Mitsudome, K. Miyagawa, Z. Maeno, T. Mizugaki, K. Jitsukawa, J. Yamasaki, Y. Kitagawa and K. Kaneda, *Angew.Chem. Int.Ed*., 2017, **56**, 9381 – 9385. (f) P. Sarkar, A. Z. Chowdhury, S. Riyajuddin, S. Biswas, K. Ghosh and S. M. Islam, *New J. Chem*., 2020, **44**, 744 – 752. (g) N. Sarkar, S. Bera and S. Nembenna, *J. Org. Chem.*, 2020, **85**, 4999 – 5009. (h) A. Kaithal, B. Chatterjee and C. Gunanathan, *J. Org. Chem.*, 2016, **81**, 11153 – 11161. (i) W. Yao, H. Fang, Q. He, D. Peng, G. Liu and Z. Huang, *J. Org. Chem*., 2019, **84**, 6084−6093. (j) Y. Pan, Z. Luo, X. Xu, H. Zhao, J. Han, L. Xu, Q. Fan and J. Xiao, *Adv. Synth. Catal*., 2019, **361**, 3800-3806. (k) X. Yu, R. Zhao, H. Wan, Y. Yang and D. Wang *Tetrahedron Lett*., 2016, *57*, 4588-4591. (l) Y. Pan, Z. Luo, X. Xu, H. Zhao, J. Han, L. Xu, Q. Fan and J. Xiao, *Adv. Synth. Catal*., 2019, **361**, 3800 – 3806. (m) S. Elangovan, J. Neumann, J.-B. Sortais, K. Junge, C. Darcel and M. Beller, *Nature Commun.*, 2016, 1 – 8. (n) V. K Pandey, S. N. R. Donthireddy and A. Rit, *Chem. Asian J.*, 2019, 14, 3255 – 3258. (o) M. Bhunia, S. R. Sahoo, A. Das, J. Ahmed, P. Sreejyothi and S. K. Mandal, *Chem. Sci*., 2019, **10**, 1 − 7.